

**UNIVERSITÉ DU QUÉBEC À CHICOUTIMI**

**MÉMOIRE PRÉSENTÉ À  
L'UNIVERSITÉ DU QUÉBEC À CHICOUTIMI  
COMME EXIGENCE PARTIELLE  
DE LA MAÎTRISE EN INGÉNIERIE**

**PAR**

**NASSER HABIBI**

**EVALUATION OF INCLUSIONS AND OXIDES IN THE AL-SI  
ALLOYS USING PREFIL TECHNIQUE**

**AOÛT 2002**



### *Mise en garde/Advice*

Afin de rendre accessible au plus grand nombre le résultat des travaux de recherche menés par ses étudiants gradués et dans l'esprit des règles qui régissent le dépôt et la diffusion des mémoires et thèses produits dans cette Institution, **l'Université du Québec à Chicoutimi (UQAC)** est fière de rendre accessible une version complète et gratuite de cette œuvre.

Motivated by a desire to make the results of its graduate students' research accessible to all, and in accordance with the rules governing the acceptance and diffusion of dissertations and theses in this Institution, the **Université du Québec à Chicoutimi (UQAC)** is proud to make a complete version of this work available at no cost to the reader.

L'auteur conserve néanmoins la propriété du droit d'auteur qui protège ce mémoire ou cette thèse. Ni le mémoire ou la thèse ni des extraits substantiels de ceux-ci ne peuvent être imprimés ou autrement reproduits sans son autorisation.

The author retains ownership of the copyright of this dissertation or thesis. Neither the dissertation or thesis, nor substantial extracts from it, may be printed or otherwise reproduced without the author's permission.

**Dedicated to my wife Narges  
and my children, Nima and Rosa  
Winter 2002**

## RÉSUMÉ

Le présent travail a été entrepris afin d'étudier le rôle des principaux paramètres du métal en fusion couramment appliqués dans les fonderies d'aluminium, tels que l'affinage de grain et la modification au strontium, de même que l'effet des éléments alliés mineurs sur la formation d'inclusion dans trois alliages Al-Si primaires largement utilisés, notamment A356, A319 et 4104, utilisant la technique Prefil (Pressure Filtration). L'appareil Prefil est l'une des techniques les plus récentes utilisées pour déterminer la propreté du métal en fusion des alliages de fonderie. En faisant passer environ 2.5 kg de métal en fusion à travers un filtre sous pression (10 psi), les inclusions/films sont concentrés dans la région au-dessus du filtre (les dimensions des pores peuvent varier de 0 à 123  $\mu\text{m}$ ). Après le test, le métal solidifié au-dessus du filtre est sectionné, monté et poli pour fins d'examen métallographique.

Puisque la qualité du métal en fusion est un aspect essentiel de la qualité des produits finis des fonderies et des centres de coulées, il est important que les classes mondiales d'opérations établissent des normes de mesure de la qualité du métal. Depuis des dizaines d'années et aujourd'hui encore, la propreté du métal a été largement supervisée en utilisant l'analyse métallographique des échantillons solidifiés. Ces échantillons peuvent être ou ne pas être filtrés.

Une série de quatre-vingt neuf expériences a été conduite (utilisant une charge de 25 kg de matériel d'alliage frais à chaque expérience). La chambre de pression et le creuset de filtration de l'appareil Prefil sont chauffés à environ 300-350°C, afin de réduire la perte de chaleur lors du transfert du métal liquide du creuset de métal en fusion jusqu'au creuset de filtration. Aussi, la température de filtration devrait être suffisamment élevée de façon à éviter que ne se produise une sédimentation des inclusions dans la louche lors du transfert.

Des échantillons Prefil contenant la partie de métal non filtrée (environ 5 mm d'épaisseur) en contact avec le filtre, ont été sectionnée, montée sur du Bakelite et polis pour fins d'examen métallographique. Les échantillons polis ont été examinés au microscope optique afin d'identifier les inclusions obtenues dans chaque cas. Le comptage des inclusions a été effectué utilisant la méthode du maillage. Les types et concentrations d'inclusions de même que les films d'oxyde produits dans ces alliages avant coulée ont été déterminés.

Il appert que les principales inclusions dans ces alliages sont  $\text{Al}_4\text{C}_3$ ,  $\text{MgO}$  et  $\text{MgAl}_2\text{O}_4$  et des oxydes dispersés. La génération de films d'oxydes - associée avec l'usage de l'agitation mécanique pour dissoudre l'affineur de grain et/ou les additions de modificateur au métal en fusion – peut être évitée en utilisant le dégazage. Les résultats du Prefil démontrent qu'un temps de maintien prolongé et l'agitation du métal jouent un rôle significatif en augmentant la quantité d'inclusions dans le métal en fusion. Le dégazage

utilisant de l'argon sec injecté au métal liquide à travers une roue motrice (vitesse 160 rpm) semble être la meilleure technique pour l'enlèvement des inclusions. Dans le cas des additions d'affineur de grain, le traitement de dégazage tend à augmenter la quantité d'inclusions de  $\text{TiB}_2$ .

## ABSTRACT

The present work was undertaken to study the role of the major melt treatment parameters commonly applied in aluminum foundries, such as grain refining and strontium modification, as well as the effect of minor alloying elements on inclusion formation in three widely used Al-Si alloys, A356, A319 and 4104 primary alloys, using the Prefil (Pressure Filtration) technique. The Prefil apparatus is one of the more recent techniques used to determine the melt cleanliness of aluminum foundry alloys. By passing ~2.5 kg of molten metal through a filter under pressure (10 psi), the inclusions/films are concentrated in the region above the filter (pore sizes in the filter can vary from 0 to 123  $\mu\text{m}$ ). After the test, the solidified metal above the filter is sectioned, mounted and polished for metallographic examination.

As liquid metal quality is an essential aspect of the quality of final products from casting foundries and casthouses, it is important that world-class operations accurately benchmark metal quality. For decades, and still today, metal cleanliness has been widely monitored using the metallographic analysis of solidified samples. These samples may or may not be filtered. A series of eighty-nine experiments was conducted (using a charge of 25 kg of fresh alloy material for each experiment). The pressure chamber and filtration crucible of the Prefil apparatus were heated to ~ 300-350°C, to reduce heat loss during transfer of the liquid metal from the melt crucible to the filtration crucible. Also, the filtration temperature would have to be high enough to avoid the possible sedimentation of inclusions in the ladle during the transfer.

Prefil samples containing the unfiltered part of the metal (~ 5 mm in thickness) in contact with the filter were sectioned, mounted in bakelite, and polished for metallographic examination. The polished samples were examined under an optical microscope to identify the inclusions obtained in each case. Inclusion counting was done using the grid method. The types and concentrations of inclusions, as well as aluminum oxide films that occurred in these alloys prior to casting were determined.

It was found that the main inclusions in these alloys are  $\text{Al}_4\text{C}_3$ ,  $\text{MgO}$ , and  $\text{MgAl}_2\text{O}_4$  and dispersed oxides. The generation of oxide films - associated with the use of mechanical stirring to dissolve grain refiners and/or modifier additions to the melt - can be avoided by employing degassing. The Prefil results show that a long holding time and metal stirring play a significant role in increasing the amount of inclusions in the melt. Degassing using dry argon injected into the liquid metal through a rotary impeller (speed ~ 160 rpm) appears to be the best technique for inclusion removal. In the case of grain refiner additions, the degassing treatment tends to increase the amount of  $\text{TiB}_2$  inclusions.

## **ACKNOWLEDGEMENTS**

It gives me a great pleasure to acknowledge all people who were involved directly or indirectly in making this work a success. It is a pleasure to convey my sincere thanks to my supervisors Professors F. H. Samuel and A.M. Samuel for their invaluable guidance during each stage of my thesis.

Financial (in the form of scholarship) and in-kind support received from the Natural Sciences and Engineering Research Council of Canada (NSERC), General Motors Powertrain Group (U.S.A), Corporation Nematik (Mexico), and the Centre Quebécois de recherche et de développement de l'aluminium (CQRDA) is gratefully acknowledged.

The author would also like to thank Mr. Alain Simard, R & D Manager, and Mr. Dany Paquin, Technologist, of ABB. Bomem Inc. for their great assistance during the course of the experimental work. I would like to express my appreciation to several colleagues, particularly Mr. Alain Bérubé and Mr. Régis Boucher for their sincere help and creation of an enjoyable working atmosphere.

Finally, I would like to record my deep gratitude to the members of my family for their consistent encouragement and support.

## TABLE OF CONTENTS

RÉSUMÉ.....	(iii)
ABSTRACT.....	(v)
ACKNOWLEDGEMENTS.....	(vi)
TABLE OF CONTENTS.....	(vii)
LIST OF FIGURES.....	x
LIST OF TABLES.....	xviii

### CHAPTER 1

DEFINITION OF THE PROBLEM.....	1
1.1 INTRODUCTION.....	2
1.2 OBJECTIVES.....	5

### CHAPTER 2

LITERATURE SURVEY.....	6
2.1 HISTORY OF ALUMINUM.....	7
2.2 TYPICAL PROPERTIES AND APPLICATION OF ALUMINUM..	8
2.3 CLASSIFICATION OF ALUMINUM ALLOYS.....	11
2.3.1 ALUMINUM CASTING ALLOYS.....	14
2.4 INCLUSIONS IN ALUMINUM ALLOYS.....	15
2.5 HYDROGEN AND GAS POROSITY.....	23
2.6 SHRINKAGE.....	30
2.7 OXIDATION PROCESS.....	30
2.8 TYPES AND SOURCES OF INCLUSIONS.....	33
2.8.1 OXIDES.....	33



2.8.2	CARBIDES.....	34
2.8.3	BORIDES.....	35
2.8.4	NITRIDES.....	36
2.9	CLASSIFICATION OF INCLUSIONS.....	36
2.10	HARMFUL EFFECTS OF INCLUSIONS.....	40
2.10.1	REDUCTION IN MECHANICAL PROPERTIES.....	40
2.10.2	POOR SURFACE QUALITY.....	42
2.10.3	REDUCTION IN FLUIDITY PROPERTIES.....	43
2.10.4	REDUCTION IN MACHINABILITY AND HIGH TOOL WEAR.....	45
2.11	EFFECT OF GRAIN REFINEMENT.....	45
2.12	EFFECT OF MODIFICATION.....	46
2.13	CHEMICAL COMPOSITION AND HEAT TREATMENT.....	48

### CHAPTER 3

INCLUSION REMOVAL TECHNIQUES.....	49
3.1 INTRODUCTION.....	50
3.1.1 FLUXING.....	50
3.1.1.1 COVERING FLUXES.....	52
3.1.2 FLOTATION.....	53
3.1.3 SEDIMENTATION.....	54
3.1.4 DEGASSING.....	55
3.1.4.1 BENEFITS OF DEGASSING AND FILTRATION....	56
3.2 FILTRATION.....	57
3.2.1 FILTRATION METHODES.....	58
3.2.1.1 Deep Bed Filtration.....	58
3.2.1.2 Cake Filtration.....	59
3.3 INCLUSIONS ASSESSMENT.....	60
3.3.1 Non-Destructive Techniques.....	60
3.3.2 PoDFA (Porous Disc Filtration Apparatus).....	60
3.3.3 Prefil (Pressure Filtration Technique).....	62
3.3.4 Qualiflash.....	66
3.3.5 LiMCA.....	68
3.3.6 Ultrasonic Technique.....	69

### CHAPTER 4

EXPERIMENTAL PROCEDURE & MEASUREMENT.....	71
4.1 MELT PREPARATION.....	72

4.2	METALLOGRAPHIC ANALYSIS.....	73
4.3	THE PREFIL SYSTEM.....	75
4.3.1	PREFIL CRUCIBLE.....	78
4.4	THE LiMCA II SYSTEM.....	80
4.5	EFFECT OF DIFFERENT CLEANLINESS LEVELS.....	82
4.5.1	Prefil results with pure aluminum charge (first set).....	82
4.5.2	LiMCA II results with a pure aluminum charge (first set)....	83
4.5.3	Prefil results with a pure aluminum charge (second set).....	84
4.5.4	LiMCA II results with pure aluminum charge (second set)...	86
4.5.5	Third Set at a Primary Aluminum Producer Plant.....	87
4.5.6	Prefil results with a pure aluminum charge (third set).....	87
4.5.7	LiMCA II results with pure aluminum charge (third set).....	90
4.5.8	TEST WITH AA4104 ALLOY.....	91
4.5.8.1	Prefil Experiments.....	91
4.5.8.2	LiMCA II Experiments.....	94
4.5.9	TEST WITH A356.2 ALLOY.....	95
4.5.9.1	Prefil Results.....	95
4.5.9.2	LiMCA II Results.....	96
4.5.10	Second Set at a Primary Plant.....	98
4.5.10.1	Prefil Results.....	98
4.5.10.2	LiMCA II Results.....	99
4.5.11	TEST WITH 319 ALLOY.....	103
4.5.12	EFFECT OF GRAIN REFINER.....	105
4.6	Prefil – Footprinter Curve Sensitivity.....	109
4.7	Curves Reproducibility.....	113
4.8	EXAMPLES OF INCLUSIONS.....	115
4.8.1	BORIDES.....	115
4.8.2	CARBIDES.....	119
4.8.3	OXIDES.....	121
4.8.4	GRAPHITE.....	133

## CHAPTER 5

CONCLUSIONS.....	135
------------------	-----

REFERENCES.....	139
-----------------	-----

## List of Figures

Figure 1.	Per capita consumption of aluminum in different Countries.....	8
Figure 2.	Inclusion concentration required to producing the indicated volume fraction as a function of particle diameter .....	16
Figure 3.	Oxidation skin inclusion (unetched).....	20
Figure 4.	Flake inclusion consist of MgO (unetched) .....	20
Figure 5.	Silicon oxide inclusions in pure aluminum.....	21
Figure 6.	TiB <sub>2</sub> inclusion in an Al 99.2 rolling slab.....	22
Figure 7.	Combined inclusion in Al 99.0 rolling slab.....	22
Figure 8.	Water-soluble inclusion in a sample from the metal pad of a melting furnace.....	23
Figure 9.	Solubility of hydrogen at atmospheric pressure in aluminum and magnesium <sup>18</sup> .....	24
Figure 10.	Typical microstructures in A356 plate castings under laboratory conditions. a) Distance from chill = 15 mm, hydrogen content = 0.19	

	cc/100g b) Distance from chill = 255 mm, hydrogen content = 0.19	
	cc/100g c) Distance from chill = 15 mm. Hydrogen content = 0.45	
	cc/100g d) Distance from chill = 255 mm, hydrogen content = 0.45	
	cc/100g.....	27
<b>Figure 11.</b>	<b>Porosity as a function of hydrogen content in sand-cast aluminums and aluminums alloy bras .....</b>	<b>28</b>
<b>Figure 12.</b>	<b>Ultimate tensile strength versus hydrogen porosity for sand-cast bars of three aluminum alloys .....</b>	<b>29</b>
<b>Figure 13.</b>	<b>Mechanical properties of 356 alloys as a function of hydrogen content .....</b>	<b>41</b>
<b>Figure 14.</b>	<b>Effect of various elements on surface tension of 99.99% Al in argon at 700–740° C (1290 to 1365° F) <sup>2</sup>.....</b>	<b>44</b>
<b>Figure 15.</b>	<b>Variation in quality index (Q) with Sr content for three different cooling rates. Melts degassed with N<sub>2</sub>-CCl<sub>2</sub>F<sub>2</sub>: band 1: cooling rate 1.5°C/s; band 2: cooling rate 0.5°C/s; band 3: cooling rate 0.08°C/s</b>	
	<b><sup>18</sup> .....</b>	<b>47</b>
<b>Figure 16.</b>	<b>Phase diagram of sodium chloride/ potassium chloride mixture.....</b>	<b>52</b>

<b>Figure 17.</b>	<b>Phase diagram of sodium chloride/ potassium chloride/ sodium fluoride mixture.....</b>	<b>53</b>
<b>Figure 18.</b>	<b>The effect of filtration on metal fluidity.....</b>	<b>56</b>
<b>Figure 19.</b>	<b>Comparison of tensile elongation of unfiltered and filtered test bars Aluminum alloy 535.....</b>	<b>57</b>
<b>Figure 20.</b>	<b>Principle of the PoDFA method of measuring melts cleanliness.....</b>	<b>61</b>
<b>Figure 21.</b>	<b>Typical output obtained from a PoDFA run showing the effect of gas composition on the performance of an in-line melt treatment device.....</b>	<b>62</b>
<b>Figure 22.</b>	<b>Pressure cell of the Prefil apparatus.....</b>	<b>64</b>
<b>Figure 23(a)</b>	<b>Schematic diagram showing, filtration behavior of aluminum alloy containing different types of inclusions.....</b>	<b>65</b>
<b>Figure 23(b)</b>	<b>Schematic diagram of Prefil reproducibility.....</b>	<b>65</b>
<b>Figure 24.</b>	<b>The Qualiflash apparatus : (a) placing the filter (b) measuring the cleanliness of the aluminum melt.....</b>	<b>66</b>
<b>Figure 25.</b>	<b>Variation in the number of steps as a function of pouring temperature for A356 alloy scrap.....</b>	<b>67</b>

<b>Figure 26.</b>	<b>Schematic of LiMCA operation.....</b>	<b>68</b>
<b>Figure 27.</b>	<b>Schematic diagram of an ultrasonic apparatus <sup>3</sup>.....</b>	<b>70</b>
<b>Figure 28.</b>	<b>Ultrasonic attenuation of molten aluminum before and after filtration.....</b>	<b>70</b>
<b>Figure 29.</b>	<b>Picture of a Prefil sample for metallographic analysis.....</b>	<b>74</b>
<b>Figure 30.</b>	<b>Schematic of Prefil disc samples.....</b>	<b>75</b>
<b>Figure 31.</b>	<b>Prefil-Footer operating principle.....</b>	<b>77</b>
<b>Figure 32.</b>	<b>Design of Prefil Crucible.....</b>	<b>78</b>
<b>Figure 33.</b>	<b>LiMCA II.....</b>	<b>81</b>
<b>Figure 34.</b>	<b>Prefil curves compared with LiMCA II measurement in pure aluminum (first set).....</b>	<b>82</b>
<b>Figure 35.</b>	<b>Inclusion level measured with the LiMCA II in pure aluminum (first set).....</b>	<b>83</b>
<b>Figure 36.</b>	<b>Prefil curves compared with LiMCA II instruments and metallographic analysis in pure aluminum (second set).....</b>	<b>84</b>
<b>Figure 37.</b>	<b>Metallographic analysis results from Prefil residues in pure aluminum (second set).....</b>	<b>85</b>
<b>Figure 38.</b>	<b>Inclusion level measured with the LiMCA II in pure aluminum (second set).....</b>	<b>86</b>

<b>Figure 39.</b>	<b>Prefil curves and metallographic analysis results in 99.7% pure aluminum (third set).....</b>	<b>87</b>
<b>Figure 40.</b>	<b>Metallographic analysis results from Prefil residues in 99.7% pure aluminum (third set) <sup>48</sup>.....</b>	<b>88</b>
<b>Figure 41.</b>	<b>Microscopic aspect of the Prefil Filter before Alpur at 100X(pure aluminum, third set).....</b>	<b>89</b>
<b>Figure 42.</b>	<b>Microscopic aspect of the Prefil filter after Alpur at 100X(pure aluminum, third set).....</b>	<b>89</b>
<b>Figure 43.</b>	<b>Inclusion level measured by the LiMCA II before Alpur in 99.7% pure aluminum (third set).....</b>	<b>90</b>
<b>Figure 44.</b>	<b>Prefil curves and metallographic analysis results in AA4104 alloy.....</b>	<b>91</b>
<b>Figure 45.</b>	<b>Metallographic analysis results from Prefil residues in AA4104 alloy.....</b>	<b>92</b>
<b>Figure 46.</b>	<b>Microscopic aspect of the Prefil filter before treatment in AA4104 alloy.....</b>	<b>93</b>
<b>Figure 47.</b>	<b>Microscopic aspect of the Prefil filter after treatment in AA4104 alloy.....</b>	<b>93</b>
<b>Figure 48.</b>	<b>Inclusion level measured by the LiMCA II before treatment in AA4104 alloy.....</b>	<b>94</b>
<b>Figure 49.</b>	<b>Prefil curves and metallographic analysis results with A356.2 alloy (first set).....</b>	<b>95</b>

<b>Figure 50.</b>	<b>Metallographic analysis results from Prefil residues in A356.2 alloy (first set).....</b>	<b>96</b>
<b>Figure 51.</b>	<b>Inclusion level measured by the LiMCA II before treatment in A356.2 alloy (first set).....</b>	<b>97</b>
<b>Figure 52.</b>	<b>Microscopic aspect of carbides greater than 3 <math>\mu\text{m}</math> in A356.2 alloy (first set).....</b>	<b>97</b>
<b>Figure 53.</b>	<b>Microscopic aspect of carbide in A356.2 alloy (first set).....</b>	<b>98</b>
<b>Figure 54.</b>	<b>Prefil curves and metallographic analysis results in A356.2 alloy (second set).....</b>	<b>99</b>
<b>Figure 55.</b>	<b>Inclusion level measured by the LiMCA II before treatment in A356.2 alloy (first set).....</b>	<b>100</b>
<b>Figure 56.</b>	<b>Metallographic analysis results from Prefil residues in A356.2 alloy (second set).....</b>	<b>101</b>
<b>Figure 57.</b>	<b>Microscopic aspect of titanium boride particles and aluminum carbides in A356.2 alloy (second set).....</b>	<b>101</b>
<b>Figure 58.</b>	<b>Microscopic aspect of <math>\text{TiB}_2</math> particles in A356.2 alloy (second set).....</b>	<b>102</b>
<b>Figure 59.</b>	<b>Prefil curves and metallographic analysis results with A319 alloy....</b>	<b>103</b>
<b>Figure 60.</b>	<b>Metallographic analysis results from Prefil residues in A319 alloy.....</b>	<b>104</b>



**Figure 61. Microscopic aspect of Prefil filter in 319 alloys.....104**

**Figure 62(a). Prefil curves and metallographic analysis results showing the effect of grain refiner on the filtration rate (fresh A356.2 alloy).....105**

**Figure 62(b). Prefil curves and metallographic analysis results showing the effect of grain refiner on the filtration rate (fresh A356.2 alloy).....106**

**Figure 63(a). Effect of modification with 200-400 ppm strontium on Prefil curves using different filter permeability.....108**

**Figure 63(b). Effect of modification with 400-600 ppm strontium on Prefil curves using different filter permeability.....109**

**Figure 64. Al<sub>2</sub>SrO<sub>3</sub> inclusion particles in a 356.2 alloy .....110**

**Figure 65. EDX analysis of O, Sr and Al observed in the white particles shown in Fig 65.....110**

**Figure 66. Correlation between Prefil curves and metallographic analysis results in pure aluminum for clean metal.....111**

**Figure 67. Correlation between Prefil curves and LiMCA II measurement in pure aluminum.....112**

**Figure 68. Correlation between Prefil curves and metallographic analysis results with A356.2 alloy.....112**

**Figure 69. Correlation between Prefil curves and metallographic analysis results with A356.2 alloy.....113**

**Figure 70. average curves and one standard deviation .....116**

<b>Figure 71.</b>	<b>Microscopic aspect of the interface.....</b>	<b>117</b>
<b>Figure 72.</b>	<b>AlB<sub>2</sub> as an inclusion in aluminum casting alloys.....</b>	<b>118</b>
<b>Figure 73.</b>	<b>(Ti-V)B<sub>2</sub> as an inclusion in aluminum casting alloys.....</b>	<b>119</b>
<b>Figure 74.</b>	<b>Microstructure of Prefil-Test residues from CFF filtered tests.....</b>	<b>120</b>
<b>Figure 75.</b>	<b>Large aluminum carbide inclusion.....</b>	<b>122</b>
<b>Figure 76.</b>	<b>Sample # 4A, Aspect of aluminum carbides.....</b>	<b>122</b>
<b>Figure 77.</b>	<b>Presence of MgO at the metal/filter interface.....</b>	<b>124</b>
<b>Figure 78.</b>	<b>Presence of MgO in the matrix.....</b>	<b>124</b>
<b>Figure 79.</b>	<b>Magnesium oxides beside the filter section.....</b>	<b>125</b>
<b>Figure 80.</b>	<b>Magnesium oxide inclusion in the matrix.....</b>	<b>125</b>
<b>Figure 81.</b>	<b>Presence of metallurgical spinel and cuboids at the interface.....</b>	<b>126</b>
<b>Figure 82.</b>	<b>An example of cuboids oxide inclusions.....</b>	<b>127</b>
<b>Figure 83.</b>	<b>Cuboids inclusion with MgO at the interface.....</b>	<b>127</b>
<b>Figure 84.</b>	<b>Presence of metallurgical spinel particles at the interface.....</b>	<b>128</b>
<b>Figure 85.</b>	<b>Spinel inclusion inside the filter section.....</b>	<b>129</b>
<b>Figure 86.</b>	<b>Presence of a spinel-like at the interface.....</b>	<b>130</b>
<b>Figure 87.</b>	<b>spinel-like inclusion.....</b>	<b>130</b>
<b>Figure 88.</b>	<b>Example of a thick and long oxide film.....</b>	<b>131</b>
<b>Figure 89.</b>	<b>Example of a thin and short oxide film.....</b>	<b>132</b>
<b>Figure 90.</b>	<b>Dispersed Al<sub>2</sub>O<sub>3</sub> beside the filter section.....</b>	<b>132</b>
<b>Figure 91.</b>	<b>Bone Ash as an example of inclusions in aluminum casting.....</b>	<b>133</b>
<b>Figure 92.</b>	<b>FeO/MnO as an example of inclusions in aluminum casting.....</b>	<b>133</b>

<b>Figure 93.</b>	<b>Presence of refractory material at the interface.....</b>	<b>134</b>
<b>Figure 94.</b>	<b>Nodular graphite as an inclusion in aluminum.....</b>	<b>135</b>
<b>Figure 95.</b>	<b>Flakes graphite as an inclusion in aluminum.....</b>	<b>136</b>

## LIST OF TABLES

<b>Table 1.</b>	Physical properties of commercially pure aluminum (99.5%).....	10
<b>Table 2.</b>	Compositions of some common aluminum-silicon casting alloys.....	15
<b>Table 3.</b>	Classification of Inclusions in Aluminum Casting Alloys.....	18
<b>Table 4.</b>	Pilling Bedworth ratios for some common metals.....	32
<b>Table 5.</b>	Typical inclusions in die cast aluminum alloys.....	38
<b>Table 6.</b>	Chemical compositions (wt %) of the as-received A356, A319 and AA4104 alloys.....	73
<b>Table 7.</b>	Technical Specifications of Prefil Crucible.....	79
<b>Table 8.</b>	Temperature Range of Crucible.....	79
<b>Table 9.</b>	Chemical Composition of Crucible (Weight Percent After firing).....	80
<b>Table 10.</b>	Inclusion Concentrations as a Function of Sr Content and Filter.....	108
	Permeability	

## **CHAPTER 1**

### **DEFINITION OF THE PROBLEM**

# CHAPTER 1

## DEFINITION OF THE PROBLEM

### 1.1 INTRODUCTION

Aluminum (with an atomic weight of 26.98 and an atomic number of 13) is well known for its low melting point ( $658^{\circ}\text{C}$ ), and low density ( $2.71\text{ g/cm}^3$  at  $20^{\circ}\text{C}$ ). Aluminum is the second most plentiful metallic element on earth, and became an economic competitor in engineering applications as recently as the end of 19<sup>th</sup> century. The emergence of important industrial developments that demanded material development consistent with the unique qualities of aluminum and its alloys, have resulted in spiralling growth in the production and use of aluminum, so that today aluminum alloys have virtually replaced iron and steel in many applications.<sup>1</sup> Pure aluminum has a tensile strength of about 13000 psi. However, substantial increases in strength can be obtained by cold working some alloys, which properly heat-treated; can approach tensile strengths of 100,000 psi.

Avner<sup>2</sup> reported that one of the most important characteristics of aluminum is its machinability and workability. It can be cast by known methods, rolled to any desired

thickness, stamped, drummed, hammered, forged and extruded to almost any conceivable shape. Commercially pure aluminum, 1100 alloy (99.0 + percent aluminum), is suitable for applications where good formability or very good resistance to corrosion (or both) is required and where high strength is not necessary. It has been used extensively for cooking utensils, various architectural components, food and chemical handling and storage equipment and welded assemblies.

Among the more widely used aluminum casting alloys A357 and A319-are more popular for automotive applications. These groups are characterized by their low specific gravity, low melting point, excellent castability, good machinability and good corrosion resistance. A356 belongs to the Al-Si-Mg family of alloys with excellent casting characteristics and heat treatable properties to provide the best tensile and physical properties.

Shivkumar et al. <sup>3</sup> reported that cast aluminum alloys have widespread applications, especially in the aerospace and automotive industries. These alloys possess excellent tensile and fatigue properties and good corrosion resistance. The major alloying element, silicon, imparts good castability and resistance to hot tearing. Also, since silicon increases in volume during solidification, the susceptibility of the casting to shrinkage defects is reduced. Consequently, alloys containing silicon are ideally suited for high volume production in aluminum foundries. Magnesium and copper are the other major alloying elements that may be present in cast aluminum alloys. Magnesium combines with silicon to form  $Mg_2Si$  and provides the ability to heat-treat the 356 and 357 family of alloys to high

strength levels. Copper in aluminum alloys such as 319, improves their as-cast and high temperature strength properties.

Miller<sup>4</sup> found that the presence of inclusions in aluminum alloy castings has been a major problem in process and quality control. There are, of course, other variables which affect ingot quality. Inclusions of various types and sizes originate in the melting process and if they are not removed prior to ingot solidification, they can result in a defective finished part.

There are different methods for measuring inclusions in the molten metal. These methods include electronic devices such as LiMCA<sup>TM</sup> technique; standard tests for measuring hydrogen levels such as the reduced pressure test or AISCAN<sup>TM</sup>. Another method is filtration of the molten metal with collection of the inclusions for subsequent metallographic examination such as PoDFA, LAIS, Qualiflash and Prefil. Among of these techniques the more recent Prefil technique is one of the easiest to use to evaluate the quality of molten metal. This technique is based on the relationship between filtration curves (Footprint) and the molten metal quality (*viz.*, amount of inclusions).

This present work focuses on the identification, evaluation and measurement of inclusions obtained in aluminum casting alloys, in particular, A356 and A319 alloys, using the Prefil technique. A correlation between the type and concentration of inclusions observed and the flow curves obtained with the Prefil apparatus has been presented.



## 1.2 OBJECTIVES

The present research work was undertaken to study the assessment of melt cleanliness in A356 and A319 aluminum casting alloys using the Prefil technique.

The work was divided into three parts to cover the following aspects:

- i) To evaluate the effectiveness of the Prefil technique in the measurement of inclusions in 356 and 319 Al-Si cast alloys.
- ii) To study the permeability of different filters used in the Prefil technique.
- iii) To study the effect of the grain refiner addition ( $\text{TiB}_2$ ) and oxides on the nature of the Prefil curves obtained. Grain refining is normally carried out by adding measured amounts of Al-Ti-B master alloys *viz.*, Al-5 wt % Ti- 1 wt % B, Al- 5 wt % Ti-5 wt %B, Al-2.5 wt %Ti-2.5 wt % B or Al-10 wt %Ti-1wt %B. In the present work, Al-5 wt % Ti-1 wt % B was used. The concentration of  $\text{TiB}_2$  was calculated in the range of 0.01-0.03-wt % Ti.

**CHAPTER 2**  
**LITRATURE SURVEY**

## CHAPTER 2

### LITRATURE SURVEY

#### 2.1 HISTORY OF ALUMINUM

The first production of aluminum on a laboratory scale was carried out by Oersted in Denmark in 1825, and in Germany by Woehler, a short time later. <sup>5</sup> In 1888, two men, Charles Martin Hall, an American, and Paul T. Heroult, a Frenchman, worked independently and discovered almost simultaneously an economical process of producing aluminum by electrolysis from a fused salt bath. This is still the basic process by which aluminum is produced today.

The Heroult process was evaluated industrially in Neuhausen, Switzerland in 1888, and the Hall process was tested at about the same time in Pittsburgh, Pennsylvania. In the relatively short time since then, aluminum production has undergone an amazing growth (see Figure 1). Since World War II, the production and consumption of aluminum has increased at a rate of more than 8% per year, as shown in Figure 1. Today aluminum is the second most widely used metal in the world. <sup>5</sup>

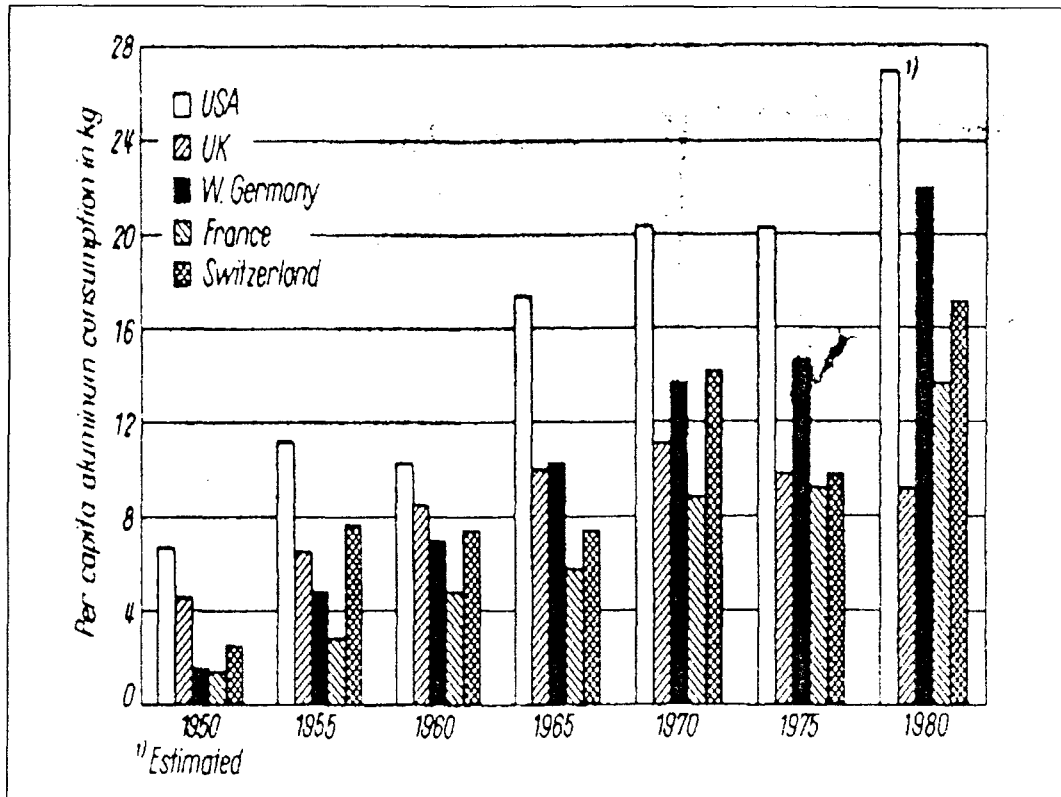


Figure 1. Per capita consumption of aluminum in different countries.<sup>5</sup>

## 2.2 TYPICAL PROPERTIES AND APPLICATION OF ALUMINUM

Aluminum has unique characteristics. Some of the typical properties of aluminum are summarized below:

- a) Aluminum is light; its density is only about one-third that of steel.
- b) Aluminium is resistant to weather, foodstuffs and a large number of liquids and gases found in every day use.

- c) Aluminum has high reflectivity. This, together with its silvery surface, provides aluminum with decorative properties suitable for interior and exterior architectural applications.
- d) The luster of the surface of aluminum can be protected with plastics, lacquers or suitable anodic finishes. In many cases the naturally occurring, clear oxide layer is sufficient to protect the surface.
- e) Aluminum alloys can equal or even exceed the strength of normal structural steel.
- f) Aluminum has high elasticity, which is very useful in certain constructions exposed to shock loading; however, its toughness is reduced significantly at low temperature, as is the case with most commercial steels.
- g) Aluminum is readily workable and easy to form and can be easily rolled and extruded to a thickness of less than 0.01 mm.
- h) Aluminum conducts electricity and heat almost as well as copper.

Table (1) lists the physical properties of aluminum.

**Table 1.** Physical properties of commercially pure aluminum (99.5%).<sup>2</sup>

Atomic Weight	26.98	-
Atomic number	13	-
Crystal structure, face centered cubic, atomic	$4.0496 \cdot 10^{-8}$	Cm
Density at 20°C	2.71	$\text{g/cm}^3$
Thermal conductivity	2.1-2.3	W/cm.k
Coeff. of thermal expansion 60°C -100°C	23.5	$1/\text{k} \cdot 10^6$
Increase in volume on changing from solid to liquid	6.5	%
Melting point	658(93)	°C (K)
Specific heat at 20°C (293 K)	0.9	J/g K
Specific heat at 658°C (931K)	1.13	J/g K
Specific heat at 700°C (937K)	1.045	J/g K
Average specific heat from 0-658°C (273-931K) solid	1.045	J/g K
Heat of fusion	396	J/g K
Heat of vaporization at 1.01325 bar (= 1 atm)	$1.1 \times 10^4$	J/g
Boiling point	2270 (2534)	°C (K)
Electrical conductivity	34 - 36	M/Oh.mm <sup>2</sup>
Resistivity at 20°C	$2.65 \cdot 10^{-6}$	Ohm .cm
Temperature coefficient of resistance	$1.15 \cdot 10^{-8}$	Ohm m/K
Electrochemical equivalent	$9.3167 \cdot 10^{-5}$	G/A .s
Modulus of elasticity E	$7.2 \cdot 10^4$	N/mm <sup>2</sup>
Shear modulus G	$2.7 \cdot 10^4$	N/mm <sup>2</sup>
Poisson s ratio	0.34	-

Aluminum alloys are used to alter the characteristics of aluminum to fit with the requirements of product development. One of the important stages is material selection, which is a crucial part in any product development and design process. The success of the launched product is determined by the resulting physical and mechanical properties, functionality and aesthetic appearance. The optimum combination of these properties can be found in aluminum with the correct aluminum alloy and temper selection. This offers limitless application opportunities and product development. The most common alloying elements for aluminum are magnesium, silicon, manganese, zinc and copper.

### 2.3 CLASSIFICATION OF ALUMINUM ALLOYS

It is convenient to divide aluminum alloys into two major categories: casting compositions and wrought compositions. A further differentiation for each category is based on the primary mechanism of property development. Many alloys respond to thermal treatment, based on phase solubility. These treatments include solution heat treatment, quenching and precipitation or age hardening. For either casting or wrought alloys, such alloys are described as heat-treatable. A large number of other wrought compositions rely instead on work hardening through mechanical reduction, usually in combination with various annealing procedures for property development. These alloys are referred to as work hardening alloys. Some cast alloys are essentially non-heat-treatable and are used only in as-cast or in thermally modified conditions unrelated to solution or precipitation effects.

Cast and wrought alloy nomenclatures have been developed. The Aluminum Association system of classification <sup>6</sup> is the most widely recognized in the United States. This alloy identification system employs different nomenclatures for wrought and cast alloys. For wrought alloys a four-digit system is used to produce a list of wrought composition families as follows:

1 xxx controlled unalloyed (pure) composition.

2 xxx alloys in which copper is the principal alloying element, though other elements, notably magnesium, may be specified.

3 xxx alloys in which manganese is the principal alloying element.

4 xxx alloys in which silicon is the principal alloying element.

5 xxx alloys in which magnesium is the principal alloying element.

6 xxx alloys in which magnesium and silicon are the principle alloying elements.

7 xxx alloys in which zinc is the principal alloying element, but other elements such as copper, magnesium, chromium, and zirconium may be specified.

8 xxx alloys including tin and some lithium, compositions characterizing miscellaneous compositions.

9 xxx reserved for future use.



Casting compositions are described by a three-digit system followed by a decimal value. The decimal “.0 ” in all cases pertains to casting alloy limits. Decimals “. 1 ” and “. 2 ” concern ingot compositions, which, after melting and processing, should result in chemistries conforming to casting specification requirements. Alloy families for casting compositions are:

1 xx.x controlled unalloyed (pure) compositions, especially for rotor manufacture.

2 xx.x Alloys in which copper is the principal alloying element, but other alloying elements may be specified.

3 xx.x Alloys in which silicon is the principal alloying element, but other alloying elements such as copper and magnesium are specified.

4 xx.x Alloys in which silicon is the principal alloying element.

5 xx.x Alloys in which magnesium is the principal alloying element.

6 xx.x Un-used.

7 xx.x Alloys in which zinc is the principal alloying element, but other alloying elements such as copper and magnesium may be specified.

8 xx.x Alloys in which tin is the principal alloying element.

9 xx.x Un-used.

### **2.3.1 ALUMINUM CASTING ALLOYS**

Aluminum casting alloys are the most versatile of all common foundry alloys and generally have the highest castability rating. As casting materials, aluminum alloys have the following characteristics:

- a) Good fluidity for filling thin sections;
- b) Low melting point relative to those required for many other metals;
- c) Rapid heat transfer from the molten aluminum to the mold, providing shorter casting cycles;
- d) Hydrogen is the only gas with appreciable solubility in aluminum and its alloys. By controlling the processing methods the hydrogen solubility can be readily controlled.
- e) Many aluminum alloys are relatively free from hot short cracking and tearing tendencies.
- f) Chemical stability.
- g) Good as-cast surface finish with a lustrous surface and few or no blemishes.

Aluminum alloy castings are routinely produced by pressure-die casting, permanent-mold casting, green sand casting, dry sand casting, investment casting, and plaster casting. All alloys are also readily cast with vacuum, low-pressure, centrifugal

and pattern-related processes such as lost foam casting. The total shipment of aluminum foundry products (all types of castings, exclusive of ingots) in the United States for 1988 was about  $10^6$  Mg, tons of which about 68% was accounted for by die-castings. <sup>6</sup> The most common aluminum silicon casting alloys are listed in Table 2.

**Table 2.** Compositions of some common aluminum-silicon casting alloys. <sup>7</sup>

Alloy	Casting Method	Element (wt %)					
		Si	Cu	Mg	Fe	Zn	Other
319.0	S,P	6.0	3.5	<0.10	<0.10	<0.10	
332.0	P	9.5	3.0	1.0	1.2	1.0	
355.0	S,P	5.0	1.25	0.5	<0.06	<0.35	
A356.0	S,P	7.0	<0.20	0.35	<0.2	<0.1	
A357.0	S,P	7.0	<0.20	0.55	<0.2	<0.1	0.05 Be
380.0	D	8.5	3.5	<0.1	<1.3	<3.0	
383.0	D	10.0	2.5	0.10	1.3	3.0	0.15 Sn
384.0	D	11.0	2.0	<0.3	<1.3	<3.0	0.35 Sn
390.0	D	17.0	4.5	0.55	<1.3	<0.1	<0.1 Mg
413.0	D	12.0	<0.1	<0.10	<2.0	-	
443.0	S,P	5.25	<0.3	<0.05	<0.8	<0.5	

S: Sand casting, P: Permanent mold casting, D: Die casting

## 2.4 INCLUSIONS IN ALUMINUM ALLOYS

According to Shivkumar et al., <sup>8</sup>, the term “inclusion” can be defined to mean “any exogenous solid or liquid phase particle present in an aluminum alloy above the liquidus temperature”. Thus titanium diboride ( $TiB_2$ ) is considered to be an inclusion, whereas titanium aluminide ( $TiAl_3$ ), which under conditions normally encountered in industry is

soluble, is not. Likewise, liquid salt droplets arising either from solid flux additions or chlorine fluxing are considered to be inclusions, whereas gas bubbles are not.

Inclusions in aluminum foundry alloys may be of two types in general: exogenous and indigenous.<sup>7</sup> Exogenous inclusions originate from outside the melt itself and include refractory particles such as alumina, silica, and silicon carbide, which result from the wear and erosion of crucible materials. Indigenous inclusions arise from either a chemical reaction within the melt itself, or else remain from some deliberate melt treatments such as fluxing or grain refinement. Figure 2 shows the number of inclusions per kg of metal required to produce the indicated volume fractions as a function of the inclusion particle diameter. As can be seen, enormous numbers are required to produce volume fractions approaching the part per million levels.

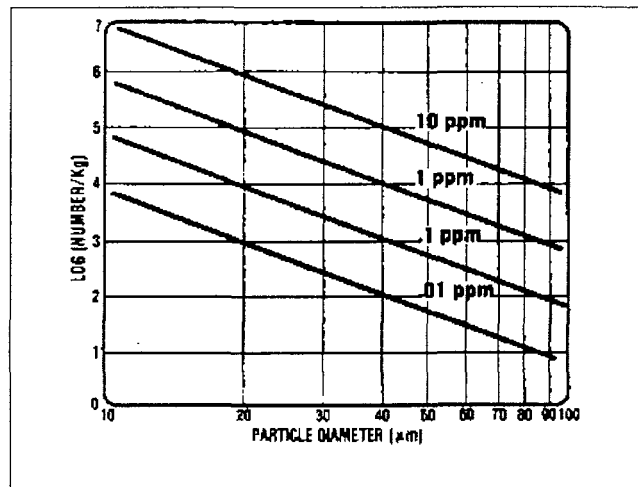


**Figure 2.** Inclusion concentration required to produce the indicated volume fraction as a function of particle diameter.<sup>9</sup>

The size at which an inclusion becomes potentially troublesome varies of course with the end-use application. In general, in critical applications, any inclusion larger than 10-20  $\mu\text{m}$  in diameter is considered to be deleterious, although even smaller inclusions can cause problems if present in sufficient quantity. It is important to understand that the analysis of inclusions is, in most cases, a trace analysis. Table 3 gives the classification of different inclusions observed in aluminum casting alloys.

**Table 3.** Classification of Inclusions in Aluminum Casting Alloys. <sup>10</sup>

<b>Inclusion</b>	<b>Description</b>	<b>Origin</b>
Carbides $Al_4C_3$	Tiny platelets or small chunks	Reduction of alumina – carbon contamination
Dispersed $Al_2O_3$	Very tiny yellowish needles or clusters	Base metal or scrap contamination
Borocarbides $Al_4B_4C$	Tiny needles	Chemical reaction from boron in primary aluminum
$TiB_2$	Cluster of tiny particles	Grain refiners – Act as nuclei in grain size refining
$MgO$	Dispersed cluster of $MgO$ particles	Chemical reaction between Mg and oxygen in furnace, ladle etc.
Cuboids	$MgO$ particles being transformed in hard crystals	Chemical reaction between $MgO$ and $Al_2O_3$ after significant time and high temperature
Spinel $MgAl_2O_4$	Hard films or chunks – Large inclusion	Chemical reaction between $MgO$ and $Al_2O_3$ after significant time and high temperature
Graphite	Small or medium size inclusion	Comes from degradation of graphite equipment (lance, impellers, etc.)
Refractory	Medium to large size inclusion Hard inclusion	Comes from degradation of furnace lining
Nitrides $AlN$	Relatively hard inclusion – Film distribution	Chemical reaction between Al and air after significant time and at high temperature
Chlorides $NaCl, MgCl_2$ , etc.	Small voids	Chemical reaction between alkaline and chlorine gas during fluxing operation or chemical flux addition
Oxide film Gamma $Al_2O_3$ $\gamma-Al_2O_3$	Elongated films	Oxidation of Al from surface turbulence, splashing, etc.
Oxide film Alpha $Al_2O_3$ $\alpha-Al_2O_3$	Thicker film distribution	Oxidation of Al from turbulence after significant time and at high temperature

According to Doutré et al.,<sup>9</sup> these observations indicate the extreme sensitivity required of any analytical technique whose purpose is to quantify metal cleanliness. There are essentially three major approaches used for measuring metal cleanliness:

- a) Chemical analysis
- b) Metallographic evaluation
- c) Techniques based upon physical principles

Wide varieties of inclusions are found in aluminum alloys. Some of them occur naturally in the system; for example, MgO, spinel and some that are intentionally added, such as those in the form of grain refiner additions, such as TiC and TiB<sub>2</sub>. For instance, in the case of grain refinement by the use of Al-Ti-B master alloys, the crystallites that are commonly believed to nucleate grains are TiB<sub>2</sub>. Many of these inclusions occur simultaneously in a melt, complicating the systematic study of their behavior.<sup>11</sup>

Longerweger<sup>12</sup> reported six basic types of non-metallic inclusions:

- 1) Oxide skin consisting of Al<sub>2</sub>O<sub>3</sub>, formed in the air during the natural oxidation of aluminum melts, and entrained within the melt as a result of turbulences (see figure 3).



**Figure 3.** Oxide skin inclusion (unetched).<sup>12</sup>

- 2) Oxide flake of MgO or magnesium spinel (Figure 4). Such inclusions are the result of unsuitable technique or the use of corroded magnesium pigs, and also possibly a consequence of the overheating of Mg-alloyed aluminum melts.

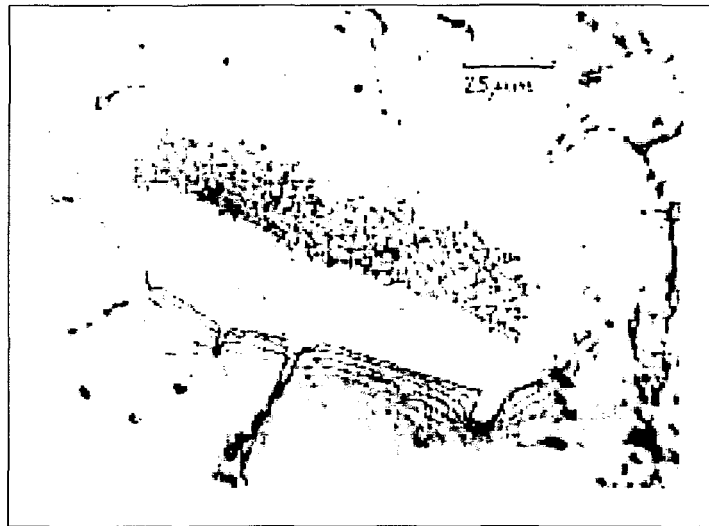


**Figure 4.** Flake inclusion consisting of MgO (unetched).<sup>12</sup>



- 3) Oxide particles, mainly  $\text{SiO}_2$  (Figure 5), that can come into the melt from outside (for example from contaminated scrap) or due to the use of poor quality silicon metal ( $\text{SiO}_2$ ).

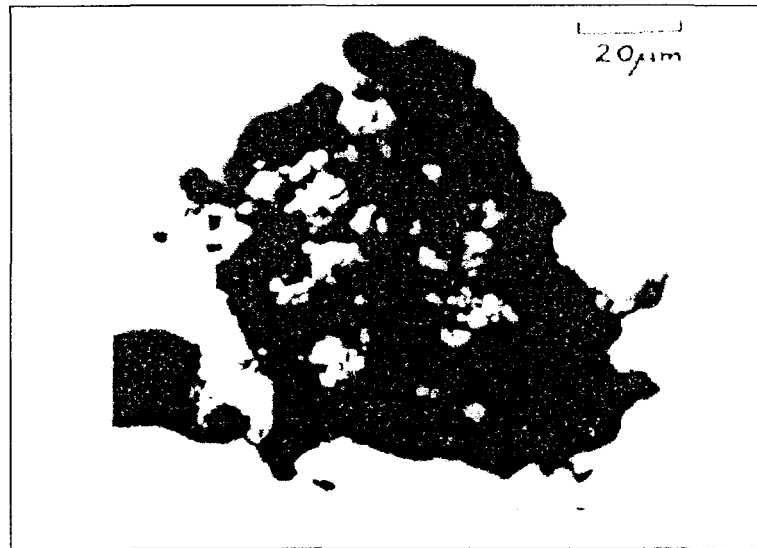


**Figure 5.** Silicon oxide ( $\text{SiO}_2$ ) inclusions in pure aluminum.<sup>12</sup>

- 4) Titanium boride clusters (Figure 6) that arise as a result of heavy grain refining, or too long holding times, or else as reaction products in the boron treatment of aluminum melts.  $\text{TiB}_2$  inclusions mostly occur together with other inclusions, such as the combination of  $\text{MgO}$  flakes and  $\text{TiB}_2$  particles shown in Figure.7.

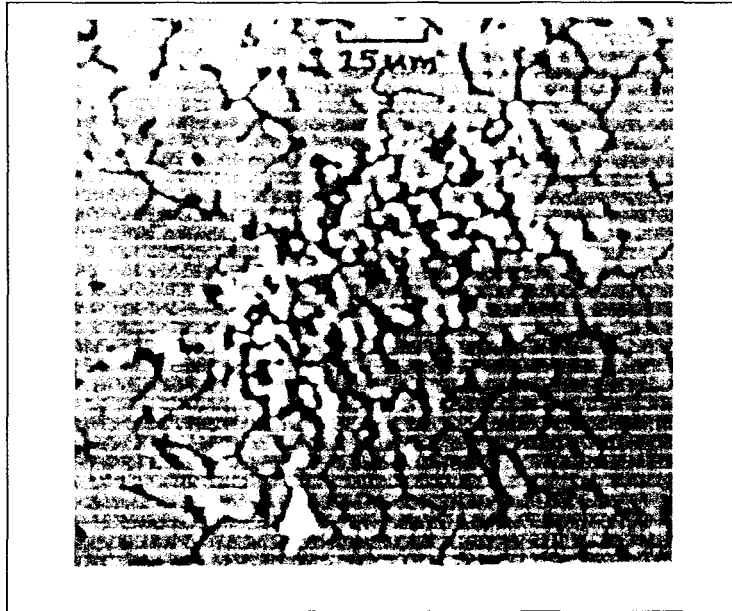


**Figure 6.**  $\text{TiB}_2$  inclusions in an Al 99.2 rolling slab.<sup>12</sup>

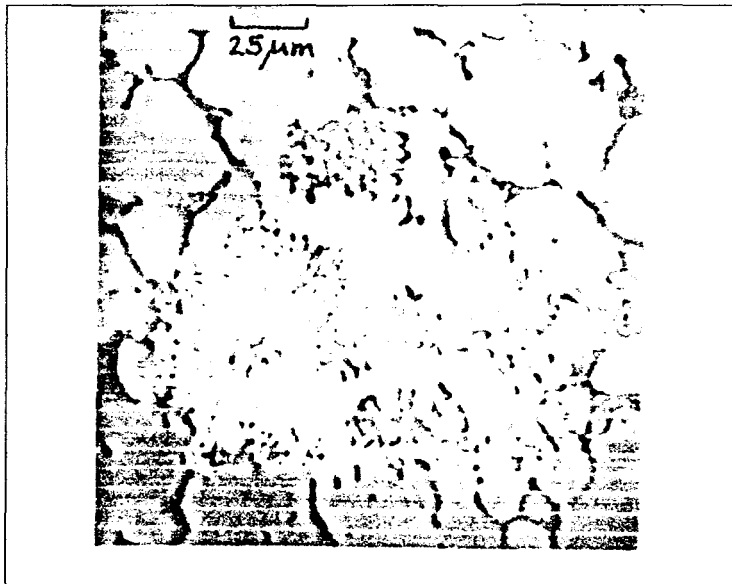


**Figure 7.** Combined  $\text{TiB}_2$ –MgO inclusion in an Al 99.0 rolling slab.<sup>12</sup>

- 5) Particles of salts (i.e., inclusions soluble in water, see Figure 8, for example). These mostly contain Al, Na, Ca, K, Cl, F, and S, and can have the following origins:

- i) Pot room metal (e.g., particles of pot flux)
- ii) Melt treatment salts
- iii) Products from the reaction of aluminum with active gases, e.g., chlorine.



**Figure 8.** Water-soluble inclusion in a sample from the metal pad of a melting furnace. <sup>12</sup>

- 6) Other non-metallic inclusions such as carbides.

## 2.5 HYDROGEN AND GAS POROSITY

The only gas with appreciable solubility in molten aluminum is hydrogen, as shown in Figure 9. Sources of hydrogen in molten aluminum include excessive molten metal

temperature, absorption from the atmosphere and from a fuel-fired furnace, combustion by-products, and scrap returns (gates, runners, trim) containing metalworking lubricants. The equation for hydrogen formation is given by:

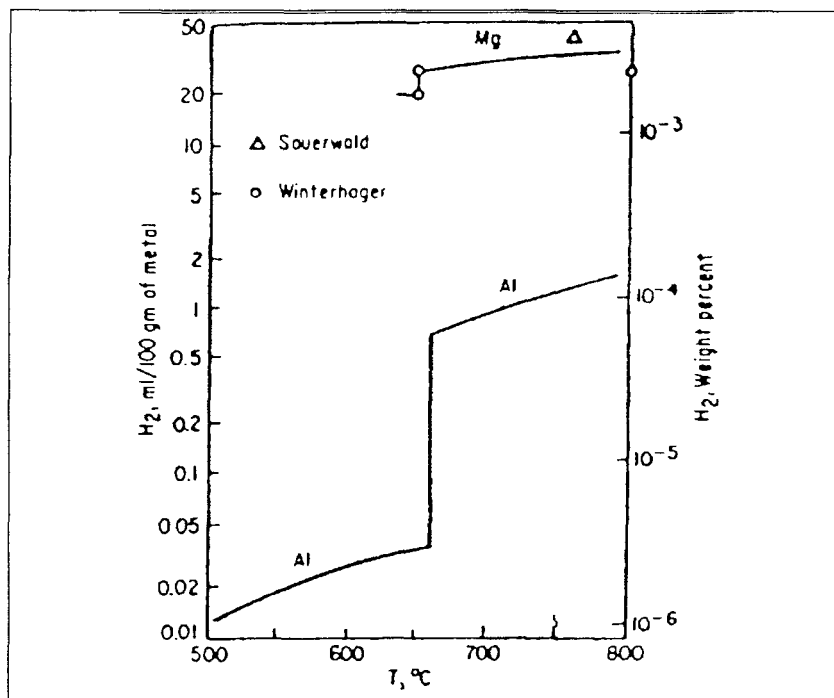
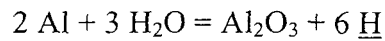


**Figure 9.** Solubility of hydrogen at atmospheric pressure in aluminum and magnesium. <sup>13</sup>

There is considerable reduction of hydrogen solubility in the solid state. As molten aluminum solidifies, this excess hydrogen is rejected from the liquid, and can manifest itself in the form of shrinkage, blowholes, porosity, or micro porosity. <sup>14</sup>

King and Reynolds <sup>15</sup> reported that one of the elements required for producing a good casting is metal cleanliness. For casting purposes, clean metal is defined as that which produces castings that contain a minimum level of porosity and inclusion defects. The level of melt cleanliness ultimately determines the scrap rate of the part being cast.

Altenpol <sup>5</sup> has reported that the most important source of hydrogen is the reaction between the liquid metal and water, which is usually present as moisture in the atmosphere. There may be several ways in which moisture may be introduced into aluminum <sup>16</sup> as described below:

- 1) By products of combustion – even with a well-defined flame, most fuels contain 10 – 20 percent water vapor as product of combustion. The direct impingement of flame on the metal surface or poor crucible wall condition would permit the introduction of hydrogen into the metal surface.
- 2) Charge materials – The surface of charged materials may contain moisture or be oxidized, which contributes to the generation of aluminum hydroxides when melted. In addition, charged ingot material may contain an initial amount of gas, which may become trapped within the melt.
- 3) Additives – Grain refining, salts, fluxes, and degassing pills are all potential sources of hydrogen due to their hygroscopic compositions. These materials

absorb moisture, which would be introduced below the metal surface, if not stored in a dry location.

- 4) Atmospheric moisture – High humidity climates present a significant source of hydrogen. The amount of hydrogen introduced into the metal is a function of metal temperature, metal surface exposure, and the amount of moisture in the air.

Kanicki and Rasmussen <sup>17</sup> have stated that the presence of hydrogen results from the propensity of molten aluminum to absorb the gas from the air around the furnace during melting, pouring, transfer and other processing operations.

Although aluminum and aluminum alloys are widely used because of their distinct properties, the presence of gas and inclusions can critically hinder their application. <sup>18</sup>

Shivkumar, Wang and Lavigne <sup>19</sup> reported that at small values of secondary dendrite arm spacing (DAS) and at relatively low hydrogen concentrations, a wide variety of pores could be detected in the microstructure. Several elongated pores were present at the cell boundaries. As the dendrite arm spacing or the hydrogen concentration increased, the pores became larger and more spherical. Typical microstructures in A356 plate castings produced under laboratory conditions are shown in Figure 10. The closer the specimen to the chill, the faster the cooling rate and the finer the DAS. As can be seen from Figure 11, the smallest pores are observed in Figure 10 (a), whereas the largest pores are observed in Figure 10(b), at higher hydrogen and DAS.

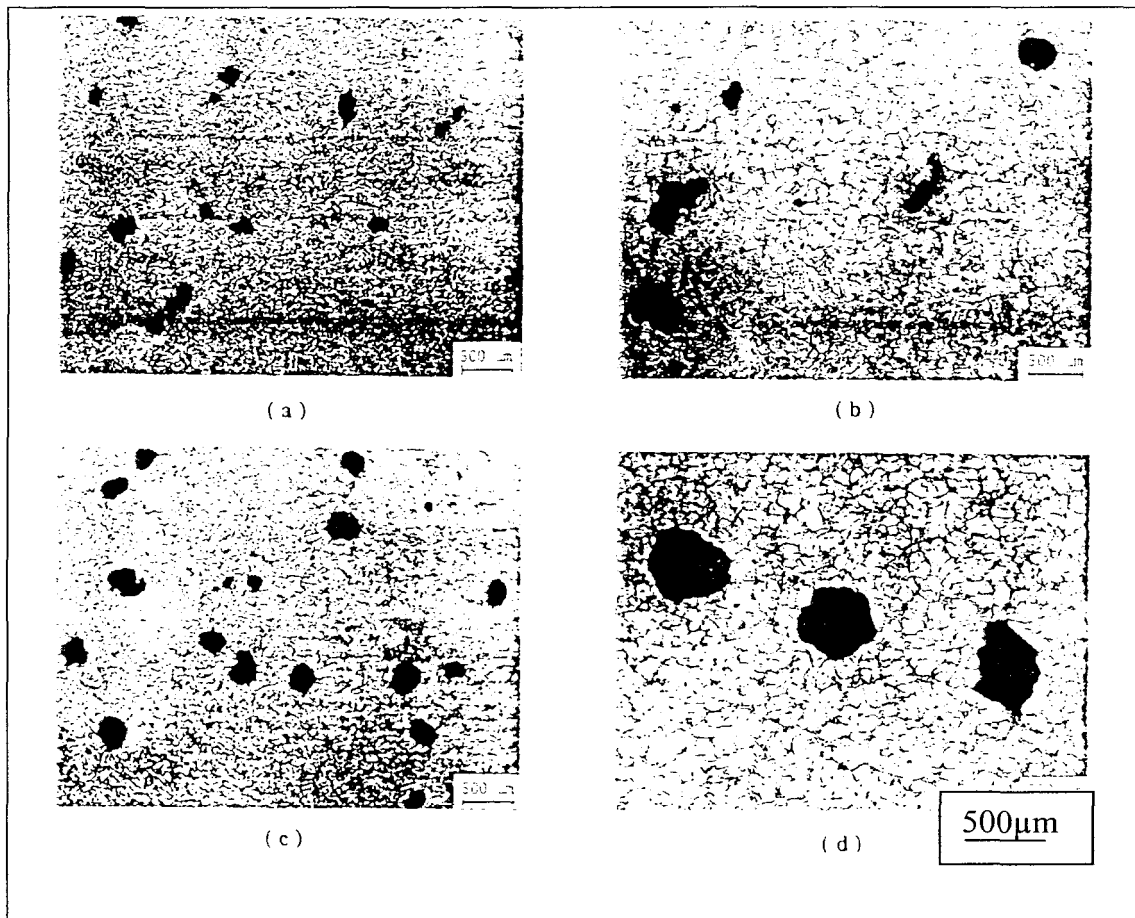


**Figure 10.** Typical microstructures in A356 plate castings under laboratory conditions. a) Distance from chill = 15 mm, hydrogen content = 0.19 cc/100g b) Distance from chill = 255 mm, hydrogen content = 0.19 cc/100g c) Distance from chill = 15 mm. Hydrogen content = 0.45 cc/100g d) Distance from chill = 255 mm, hydrogen content = 0.45 cc/100g.<sup>19</sup>

In general, two types of porosity may occur in cast aluminum: gas porosity, and shrinkage porosity. Gas porosity, which is generally fairly spherical in shape, results either from the precipitation of hydrogen during solidification (because the solubility of this gas is much higher in the molten metal than in the solid), or from the occlusion of gas bubbles during the high-velocity injection of molten metal in die casting operations. The

precipitation of molecular hydrogen during the cooling and solidification of molten aluminum results in the formation of primary and/or secondary voids. Interdendritic porosity is encountered when hydrogen contents are sufficiently high that hydrogen rejected at the solidification front results in solution pressures above atmospheric pressure.

Secondary (micron-size) porosity occurs when dissolved hydrogen contents are low and void formation is characteristically subcritical. Nevertheless, hydrogen porosity adversely affects mechanical properties in a manner that varies with the alloy. Figure 11 shows the relationship between actual hydrogen content and observed porosity, while Figure 12 shows the effects of porosity on the ultimate tensile strength (UTS) of selected aluminum alloys.

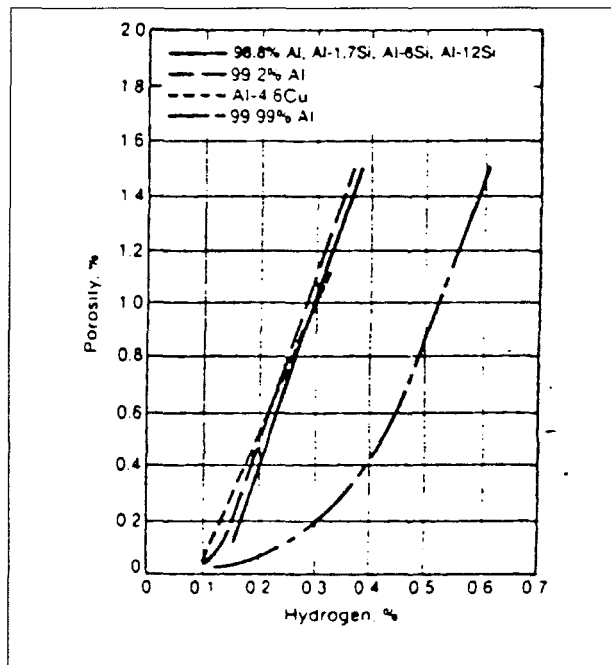


**Figure 11.** Porosity as a function of hydrogen content in sand-cast aluminum and aluminum alloy bars.<sup>6</sup>



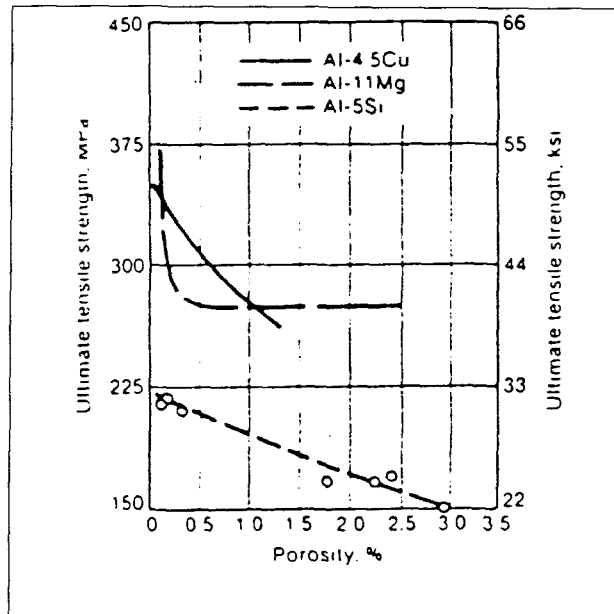


**Figure 12.** Ultimate tensile strength versus hydrogen porosity for sand-cast bars of three aluminum alloys.<sup>6</sup>

According to Meredith<sup>20</sup>, the most commonly used method for removal of dissolved hydrogen from molten aluminum is the injection of dry nitrogen gas into the melt via a lance. This is one of the simplest and cheapest means of reducing the hydrogen gas level in molten aluminum. However, the efficiency of this operation is relatively low due to the large bubbles produced from a lance.

Pallet<sup>21</sup> reports that the two main types of defects are those due to inclusions and dissolved gas. Inclusions can be removed by a fluxing treatment of the bulk liquid metal and a final filtration of the metal before it is poured in the mold. The only gas with significant solubility in aluminum and its alloys is hydrogen, and if not reduced to a low level prior to casting, will lead to gas porosity in the solidified casting.

## 2.6 SHRINKAGE

The other source of porosity is the liquid-to-solid shrinkage that frequently takes the form of interdendritically distributed voids may be enlarged by hydrogen and the size of such porosity also increases as the solidification rate decreases, since larger dendrites result from slower solidification. It is not possible to establish an inherent rating with respect to anticipated porosity because castings made by any process can vary substantially in soundness – from nearly completely sound to very unsound – depending on the casting size and design, as well as on the foundry techniques. <sup>6</sup>

Flemings <sup>22</sup> reported that most metals and alloys contract on solidification. The volume change that results from the liquid-solid contraction, is in the range of about 3 to 6 percent for metals, and much higher for refractory oxides. With the use of properly designed risers, it is possible to achieve sound castings, in spite of this shrinkage.

## 2.7 OXIDATION PROCESS

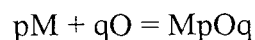
When a bath of molten metal is held in a furnace over long periods of time, the surface of the metal exposed to the air or the furnace atmosphere will undergo oxidation. The phenomenon of oxidation is important as:

- a) The preferential oxidation of one of the alloying elements in the aluminum alloys causes loss of that element during melt-down.

- b) The oxide formed, whether of a solid crusty material or a liquid film floating on the surface, will invariably become entrained in the molten metal during transfer from the breakdown furnace to the holding furnace, and become trapped as inclusions in the finished casting.

In order to understand the oxidation phenomenon occurring in the melting furnace, we first must identify the metallic element that is oxidized, and then determine the nature of the oxide product that is being formed. Generally, the oxide forming on the surface layer of a molten alloy will be the oxide of the alloying element that has the greater affinity for oxygen. This element can be determined by comparing the standard free energies of the formation of different oxides. The one with the highest will preferentially oxidize on the surface of the melt.

In their classical investigations on the oxidation of metals at high temperature, Pilling and Bedworth (PB) showed that the reaction with oxygen proceeds at a diminishing rate, if the volume of the oxide layer formed exceeds the volume of metal from which it is produced. If a metal oxidizes according to the equation



Then the ratio given below (called the Pilling-Bedworth ratio) should be greater than one.

$$P.B. = \frac{\frac{\text{MolecularWeightMpOq}}{\text{DensityMpOq}}}{\frac{P \times \text{AtomicWeightM}}{\text{DensityM}}}$$

Table 4 gives the Pilling-Bedworth ratios for some common alloying elements in aluminum alloys.

**Table 4.** Pilling Bedworth ratios for some common metals. <sup>23</sup>

Metal	Density Of Metal (gm/cm <sup>3</sup> )	Density Of Oxides (gm/cm <sup>3</sup> )	Pilling-Bedworth (Ratio)
Cu	8.92	6.40	1.74
Fe	7.86	5.10	2.18
Ni	8.90	7.45	1.50
Mg	1.74	3.69	0.78
Al	2.70	4.00	1.27
Zn	7.14	5.47	1.64
Pb	11.34	9.53	1.27
Sn	7.31	7.00	1.33
Ca	1.55	3.32	0.65
Na	0.97	2.27	0.58
Be	1.85	3.05	1.68

If the oxide layer on the surface of a molten bath is composed of the oxide of a metal with a Pilling-Bedworth ratio greater than unity, then a dense, continuous oxide film is formed on the surface of the melt, which inhibits the rate of oxidation because the oxygen must diffuse through the oxide layer to the molten metal, or the metallic element must diffuse through the oxide layer to the atmosphere in order for the reaction to occur. Thus, the oxidation of the bath will occur rapidly at first, and then at a slowly diminishing rate, until it appears to stop completely. If, on the other hand, the oxide layer is formed from a metal with a Pilling-Bedworth ratio of less than 1, then a crusty, solid, porous layer will be formed on the melt surface. The oxidation of this melt will occur rapidly consuming the metallic species and forming copious amounts of dry, lumpy dross. <sup>23</sup>

## 2.8 TYPES AND SOURCES OF INCLUSIONS

Natural impurities in aluminum alloys include both metallic and non-metallic constituents. Iron and silicon in the primary metal are important cases of metallic impurities. The main non-metallic impurities are hydrogen, oxides ( $\text{Al}_2\text{O}_3$ ,  $\text{MgO}$ ,  $\text{Al}_2\text{MgO}_4$ ,  $\text{SiO}_2$ ,  $\text{Fe}_3\text{O}_4$ ,  $\text{FeO}$ ), and carbides (mainly  $\text{Al}_4\text{C}_3$ ), nitrides (mainly  $\text{AlN}$ ) and borides ( $\text{TiB}_2$  and  $\text{VB}_2$ ). Oxides commonly appear in the form of films, cluster or lumps (especially in the case of  $\text{SiO}_2$ ), carbides in the form of rectangular and hexagonal discs, borides in the form of clusters, and  $\text{AlN}$  in the form of films.

There are many sources of inclusions that exist in a commercial foundry operation.<sup>24</sup> These include the incoming ingot or scrap, the gates and risers with associated cutting lubricants or molding materials, furnace refractory particles, flux inclusions, etc. The lists of compounds found in commercial melt inclusions include oxides, carbides, nitrides, borides, phosphides and sulfides, as well as complexes formed from high melting constituents and sludge or intermetallic inclusions.

Simensen<sup>25</sup> has explained that the common types of inclusions are oxides, carbides, nitrides, chlorides and Mg-rich particles.

### 2.8.1 OXIDES

All aluminum solids have an oxide coating or oxide skin on the surface. When these are melted, the oxides ( $\text{Al}_2\text{O}_3$ ) remain in the melt. Magnesium oxide ( $\text{MgO}$ ) and

magnesium aluminates or spinel ( $\text{Al}_2\text{O}_4\text{Mg}$ ) are the other most common oxides that are present in aluminum alloys. Oxygen in aluminum is commonly found as oxides films and in the form of clusters of oxide particles. The concentration of oxides in commercial aluminum lies in the range of 0.1 to 100 ppm.<sup>26</sup> The kind and amount of oxides formed in the melt are determined by the following parameters:

- i) Type of furnace;
- ii) Type of charge (fresh or scrap);
- iii) Alloying elements present;
- iv) Temperature of the melt;
- v) Stirring of the melt or turbulent purging, during which the surface oxide skin covering the molten metal can get carried into the liquid metal.

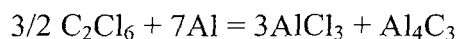
### **2.8.2 CARBIDES**

There are three sources of carbide introduction into the molten metal.<sup>27</sup>

- i) Reaction between the air and melt,
- ii) Brick refractory lining of furnace,
- iii) Charge and tools.

The common carbide in aluminum is aluminum carbide,  $\text{Al}_4\text{C}_3$ . The carbide particles are hexagonal or rectangular gray discs and are normally found as clusters, isolated or together with oxides and boride particles. The size of these carbide particles lies between 0.1 and 10  $\mu\text{m}$ .<sup>28</sup>

Eckret<sup>29</sup> reported that carbide formation could produce different type of inclusions. Aluminum carbide ( $\text{Al}_4\text{C}_3$ ) may be formed during the aluminum smelting process and frequently results from poor quality secondary ingot or pig. These carbides are generally innocuous due to their small size (1 – 10 microns). Carbides can also be formed from the use of certain solid degassing tablets that contain hexachloroethane ( $\text{C}_2\text{Cl}_6$ ) through the reaction



$\text{Al}_4\text{C}_3$  particles can be as large as 50 microns, and most of them float to the surface along with the  $\text{AlCl}_3$  vapor formed in the reaction.

### **2.8.3 BORIDES**

Ordinary aluminum contains less than 1-ppm borides, whereas grain-refined material can contain 10-100 ppm borides. The common borides are  $\text{TiB}_2$  and  $\text{VB}_2$ , but  $\text{ZrB}_2$  and  $\text{CrB}_2$  have also been detected in aluminum melts. Boride particles are hexagonal or rectangular discs, 0.1-10  $\mu\text{m}$  in diameter. These inclusions are normally found in clusters 1-50  $\mu\text{m}$  in cross-section, situated either at grain boundaries or near the center of the grain.<sup>28</sup>

According to Simmons<sup>30</sup> these inclusions very often originate from grain refiner additions to the alloy melt and can include  $TiB_2$  and  $VB_2$  particles of 0.1 to 10  $\mu m$  in diameter, which can agglomerate into cluster up to 80  $\mu m$  across.

#### **2.8.4 NITRIDES**

Simenson and Berg<sup>28</sup> have reported that the chemical analysis of commercial materials shows that aluminum contains 1 to 4 ppm nitrogen and magnesium alloys, 2 to 5 ppm nitrogen.

Apelian and Shivkumar<sup>31</sup> found commercial aluminum alloys contain 1 to 5 ppm of nitrogen or 3 to 12 ppm of nitrides. The nitrides have been identified by X-ray diffraction to be  $AlN$ , and possibly oxy-nitrides. These nitrides are commonly found in association with oxides, and are formed by the reaction between the melt and the atmosphere.

## **2.9 CLASSIFICATION OF INCLUSIONS**

The principal mechanism operating during the filtration of fluid containing solid inclusions through a fine filter is cake filtration. The build up of a cake and its subsequent permeability is a dynamic process that is critically dependent on the type, size, shape and mixture of inclusions present in relation to the filter itself. In the case of liquid metals, temperature, viscosity and the surface tension of the fluid also influence the characteristic



behavior of the system. Based upon Alcan's classification system, inclusions are divided into two major groups:

- i) Total inclusions that take into account all types of inclusions existing in the cake above the filter.
- ii) Harmful inclusions which are the sum of  $\text{Al}_4\text{C}_3$  inclusions  $>3 \mu\text{m}$ , dispersed  $\text{Al}_2\text{O}_3$ ,  $\text{MgO}$ ,  $\text{MgAl}_2\text{O}_4$  and potential chlorides. The  $\text{Al}_4\text{C}_3$  inclusions  $<3 \mu\text{m}$  and  $\text{TiB}_2$  inclusions are not considered harmful.

Inclusions in daily foundry melting operations may include dross, salts, furnace oxides, unmelted elements, corundum or sludge. The oxidation of alloying elements such as Si, Fe, Cu, Zn, Mn, Cr, and Mg lead to the formation of oxide inclusions. Non-metallic inclusions may be generated from furnace lining and refractories. These inclusions include oxides, spinels, carbides and nitrides.

In most cast components, inclusions with particle sizes greater than  $10 - 20 \mu\text{m}$  can have a drastic effect on the quality of the casting. Even if the volume fraction of inclusions is small, an enormous number of inclusions may be present in the melt. If the average inclusion size is about  $40 \mu\text{m}$ , then at an inclusions concentration of 1 ppm, 1 lb of metal will contain about 5000 particles. Thus, from a statistical point of view the number of inclusions in the melt is significant.<sup>32</sup>

Typical inclusions that may be present in die cast aluminum melts are shown in Table 5. In general, most of these inclusions exhibit a complex structure, and are very hard and brittle. Inclusions in die-cast alloys may originate from several sources.

**Table 5.** Typical inclusions in die cast aluminum alloys <sup>8</sup>

Type	Formula	Morphology	Density (g/cm <sup>3</sup> )	Range(μm)
Oxides	Al <sub>2</sub> O <sub>3</sub>	Particles;Skins	3.97	0.2–30 to 10-5000
	MgO	Particles;Skins	3.58	0.1-5 to 10-5000
	MgAl <sub>2</sub> O <sub>4</sub>	Particles;Skins	3.6	0.1-5 to 10-5000
	SiO <sub>2</sub>	Particles	2.66	0.5 to 5
Salts	Chlorides Fluorides	Particles	1.98- 2.16	0.1 to 5
Carbides	Al <sub>4</sub> C <sub>3</sub>	Particles	2.36	0.5 to 25
	SiC		3.22	
Nitrides	AlN	Particles-Skins	3.26	10 to 50
Borides	TiB <sub>2</sub>	Particle-Cluster;	4.5	1 to 30
	AlB <sub>2</sub>	Particles	3.19	
Sludge	Al (FeMnCr) Si	Particles	>4.0	-

According to Neff, <sup>33</sup> typical aluminum die casting alloy compositions contain aluminum, silicon, copper, zinc and magnesium. Small amounts of other metals such as chromium and manganese may also be present. In general, all of these elements can oxidize to form oxide inclusions. Other non-metallic inclusions can originate from fluxing salts, furnace lining, refractories and other vessels used in contact with the molten metal. These include oxides, spinel, carbides and nitrides. Metal working lubricants, and other extraneous debris coming from remelt operations can also act as sources of inclusions.

Sludging occurs predominantly in die casting alloys, which contain appreciable amounts of iron, chromium, and manganese when these alloys are held at low temperatures. This sludge is very hard. The hardness of some sludge particles has been measured to be about 9.5 on the Moh's scale compared to 10 for diamond. The tendency for sludge formation is temperature dependent and may be estimated in terms of a sludge factor (SF), given by the formula:

$$SF = Fe \% + 2 \% Mn + 3 \% Cr$$

It is suggested that the sludge factor should be maintained below  $\sim 1.9$  in order to minimize the tendency for sludge formation. Sludge is a very dense, intermetallic compound that precipitates from a molten bath of aluminum alloy and collects in the furnace as mushy material. It is often termed "sand", "sugar" or "silicon drop-out" by die casters. The formation of this sludge is detrimental to the die-casting operation for three reasons:

- a) The formation of this precipitate causes loss of iron, magnesium and chromium from the die-casting alloys.
- b) The particles of the sludge phase are extremely hard and brittle. If these particles get carried along in the molten aluminum as it is ladled into the die-casting machine, they become trapped in the die-casting. During machining operations, these hard, particles can cause excessive tool wear and breakage of drills.

- c) The accumulation of sludge at the bottom of the melting furnace drastically reduces the capacity of the furnace.

According to Simensen and Berg,<sup>28</sup> the common types of inclusions in aluminum can be classified as oxides, nitrides, carbides, fluorides, and borides. In addition, chlorides and  $\text{CaSO}_4$  or  $\text{CaS}$  have also been observed. Intermetallic particles that nucleate in the melt are another type of inclusion, such as  $\text{Al}_3\text{Zr}$  in Al - Zr alloys. The common oxide in aluminum is  $\text{Al}_2\text{O}_3$ . Commercial aluminum contains 3 to 8 ppm oxygen or the equivalent of 6 to 16 ppm oxide according to neutron activation analysis. X-ray diffraction analysis of isolated oxide particles on filters has shown that these oxides are  $\alpha\text{-Al}_2\text{O}_3$  and  $\gamma\text{-Al}_2\text{O}_3$ . The dominant oxides in Al-Mg alloys are  $\text{Al}_2\text{MgO}_4$  (or spinel) and  $\text{MgO}$ , which form in air at low temperatures.

## 2.10 HARMFUL EFFECTS OF INCLUSIONS

### ***2.10.1 REDUCTION IN MECHANICAL PROPERTIES***

As can be expected, defects such as gas porosity, hard spots, and inclusions will have a detrimental influence on the mechanical properties for most foundry casting

processes. As mentioned previously, with an increase in gas porosity, tensile strength and elongation are reduced. Figure 13 shows how hydrogen content and porosity affects the strength of 356 aluminum casting alloy. <sup>14</sup>

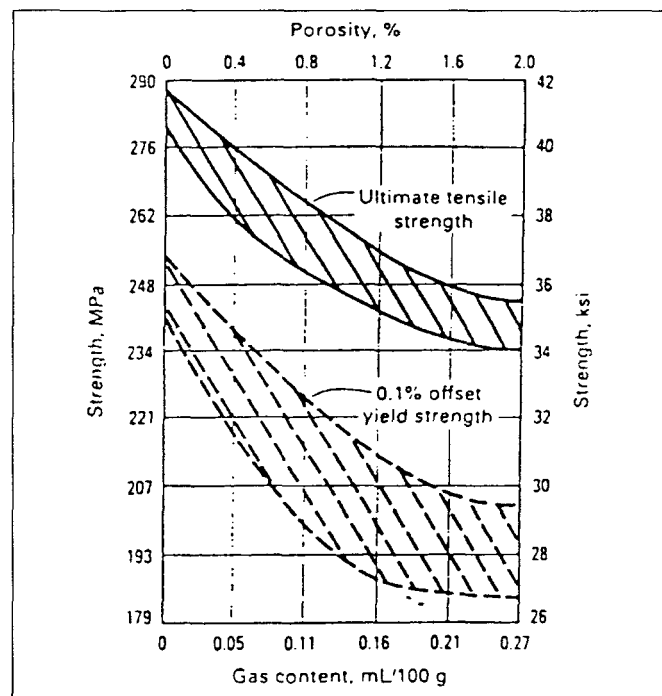


**Figure 13.** Mechanical properties of 356 alloys as a function of hydrogen content <sup>14</sup>

Aluminum or aluminum alloys can form a range of oxides whose hardness may vary depending on the composition, and cause a decrease in mechanical properties.

Kato, Ueda and Kobayashi <sup>34</sup> investigated the relationship between toughness and the inclusions originating from the impurities in Al-Zn-Mg-Cu alloys. They observed that

filtration reduced the coarse inclusions resulting from iron impurities, but did not influence the toughness much.

Extensive tests carried out at CTIF, France, have shown that the larger the size of inclusions, the greater is the reduction in strength properties.

Schmahl and Davidson's investigation of filtration found that ceramic foam filters offer several key benefits that improve the quality of premium aluminum castings.<sup>35</sup> These include: i) improved mechanical properties ii) reduced dye-penetrant indications iii) reduced x-ray evidence of non-metallic inclusions iv) reduced rework/scrap and v) improved machining properties.

Kanicki and Rasmussen<sup>17</sup> have reported that foundries of all types are increasingly finding out that the cleanliness of their molten metal is important in producing castings with predictable mechanical properties.

### ***2.10.2 POOR SURFACE QUALITY***

Inclusions have an adverse effect on surface appearance, and a severe effect on mechanical properties and on machining. Oxide films give a poor surface appearance to the casting, particularly for aluminum bronze alloys. Melting under flux cover and fluxing - off the oxide films are universal practices.<sup>36</sup>

Devaux et al.<sup>37</sup> reported that the most important factors for rejected castings are surface defects, leakage and hard spots.

### ***2.10.3 REDUCTION IN FLUIDITY PROPERTIES***

Fluidity depends on two major factors:

- a) The intrinsic fluid properties of the molten metal
- b) The casting conditions

The properties usually thought to influence fluidity are viscosity, surface tension, the character of the surface oxide film, the inclusion content and the manner in which the particular alloy solidifies. Casting conditions that influence fluidity include part configuration (*viz.*, physical measures of the fluid dynamics of the system, such as liquid static pressure drops, casting head, and velocities), mold material, mold surface characteristics, heat flux, rate of pouring and the degree of superheat.

Measured viscosities of molten aluminum are quite low and fall within a relatively narrow range. The kinematics viscosity is less than that of water. Thus viscosity is not strongly influential in determining casting behavior.

A high surface tension has the effect of increasing the pressure required for liquid metal flow. A number of elements influence surface tension, primarily through their effect on the surface tension of the oxide. Figure 14 illustrates the effect of selected elements on the surface tension of aluminum.

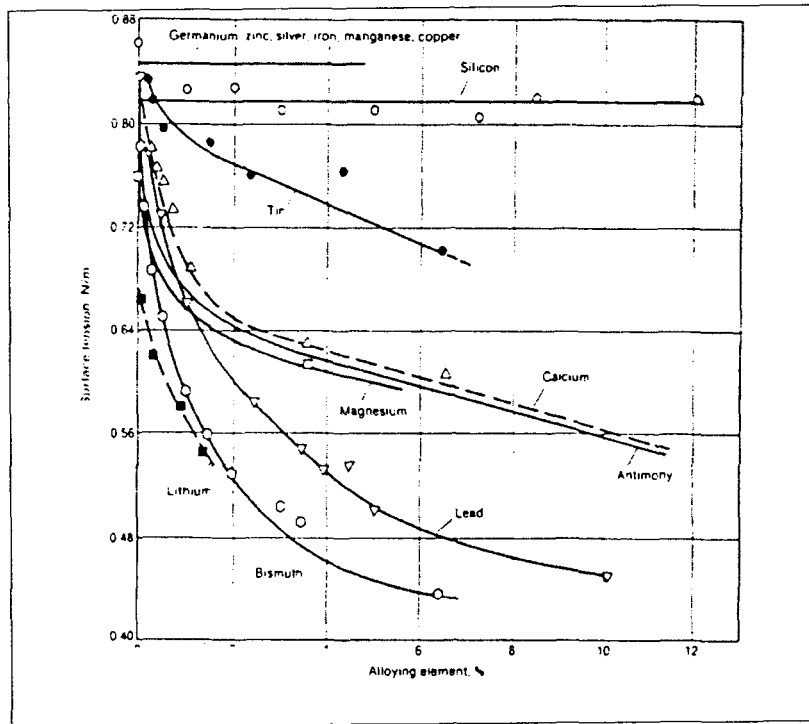


**Figure 14.** Effect of various elements on surface tension of 99.99% Al in argon at 700–740°C (1290 to 1365°F).<sup>6</sup>

In aluminum alloys, the true effect of surface tension is overpowered by the influence of surface oxide film characteristics. The oxide film on pure aluminum, for example, triples the apparent surface tension<sup>6</sup>. Inclusions in the form of suspended insoluble nonmetallic particles dramatically reduce the fluidity of molten aluminum.



#### ***2.10.4 REDUCTION IN MACHINABILITY AND HIGH TOOL WEAR***

Hard spot inclusions in aluminum alloy castings increase tool wear during machining. In aluminum, the hard spot inclusions are mainly MgO and boride particles. A fifty percent decrease in tool wear has been demonstrated in die castings obtained from metal filtered in a packed bed filter, as compared to castings poured from unfiltered metal. The poor machinability of aluminum die-castings is usually the result of intermetallics, *viz.*, sludge inclusions.<sup>36</sup>

#### **2.11 EFFECT OF GRAIN REFINEMENT**

Grain refinement is the control of the grain size of the primary phase crystallizing during solidification, through the control of the nucleation and growth of the phase<sup>23</sup>. A small amount of grain refiners are often added to control the grain structure. The grain size depends on the number of nuclei present in the liquid. The grain refinement provides nucleating sites for the formation of primary  $\alpha$ -Al dendrites. However, small amounts of fine porosity are also associated with grain refinement.

TiB<sub>2</sub> particles are found to be the most effective grain refining nuclei. The amount of TiB<sub>2</sub> used is usually calculated on the basis of a 0.02 wt % Ti addition. The most widely used grain refiners are master alloys of titanium (Ti), or titanium and boron (B). In aluminum alloys, grain refiners generally contain from 3-10 % Ti and 0.2-1 % B<sup>27</sup>. The

concentration of Ti and B in master alloys is typically 5 and 1 wt%, respectively (Al-5Ti-1B).

A finer grain size affords a more uniform distribution of the low melting point intermetallic compounds and of the shrinkage porosity that results in the casting. This uniform dispersion of fine porosity and fine intermetallic particles provides a greatly improved machinability to the alloy. The beneficial effects of fine grain size on the mechanical properties, shrinkage, and hot-tearing characteristics of aluminum alloys have become more widely appreciated in recent years.<sup>38</sup>

Easton and St John<sup>39</sup> reported that industrial trials show that the severity of the defects is accentuated by the addition of a grain refiner beyond an optimum level. Subsequent laboratory casting also found that the addition of the grain refiner beyond this optimum level increased the size of the defect at hot spots in the casting.

## 2.12 EFFECT OF MODIFICATION

In Al-Si alloys, the mechanical properties are affected by the morphology of the eutectic silicon. In the as-cast condition, the silicon precipitates in the form of coarse acicular plates, which provide easy paths for fracture. Addition of sodium or strontium can change the shape of the silicon to a fibrous form that results in higher tensile properties and an appreciably improved ductility.<sup>27</sup> This process is known as modification. Figure 15 illustrates the desirable effects on mechanical properties that can be achieved by modification.

In addition to chemical modification (accomplished by the introduction of Na, Sr or Sb into the molten metal), modification can also be achieved by the application, during solidification, of a very steep thermal gradient at the liquid-solid interface. The modification process exhibits the same contact time phenomenon and fading time phenomenon as the grain refining process. The contact time will vary depending on whether the modifier is introduced as a pure element, a salt or a master alloy.<sup>23</sup>

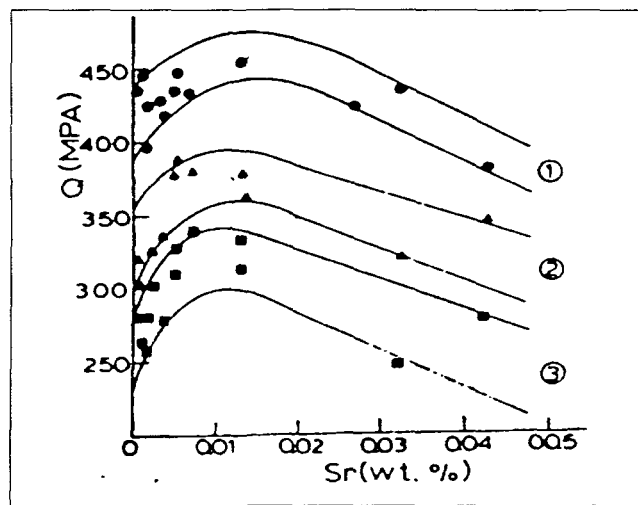


**Figure 15.** Variation in quality index (Q) with Sr content for three different cooling rates. Melts degassed with  $N_2-CCl_2F_2$ : band 1: cooling rate 1.5° C/s; band 2: cooling rate 0.5° C/s; band 3: cooling rate 0.08° C/s.<sup>13</sup>

A common method used to reduce the amount of oxidation of a metal is through the addition of an element that has a higher affinity for oxygen than the oxidizing species. In

the case of aluminum alloys, strontium is a suitable candidate for such purposes, since it is already used commonly in the melt treatment of Al-Si-Mg foundry alloys.<sup>40</sup>

## 2.13 CHEMICAL COMPOSITION AND HEAT TREATMENT

Mechanical properties of a casting depend not only on the choice of alloy but also depend somewhat on other considerations linked with the alloy. Variations in chemical composition, even within specified limits, can have a measurable effect. Metallurgical considerations such as coring, phase segregation, and modification can also alter properties. Modification is commonly used for those aluminum alloys containing 5% or more silicon. In hypoeutectic aluminum-silicon (Al-Si) alloys (Si less than 11.7%), the coarse silicon eutectic is refined and dispersed by modification. The modified structure increases both ductility and mechanical strength. Modification is accomplished by the addition of small amounts (0.02 %) of sodium or strontium. Making these additions often introduces gas into the melt. In the hypereutectic Al-Si alloys (Si greater than 11.7 %), refinement of primary silicon in sand and permanent mold castings is accomplished by adding 0.05% P (phosphorus modification is required only in those die castings that have thick walls). In these alloys, the phosphorous addition provides moderate improvements in strength and machinability. Where heat treatment is required, the choice of temper affects the properties. Heat-treating variables such as solution time and temperature of the quenching medium, and quench delay can also alter properties.<sup>7</sup>

## **CHAPTER 3**

# **INCLUSION REMOVAL TECHNIQUES**

## **CHAPTER 3**

### **INCLUSION REMOVAL TECHNIQUES**

#### **3.1. INTRODUCTION**

A variety of techniques have been used to produce clean metal. These include sedimentation processes, flotation, fluxing and degassing. Sedimentation processes are effective for particles whose density is significantly greater than that of aluminum. Furthermore, only particles greater than about 30  $\mu\text{m}$  settle to the bottom within reasonable times (about 2 hrs). Flotation techniques can be used to remove small particles ( $<10 \mu\text{m}$ ) suspended in molten aluminum.<sup>8</sup>

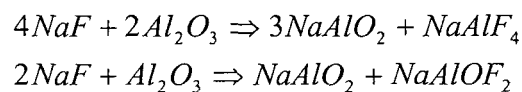
##### **3.1.1 FLUXING**

Guidelines for choosing the type of flux for a particular application will be explained along with some details on how to optimize cast-effectiveness. Alumina ( $\text{Al}_2\text{O}_3$ ) is a very stable compound, which cannot to be reduced to aluminum under ordinary melt conditions. For cleaning the melt from  $\text{Al}_2\text{O}_3$ , it is necessary to use a salt mixture of fluxes, which will react with impurities either mechanically or chemically, or both, and bring them into the dross. These fluxes are divided in two major groups:

which will react with impurities either mechanically or chemically, or both, and bring them into the dross. These fluxes are divided in two major groups:

- a) **PASSIVE FLUXES:** which will protect only the surface of the molten aluminum from oxidation and more or less prevent the pick-up of hydrogen by the melt.
- b) **ACTIVE FLUXES:** which will react chemically with aluminum oxide and effectively clean the melt.

Most fluxes have a lower density than the aluminum alloys to allow them to float on top of the melt. For maximum effect, these fluxes should be brought into direct contact with as much of the metal as possible. This is done by stirring the melt either by hand with suitable tools, vigorous rabbling or by mechanical means whereby the metal is moving continuously, as is the case in rotary furnaces. For the removal of  $Al_2O_3$  the presence of halides, particularly fluorides, is very useful. The solubility of  $Al_2O_3$  increases with sodium fluoride,



At ( $\sim 600^\circ$  C) aluminum is only slightly soluble in cryolite and therefore fluxes will chemically dissolve only a little alumina. Most  $Al_2O_3$  will be removed by the flux mechanically enveloping the particles and transporting them into dross. <sup>41</sup>

### 3.1.1.1 COVERING FLUXES

These types usually form a layer of molten slag on the surface of the molten aluminum metal to protect it against oxidation and reaction with the humid atmosphere. The basis of these fluxes is a mixture of alkali-chlorides with or without the addition of fluorides. The eutectic of NaCl – KCl melts at 660° C as shown in Figure 16.

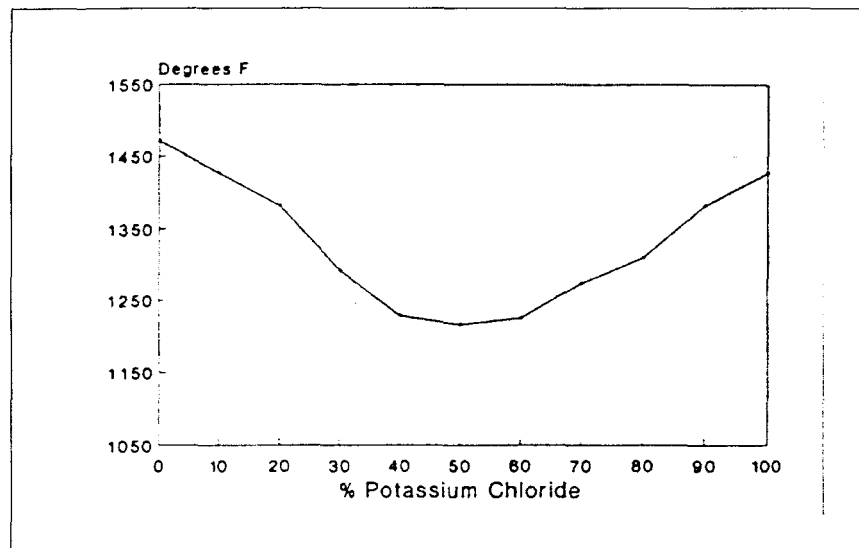


**Figure 16.** Phase diagram of sodium chloride/ potassium chloride mixture. <sup>41</sup>

The ternary diagram for NaCl, KCl and NaF is shown in Figure 17. These three compounds form the basis of most covering fluxes. For effective protection from oxidation and for a thorough cleaning effect, the best results are obtained if the flux is molten. <sup>41</sup>



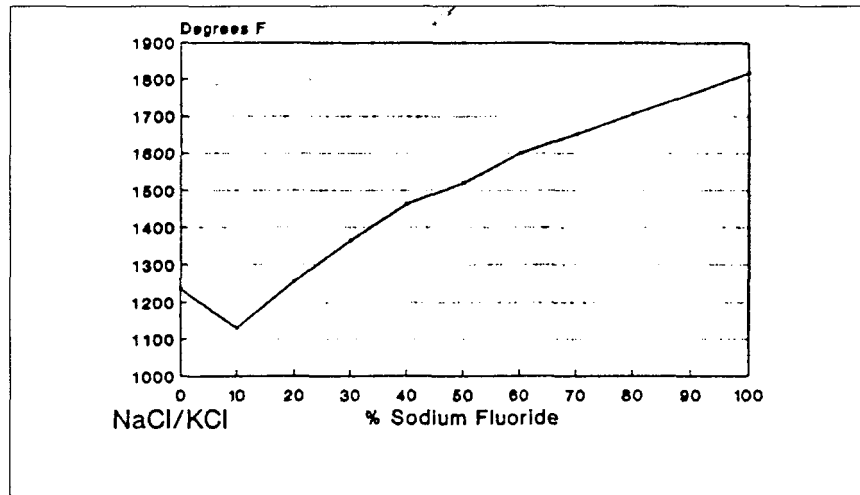


**Figure 17.** Phase diagram of sodium chloride/ potassium chloride/ sodium fluoride mixture.<sup>41</sup>

### 3.1.2 FLOTATION

Among the various melt treatment techniques, flotation, or fluxing, is most widely used in the foundry. In this melt treatment process, a reactive or inert gas, or combination of both types of gases, is purged through a rotating impeller, or non-holding lance into the liquid metal. The most commonly used reactive gases are chlorine and fluorine and the most commonly used inert gases are argon and nitrogen. While the gas, in the form of discrete bubbles, rises to the surface, it encounters the inclusions and carries them to the top of the melt.<sup>42</sup>

Flotation techniques can be used to remove small particles ( $< 10 \mu\text{m}$ ) suspended in molten aluminum. Particle flotation mechanisms have been comprehensively investigated and found to be the result of two elementary capture operations: inertial impaction and peripheral interception. Inertial impaction occurs when the inertia of an inclusion particle

exceeds that of a local fluid volume element, resulting in departure from liquid flow streamlines around a rising gas bubble. This mechanism results in the impaction of an inclusion on the gas bubble surface. If attachment to the bubble occurs and viscous shear forces do not cause detachment, the inclusion is separated from the melt by flotation. Since inertial impaction is gas-bubble and inclusion-diameter dependent, particles larger than 80  $\mu\text{m}$  can be removed by these means with bubble diameters as great as 10  $\mu\text{m}$ .

The second mechanism of particle flotation, peripheral interception, is the predicted problematic equatorial contact of an inclusion and a rising gas bubble. Inclusions greater than 30-40  $\mu\text{m}$  may be separated from the melt by flotation.

### ***3.1.3 SEDIMENTATION***

The specific gravity of most reinforcements used in aluminum MMCs is usually higher than that of molten aluminum, which leads to their settling or “sedimentation” in the melt.<sup>43</sup>

In this case 100 gr of metal is heated to 1300-1380°F (704°C - 748°C) and transferred to a well-insulated, closed crucible. The melt is centrifuged at high speeds. The inclusions, which have a higher density than the melt, settle at the bottom of the crucible during centrifuging. Centrifuging principles have also been utilized to develop a practical technique in large furnaces. Once the inclusions are concentrated in a certain volume, light microscopy and quantitative metallographic techniques can be used to obtain information

on the morphology and distribution of inclusions. The Preconcentration of inclusions by centrifugation was investigated at Alcan in the early 1950's.

### **3.1.4 DEGASSING**

Taylor <sup>44</sup> has reported that gas porosity is one of the major causes of foundry scrap. Gas porosity is caused by hydrogen gas, which is the only gas with any significant solubility in molten aluminum. Commercial aluminum alloys are generally degassed to reduce the hydrogen level in the melt <sup>8</sup>. It has been observed that suspended particles float to the top of the molten metal along with the purge gas. This behavior has been observed with nitrogen and argon. Small amounts of chlorine or fluorine enhance the rate at which particles float to the surface. The degassing process is especially effective at small purge gas bubble size. Hydrogen gas is bubbled through molten aluminum under controlled conditions to remove oxide particles. This treatment may increase the hydrogen content of the melt. However at high solidification rates such as those employed in die-casting, the increase in hydrogen may not cause severe problems. Important parameters in degassing are:

- |                 |                      |                      |
|-----------------|----------------------|----------------------|
| a) type of gas  | b) gas pressure      | c) gas flow rate     |
| d) lance design | e) lance movement    | f) bath agitation    |
| g) holding time | h) inclusion content | i) final gas content |

### 3.1.4.1 *BENEFITS OF DEGASSING AND FILTRATION*

i) Improved fluidity

Figure 18 shows the increased fluidity or flow ability of clean liquid metal compared to contaminated metal. This facilitates the filling of the mould and improves the capability of casting intricate sections.

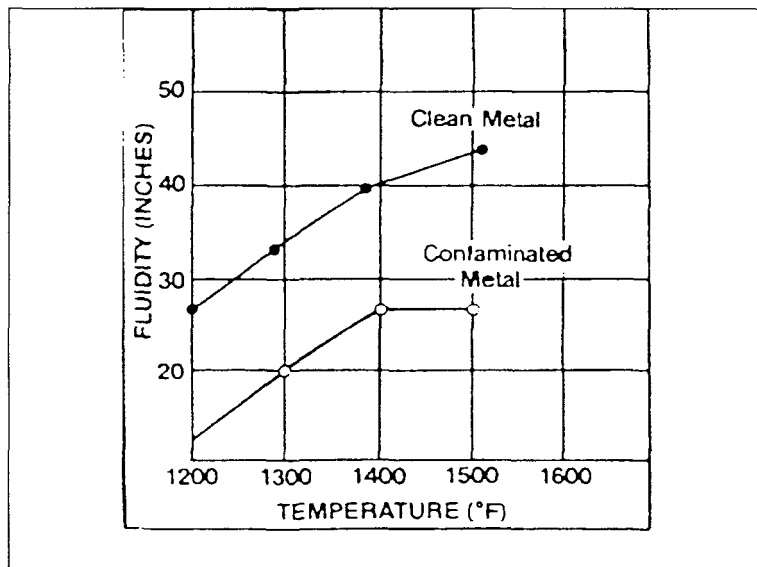


**Figure 18.** The effect of filtration on metal fluidity. <sup>14</sup>

ii) Improved mechanical properties

The removal of hydrogen and/or inclusions can result in marked improvement in the tensile yield and elongation properties as shown in Figure 19.

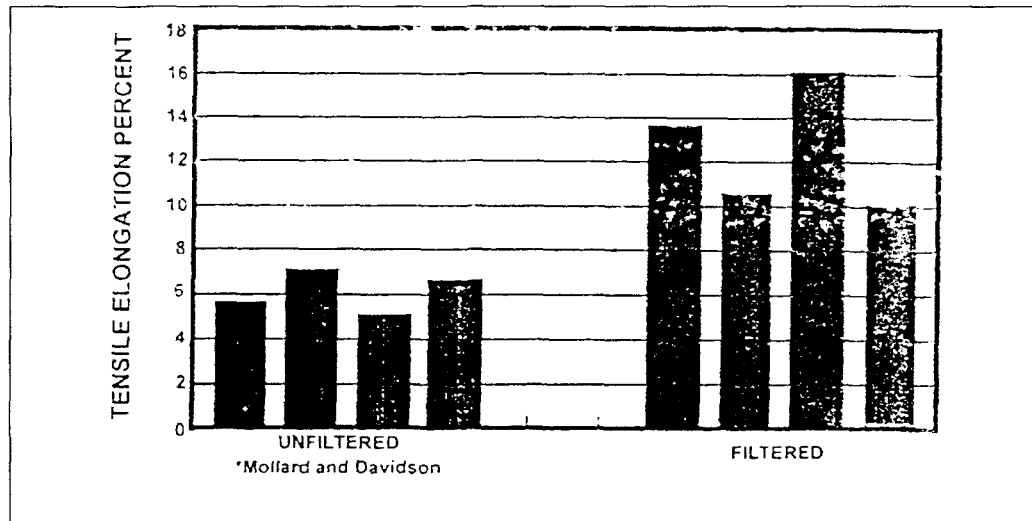


**Figure 19.** Comparison of tensile elongation of unfiltered and filtered test bars of aluminum alloy 535. <sup>45</sup>

iii) Improved machinability

Hard spots can be eliminated or reduced, resulting in easier machinability and longer tool life.

v) Greater foundry productivity and profitability.

Degassing and filtration processes can significantly improve yields and reduce rejects and rework, certainly resulting in better foundry financial performance, as well as providing greater customer satisfaction and product marketability. <sup>14</sup>

### 3.2 FILTRATION

Filtration is the separation of solid material from a liquid. In the non-ferrous industry, the molten metal processing technique of filtration means the removal of oxide

particles, intermetallic compounds, sludge crystals, and furnace refractory particles from the molten metal prior to casting.

Today there are several types of porous ceramic foams and porous ceramic sintered compacts available that permit the caster to filter the metal by a variety of techniques. These filters are produced from alumina, mulite, zirconia, and zircon in a range of porosities from twenty to fifty pores per inch.<sup>23</sup>

### ***3.2.1 FILTRATION METHODS***

Two fundamental types of filtration have been identified: deep bed filtration and cake filtration. Modern metal filters operate by each of these mechanisms, although in a given filter type, one type may be more important than the other<sup>31</sup>.

#### **3.2.1.1 Deep Bed Filtration**

In deep bed filtration, foreign particles are trapped within the body of the filter itself as the liquid metal flows through the filter. Usually, these particles are smaller than the filter pore size, and entrapment depends on them contacting the pore walls and then being bonded in place. Inertial forces trap a particle if its weight prevents it from following the fluid flow line. It then simply deposits onto the filter wall. Particles may also directly intercept the pore wall (i.e., hit it), or they may be placed there by hydrodynamic effects resulting from the lower liquid velocity near the wall, which can cause the particles to rotate inside the pore surface.<sup>31</sup>

When particles contact the inertial filter surface, they are held in place by electrostatic forces of the Van Der Waals type. These bonding forces are very weak, and particles, or clusters of particles, may become detached and washed from the filter by sudden increases in flow rate, mechanical vibration of the filter, or by backwashing.

Smaller inclusions ( $<20\mu\text{m}$ ) are removed by the deep bed mechanism, which becomes more important as the pore size of the filter decreases; consequently, the flow path becomes more tortuous, and the filter thickness increases. Although all filters will exhibit some deep bed characteristics, particularly early in the filter life, this mechanism is most important in bonded particle and bed filters.

#### **3.2.1.2 Cake Filtration**

Cake filtration occurs on the filter surface, and is essentially a sieving action. Initially, particles with sizes larger than the filter pore size are trapped on the inlet side of the filter. The spaces, which remain between these trapped particles, are finer than the original pores of the filter, and so smaller particles can now be stopped. Eventually a cake of trapped material builds up, and this filter cake itself acts as a filter. In cake filtration, the function played by the original filter is only to initially trap the largest foreign particles and then to act as a support mechanism for the filter cake. Of course, eventually the filter cake will become so thick that it will unduly impede liquid flow and the filter will become clogged.

Both cake and deep bed filtration, occurring in modern ceramic foam filters (CFF), come in different pore sizes e.g., 10 ppi, 20 ppi, where ppi represents pores per inch. The most effective filtration takes place during the deep bed period. Eventually, the filter becomes clogged with inclusions that the cake filtration predominates. When this stage is reached, the filter is essentially plugged, and will no longer pass molten aluminum.

### 3.3 INCLUSIONS ASSESSMENT

There are several techniques for measuring the inclusions in aluminum castings, including PoDFA, Prefil, Qualiflash, and non-destructive methods such as LiMCA and Ultrasonic.

#### *3.3.1 Non-Destructive Techniques*

Non-destructive testing is a basic management and engineering method of vital significance in modern industries. By definition, non-destructive tests are different from other tests and measurements which damage or impair the serviceability of the items tested.

<sup>46</sup> Prominent non-destructive techniques that are currently being applied commercially include the Ultrasonic Test and LiMCA.

#### *3.3.2 PoDFA (Porous Disc Filtration Apparatus)*

Direct examination of a polished section provides information on the type and morphology of inclusions. However, in order to obtain fairly accurate results, it is imperative that the inclusions be preconcentrated in a small area. The sample that is to be



analyzed is melted and made to pass through a filter. The residue on the filter is analyzed to obtain quantitative information on inclusion concentrations. <sup>9</sup>

PoDFA technique is based on the principle shown in Figure 20. Approximately 2kg of metal, taken directly from a melt that has to be analyzed, are made to pass through a filter. A balance located below the filter crucible enables the operator to precisely obtain the right amount of metal that filters through. The filter with the residue is then sectioned

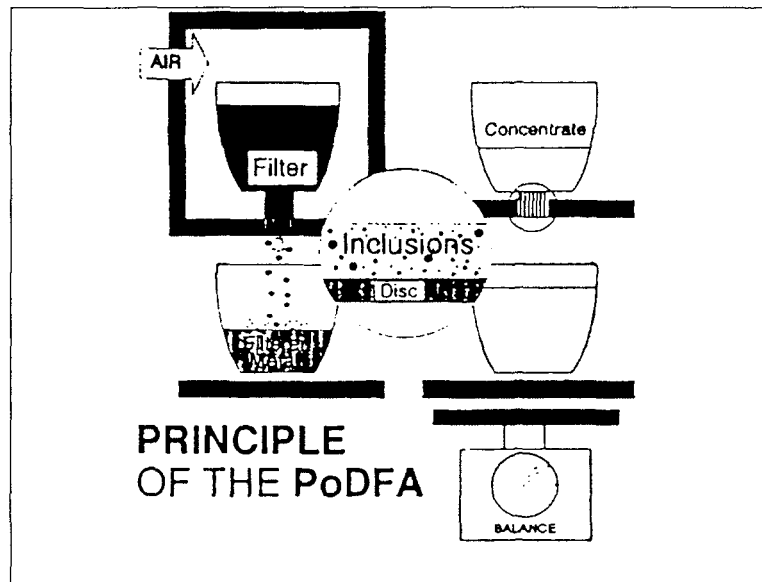


**Figure 20.** Principle of the PoDFA method of measuring melt cleanliness. <sup>8</sup>

vertically along the central plane and prepared for metallographic examination. The inclusion concentration is reported in  $\text{mm}^2/\text{kg}$  indicating the area of inclusions in the sectioned part. A typical graph obtained from the PoDFA technique that shows the effect of gas composition on the performance of an in-line melt treatment device is shown in Figure 21. Measurement of the rate of filtration has also been examined as a potential method of metal cleanliness assessment. The amount of filtrate collected and the temperature of the

metal may be recorded as a function of time using a microprocessor. This technique may distinguish between very dirty metal ( $> 1\text{mm}^2/\text{kg}$ ) and relatively clean samples. The technique is sensitive at inclusion concentrations of less than  $1\text{mm}^2/\text{kg}$ .

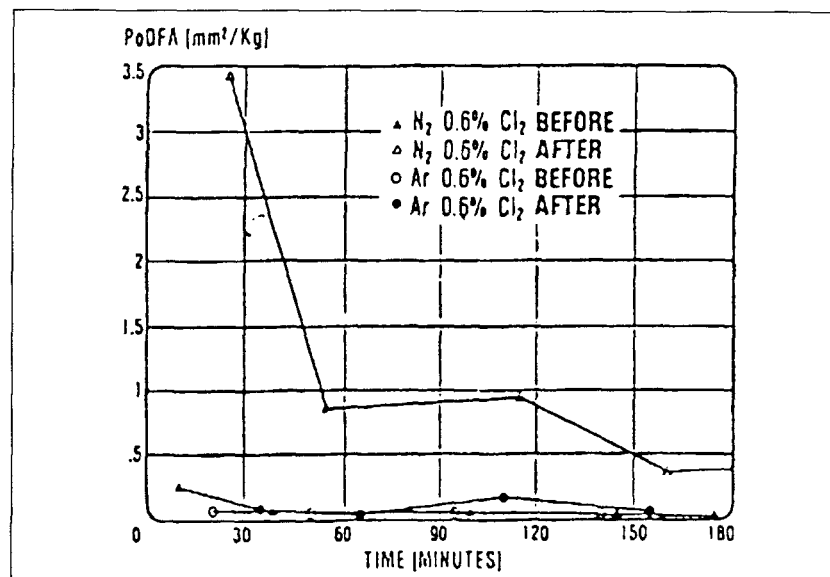


**Figure 21.** Typical output obtained from a PoDFA run showing the effect of gas composition on the performance of an in-line melt treatment device.<sup>8</sup>

### 3.3.3 Prefil (Pressure Filtration technique)

The principle mechanism operating during the filtration of a fluid containing solid inclusions through a fine filter is "cake filtration". The build-up of a cake and its subsequent permeability is a dynamic process that is critically dependent on the type, size, shape, and mixture of inclusions present in relation to the filter itself. In the case of liquid

metals, temperature, viscosity and the surface tension of the fluid also influence the characteristic behavior of the system. The net result of these influences, under highly controlled standard conditions, is a characteristic called the "filtration behavior curve" or "footprint", which can be used to define or benchmark the quality of a given metal supply.

The Prefil technique has the advantage of providing in-situ results in the form of flow rate charts. These charts minimize the need for time consuming metallographic examinations for inclusion analysis demanded by other pressure filtration techniques such as PoDFA. Experiments carried out using the Prefil technique indicate that for obtaining appropriate results, the pressure chamber and filtration crucible of the Prefil apparatus should be heated to 300 - 350°C, to reduce heat loss during transfer of the liquid metal from the melt crucible to the filtration crucible. Also, the filtration temperature should be high enough to avoid the possible sedimentation of inclusions in the ladle during the transfer.<sup>47</sup> The machine consists of a simple two-stage pressure cell (with prime and run sequences), and a refractory crucible containing the filter, as shown schematically in Figure 22.

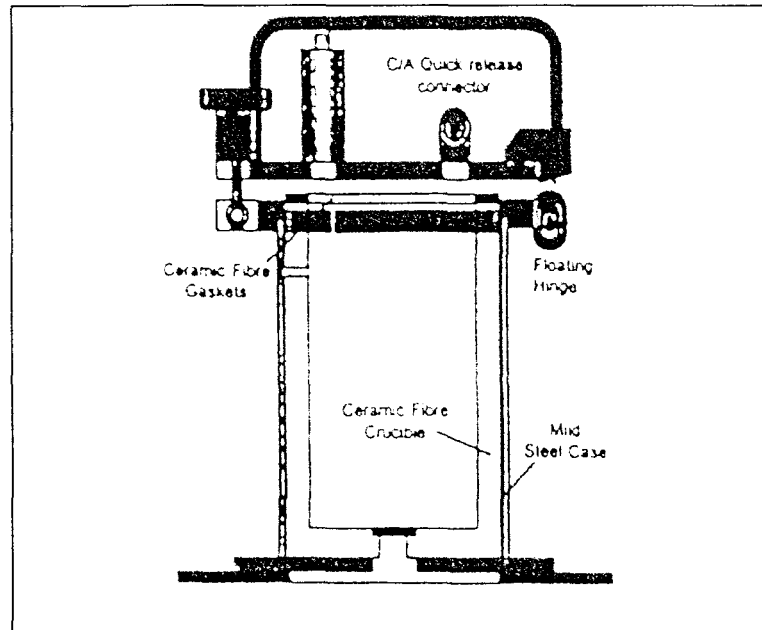


**Figure 22.** Pressure cell of the Prefil apparatus.<sup>47</sup>

The amount of metal filtered (as a function of filtration time) is recorded by means of a digital balance. The machine is equipped with on-board data logging and software for footprint characterization. The crucible is made of a low-heat capacity, high insulating fibrous material. Thus, no preheating prior to testing is required. Inclusions, which build up on the filter surface, are metallographically examined, identified and counted. Based on such quantitative analyses of inclusions, the corresponding filtration (or flow) curve can then be characterized. These flow curves then provide the means for an on-line assessment of the melt cleanliness. Figure 23(a) shows the schematic flow curves obtained with the Prefil apparatus for various melt conditions.

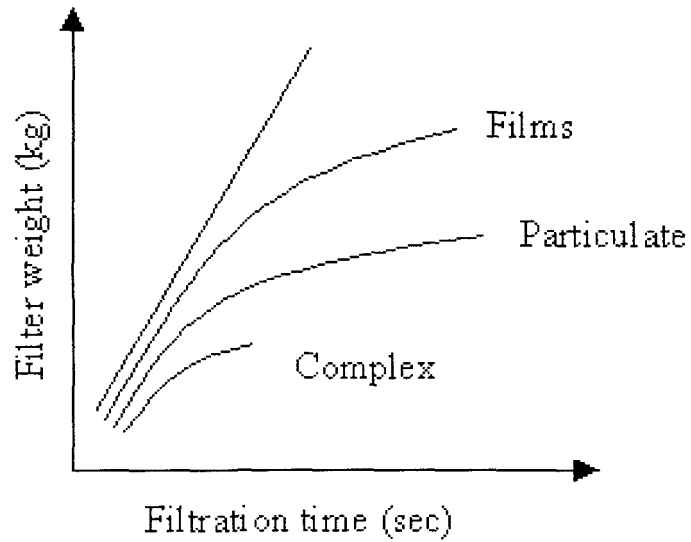


Figure 23 (a) Schematic diagram showing filtration behavior of aluminum alloy containing different types of inclusions.<sup>47</sup>

Figure 24(b), depicts the reproducibility of flow curves obtained from consecutive Prefil tests for the same melt condition.

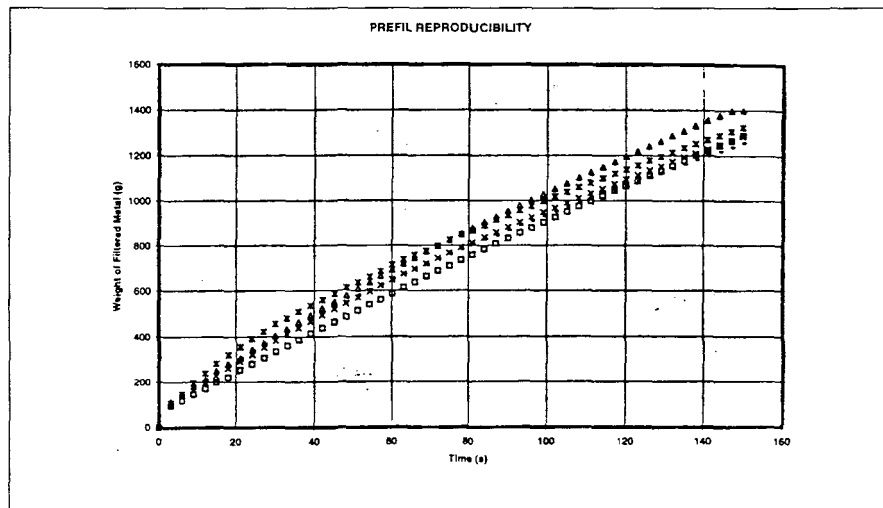
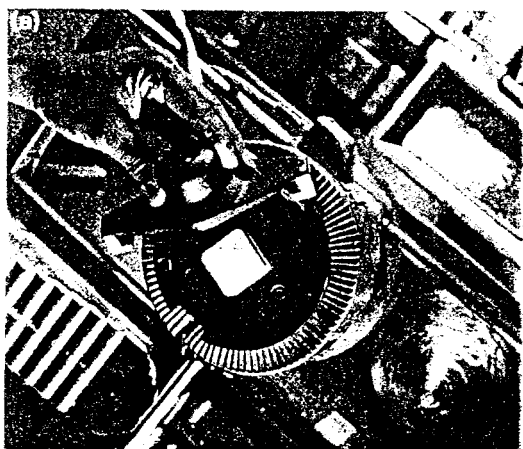


Figure 23(b) Schematic diagram of Prefil reproducibility.<sup>47</sup>

### 3.3.4 *QUALIFLASH*

Qualiflash is a melt cleanliness assessment apparatus used for measuring oxide films or particles in molten aluminum.<sup>48</sup> It gives immediate and reproducible results that allow the foundry man to quickly and easily decide whether a bath is ready to be poured, or must undergo another deoxidation treatment, or be treated further. Based on a filtration technique, the melt cleanliness is determined through the clogging of an extruded ceramic filter by oxides and inclusions.

This is a simple filtration technique where the melt cleanliness is gauged by the number of steps covered by the liquid metal that filters through into a step-like ingot mold placed underneath the filter.<sup>49</sup>



(a)



(b)

**Figure 24.** The Qualiflash apparatus: (a) placing the filter (b) measuring the cleanliness of the aluminum melt.<sup>49</sup>

The Qualiflash apparatus is shown in Figure 24. It essentially consists of a temperature-controlled funnel-shaped shell with a 15-ppi ceramic filter fitted at the bottom, beneath a filtering section plate with a hole at its center. A step-like ingot mold containing ten steps is placed directly underneath the shell.<sup>50</sup> The funnel shell, filtering plate and receiving ingot are made of steel. The temperature of the funnel shell is kept around 430°C. The degree of melt cleanliness is determined by counting the number of steps that have been covered by the filtered metal in the mold. The number of steps observed in each case is strongly related to the amount of oxide films that exist in the liquid metal prior to filtration. Such a relationship is expressed in terms of the quality temperature index (QTI). The results on the effect of pouring temperature for the same charge are shown in Figure 25.

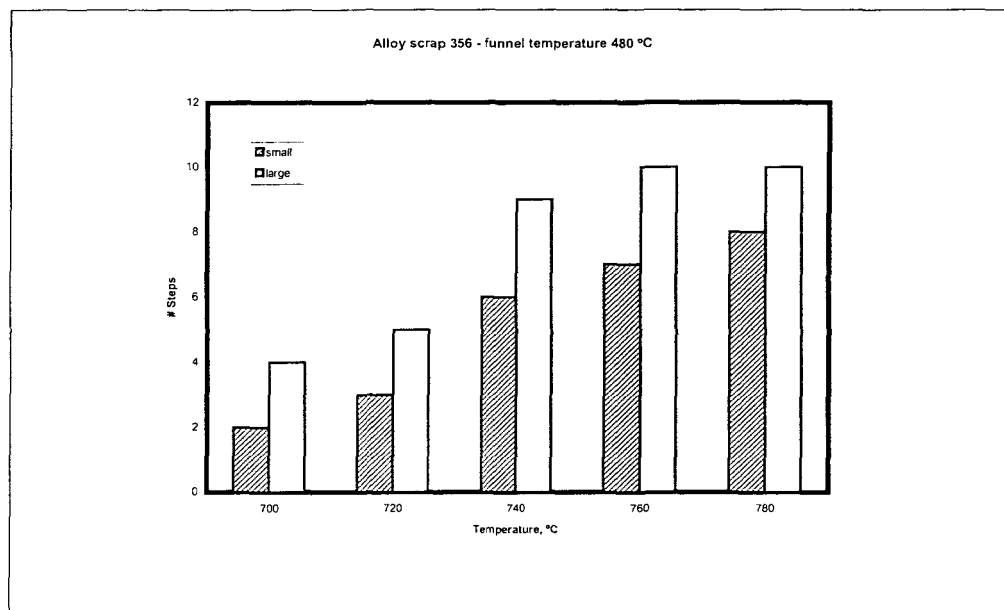


**Figure 25.** Variation in the number of steps as a function of pouring temperature for A356 alloy.

### 3.3.5 LiMCA

The LiMCA II system was used as an on-line measurement of inclusion concentrations upstream and downstream of ceramic foam filters.<sup>51</sup>

This is a non-destructive technique, and is based on the electrical sensing zone (ESZ) principle, where the presence of non-conducting particles is detected by their local effect on the electrical conductivity of the conductive fluid in which they are suspended (see Figure.26). The method allows for measurement of the inclusion concentration in the melt, along with their size distribution for every minute during the casting process. The results of the measurements are displayed instantaneously.

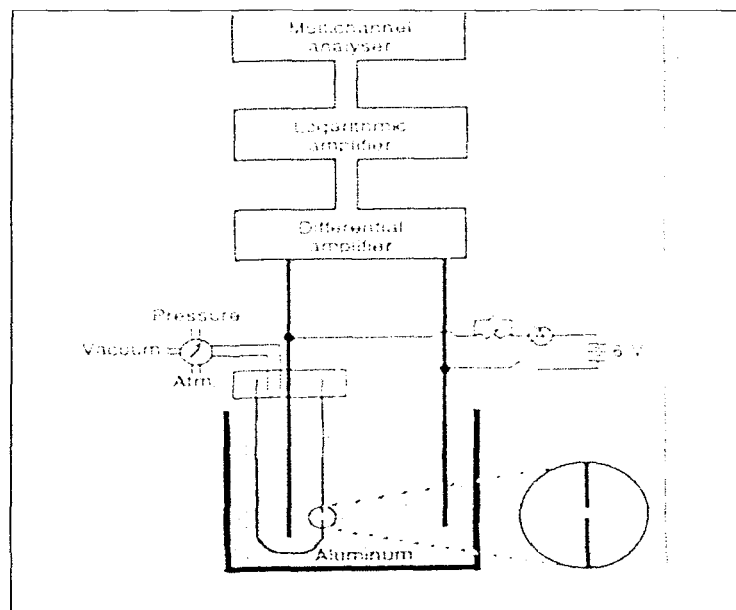


**Figure 26.** Schematic of LiMCA operation.<sup>27</sup>



The LiMCA unit consists of a probe, a current source, and a signal processing system. The probe consists of two electrodes and a sampling tube made of non-conducting material (e.g., glass) and having a small orifice (300  $\mu\text{m}$ ) on its surface. The tube is immersed in liquid metal; negative pressure is applied inside the tube to flow metal into the orifice. A constant electric current is applied between the two electrodes. This current must circulate through the orifice where it is carried by incoming liquid metal. The voltage drop across the orifice is monitored. For pure metal/alloy, the drop remains constant, but when non-electrically conducting inclusions pass through the orifice, a slight increase in voltage drop is observed. The signal processing system translates the voltage fluctuation and the distribution of their amplitudes to particle densities, and volume distributions are expressed as histograms, showing the particle density per particle size interval.<sup>52</sup>

### ***3.3.6 ULTRASONIC TECHNIQUE***

This is a non-destructive technique since it allows detection of inclusions via wave analysis, and is based on the principle of the energy dissipation of a sound pulse. To measure inclusions using this technique, a signal from a piezoelectric crystal is sent through the metal by a transmitter (figure 27). When the signal passes through the melt, some amount of its energy is reflected at inclusions. The reflection results in the reduction of the signal energy. The reduced energy signals are collected by a receiver and displayed on an oscilloscope.

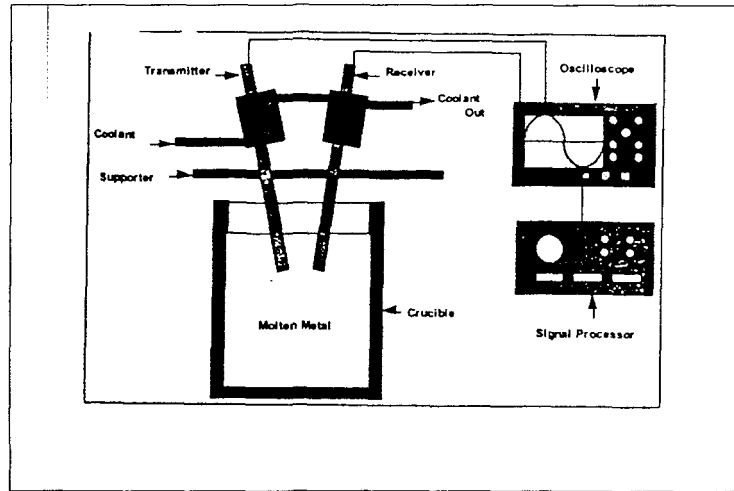


**Figure 27.** Schematic diagram of an ultrasonic apparatus. <sup>27</sup>

These signals give an indication of the content and size of inclusions and a counter records the data. With the ultrasonic technique, both nonmetallic and metallic inclusions can be detected. Figure 28 shows how the ultrasonic signal is attenuated before and after filtration (where the filtration removes the inclusions).

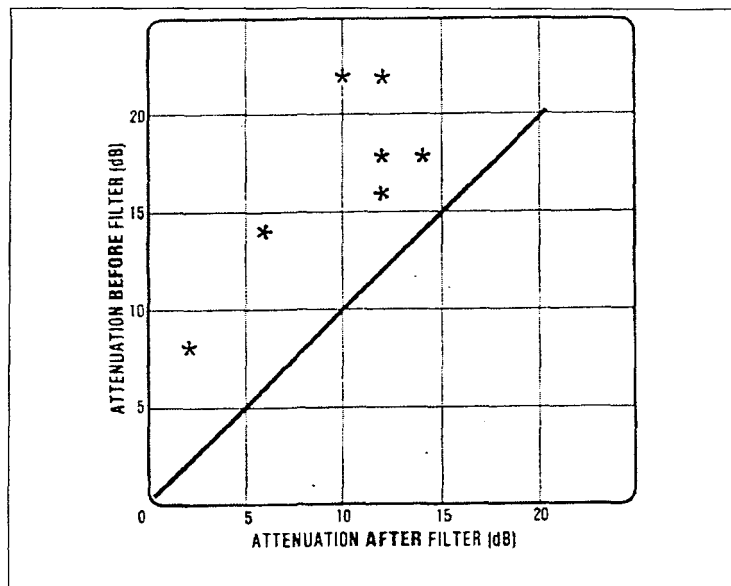


**Figure 28.** Ultrasonic attenuation of molten aluminum before and after filtration. <sup>27</sup>

## **CHAPTER 4**

# **EXPERIMENTAL PROCEDURE & MEASUREMENTS**

## **CHAPTER 4**

### **EXPERIMENTAL PROCEDURE & MEASUREMENTS**

#### **4.1. MELT PREPARATION**

Table 6 shows the chemical compositions of the A356, A319 and AA4104 alloys used in the present study. The alloys were received in the form of 12.5 Kg ingots that were cut into two halves. The cut pieces were cleaned with ether and dried in an electric oven prior to being transferred into the melting crucible. Melting was done in an electrical resistance furnace, using a silicon carbide crucible of 35 kg capacity.

When the melt temperature reached  $735 \pm 5$  °C, the required melt treatment was given, followed by repeated surface skimming and degassing with pure dry argon using a graphite impeller for 15 minutes at 135 rpm. In order to investigate the effect of different inclusion/melt conditions, tests were performed in two laboratories and in a primary aluminum plant. Cleanliness measurements were conducted using automotive alloys (356, 319, 4104) and pure aluminum.

**Table 6.** Chemical compositions (wt %) of the as-received A356, A319 and AA4104 alloys

Alloy	Si	Mg	Fe	Zn	Cu	Al
A356	7.0	0.35	<0.20	<0.1	<0.20	Bal
A319	6.0	<0.10	<1.0	<1.0	3.5	Bal
AA4104	4-10.5	1-2	0.8	0.2	0.25	Bal

#### 4.2. METALLOGRAPHIC ANALYSIS

Metallographic analysis consists of examining the residue of unfiltered metal at the surface of the Prefil filter. Because the Prefil instrument uses a very fine porous filter, inclusions in the melt are concentrated at the disc surface by a factor of 10,000. This technique can distinguish inclusions as small as 1  $\mu\text{m}$  (Figure 29).

After removing the excess metal, the sample is sectioned through the central plane perpendicular to the disc, mounted and polished to a mirror-like finish. The polished sample is then analyzed under an optical microscope by a specially trained metallographer. The types and concentration of inclusions are determined. Using a grid method based on the PoDFA technique, the total inclusion area is obtained, and then divided by the weight of the filtered metal that has passed through the filter. This technique can distinguish inclusion

types and differentiate between the levels of boride, carbide, spinel and other detrimental types of inclusions which are present within an individual sample. <sup>(9,47)</sup>

The total inclusion concentration, expressed in area per mass of metal ( $\text{mm}^2/\text{kg}$ ), is defined by:

$$\text{Total Inclusion Concentrate Area per Kilogram of Filtered Metal (mm}^2/\text{kg)} = \frac{\text{Total Number of Squares Measured} \times \text{Area per Small Square at Chosen Magnification (mm}^2)}{\text{Weight of Filtered Metal (kg)}} \times \frac{\text{Nominal Chord Length (12.7 mm)}}{\text{Chord Length Measured (mm)}}$$

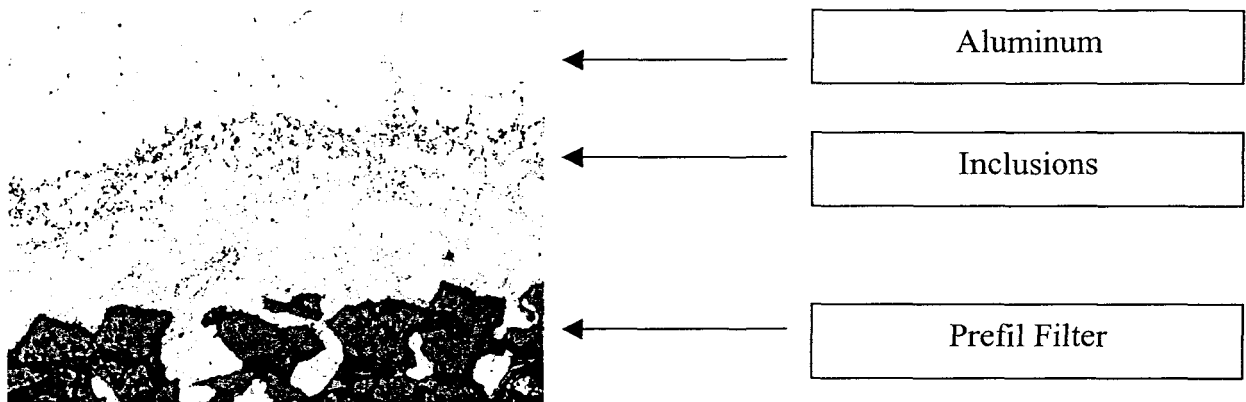


**Figure 29.** Picture of a Prefil sample for metallographic analysis.

Figure 30 shows an example pattern of disc area. The pattern is the same for all polished samples. The first sample is the one with the disc down.

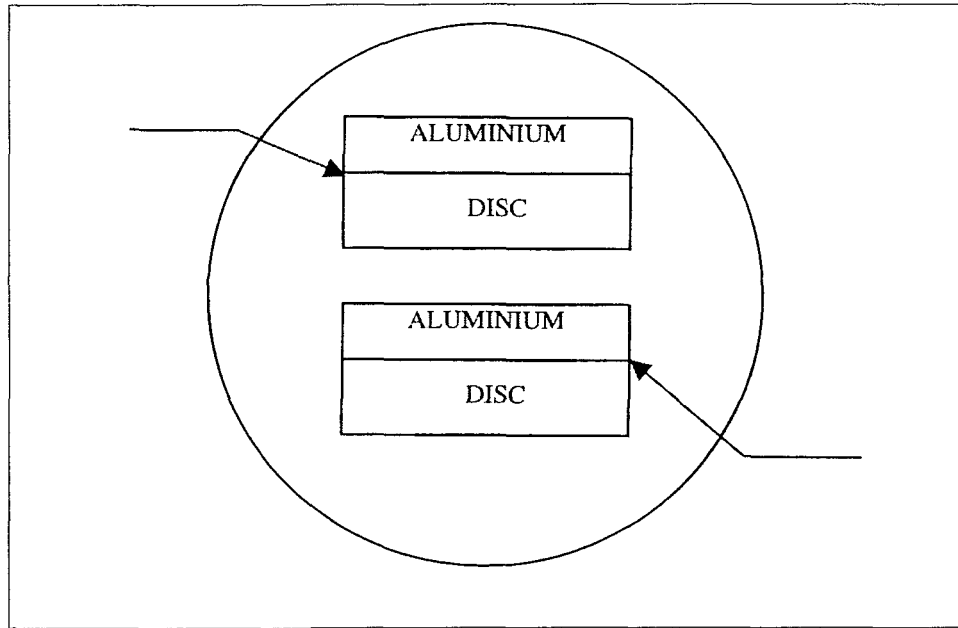


**Figure 30.** Schematic of Prefil disc samples.<sup>10</sup>

#### 4.3. THE PREFIL SYSTEM

The Prefil operating principle is illustrated in Fig 32.<sup>(53,54)</sup> A ready to use crucible, equipped with a porous filter disc at the bottom, is first preheated and installed in the pressure chamber. A sample of metal in a ladle is then taken and poured into the crucible. The pressure chamber is thereafter closed and the test starts. The system applies pressure in the chamber when the metal temperature reaches the value specified for the test, forcing the liquid metal to flow through the porous filter and into the weigh ladle located beneath the crucible. Throughout the test, the system continuously weighs the metal in the weigh ladle and displays a curve of the accumulate weight versus the elapsed time. The cleaner the

metal, the faster it will flow through the filter and the higher this curve will be. Building a database makes it possible to determine extremes of metal cleanliness found at a specific location. The results for a given alloy, obtained at a given filtration temperature and location, can be judged against the foot print database and used for shop floor quality control.

When the test is completed, the pressure is automatically released from the pressure chamber and lid unlock. The system automatically saves the test data. The metal in the ladle is removed and the system is prepared for the next test. Optionally, the metal residue above the filter can be saved. Metallographic examination of the material trapped by the filter can confirm the results and extend the interpretation. Prefil<sup>55</sup> is the only inclusion analyzer that provides a direct result and, at the same time, a sample for further metallographic analysis. These two qualities, along with its rugged design, make the Prefil-Footer a powerful solution for performing inclusion quality control on a day-to-day basis, and/or on a more in-depth audit basis for process optimization.

For Prefil experiments, two types of ceramic filters were used *viz.*, standard permeability (average filter pore size ~90 $\mu$ m-sp) and high permeability (average filter pore size~130 $\mu$ m-hp). Unless mentioned, standard permeability filters were applied.



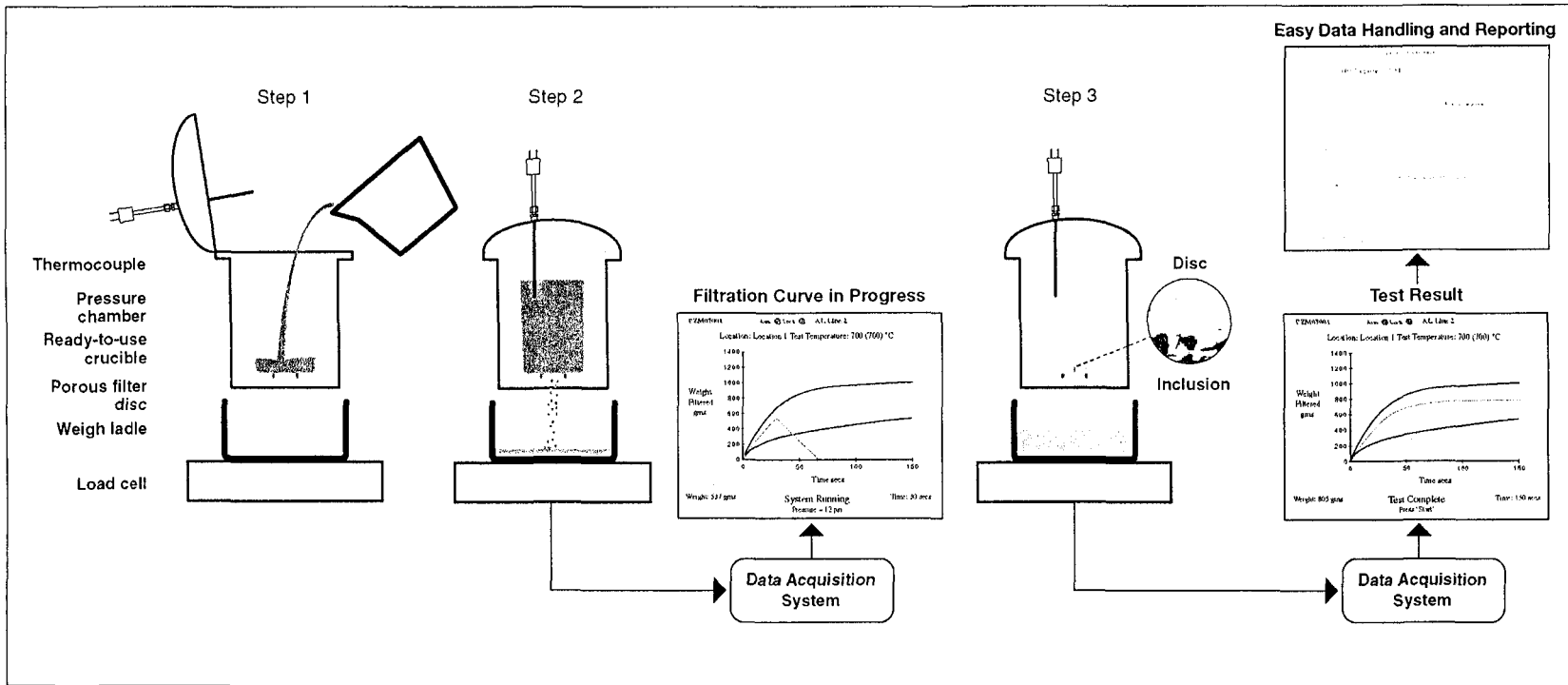
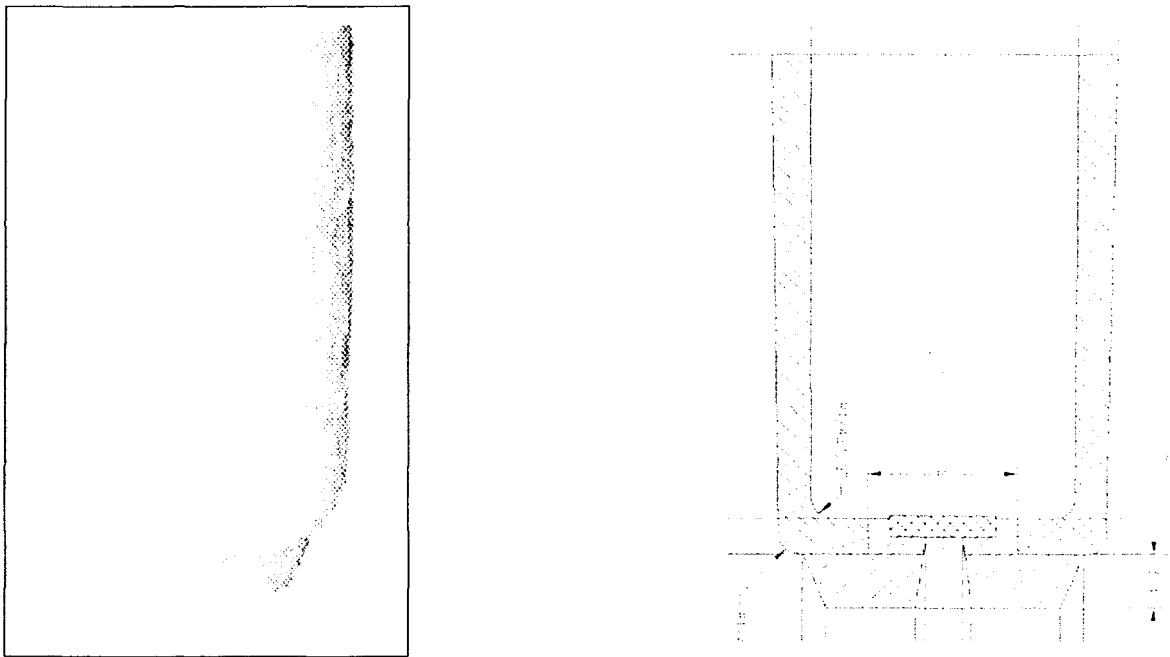


Figure 31. Prefil-Footer Operating Principle.

### 4.3.1 *PREFIL CRUCIBLE*

A schematic figure of the new crucible type used for the Prefil apparatus is shown in Figure 32. The new crucible was designed in order to meet four goals: high thermal insulation, alignment in the pressure chamber, solidity and tightness at the base. This crucible consists of a ceramic base directly molded around the Prefil disc and fiber crucible. In this design, the disc and crucible are attached to the ceramic base in the molding process, eliminating the need for high-temperature ceramic glue. Tables 7-9 provide various details related to the new crucible.



**Figure 32.** Design of the new Prefil crucible.<sup>56</sup>

**Table.7** Technical Specifications of Prefil Crucible. <sup>56</sup>

Porous Ceramic Filter	inches	mm
Diameter	1.256 ± 0.006	31.9 ± 0.15
Thickness	0.232 <sup>+0.006</sup> <sub>-0.003</sub>	5.9 <sup>+0.16</sup> <sub>-0.08</sub>
Inlet Filtration Area	1/2	12.7
Outlet Filtration Area	5/16	7.9
Outside Diameter	4 <sup>21/32</sup> ± 1/4	11.8 ± 0.6
Inside Diameter	3 <sup>19/32</sup> ± 1/32	9.13 ± 0.08
Crucible Height	7 ± 1/32	17.78 ± 0.08

Material (alumina and silica)-typical pore size (90 microns)- permeability (53 ± 5 Darcy)

The new crucible material characteristics include:

- Synthetic Vitreous Fiber vacuum formed
- 1832°F (1000°C) maximum temperature rating
- Very low thermal conductivity and heat storage
- Non-wetting to molten aluminum
- High resistance to thermal shock

The filter is produced from a calcium-magnesium-silicate material. The fibers are formed using a melt spinning process. The fibers contain no organic components. The crucible is vacuum formed and dried in an oven and provides excellent chemical stability and resistance to chemical attack. Exceptions include hydrofluoric acid, phosphoric acid, and strong alkalis.

**Table.8** Temperature Range of Crucible.<sup>56</sup>

Temperature	°F	°C
Melting Point	2327	1270
Continuous use limit	1832	1000

**Table.9** Chemical Composition of Crucible (Weight Percent After firing).<sup>56</sup>

Component	SiO <sub>2</sub>	CaO	MgO	Other
Wt %	65	29	5	1

#### 4.4 THE LiMCA II SYSTEM

The LiMCA II system was designed to measure inclusions in high-quality, inclusions-critical products, such as thin-gauge sheet for can body stock, or foil and plates.<sup>52</sup> It is ideally suited for large cast house applications in process development, process control and quality assurance.

A LiMCA (Liquid Metal Cleanliness Analysis) system directly measures the density of non-conductive particles, suspension in a metal melt, and performs a real-time analysis of the volumetric distribution of these inclusions. One clear advantage of the LiMCA II is that it is a completely objective user-independent method. A LiMCA II instrument can measure inclusions from 20  $\mu\text{m}$  to 300  $\mu\text{m}$ .

Equipped with signal and data processing electronics, the instrument can determine the density and volumetric distribution of the particles in the melt by analyzing the frequency and distribution of the amplitudes of voltage fluctuations. The density of particles is shown by a number (an index of cleanliness) expressed in thousands of particles

per kilogram of melt (K/kg) or also per volume fraction (part per billion, PPB). A schematic of the LiMCA II system is shown in Figure 33.

Chen et al.<sup>57</sup> have stated that it should be noticed that the LiMCA II results can be expressed in two ways: i) the total number of the inclusion particles detected (in thousands per kilogram metal, e.g., 5 K/kg), which is commonly used in the current literature, or ii) a volumetric concentration in ppm or ppb.

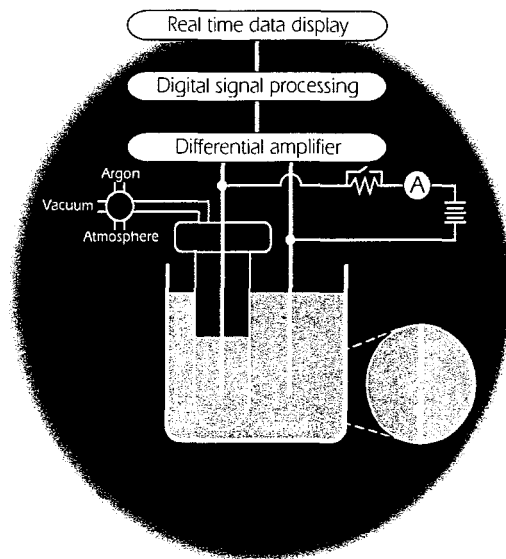
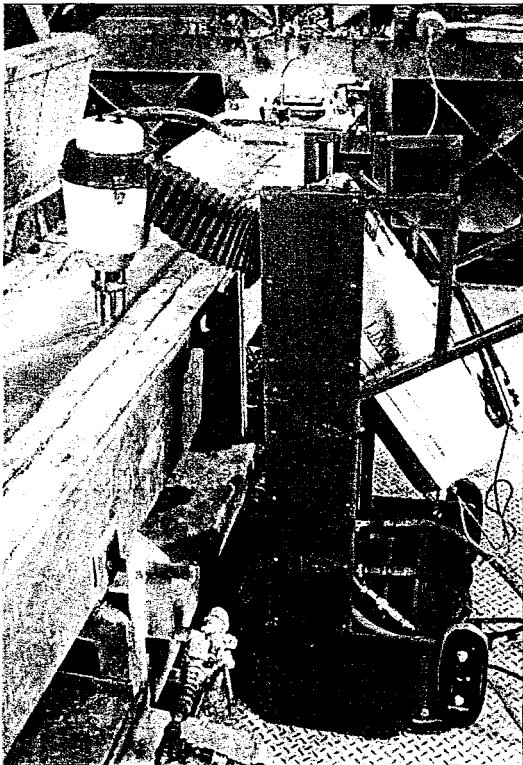
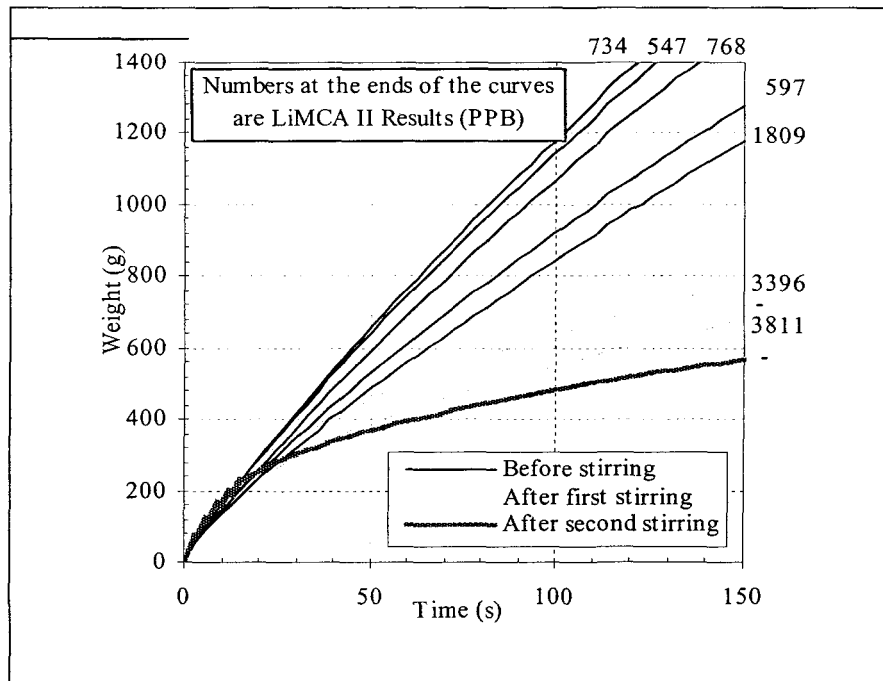


Figure 33. LiMCA II

## 4.5 EFFECT OF DIFFERENT CLEANLINESS LEVELS

### 4.5.1 PREFIL RESULTS WITH PURE ALUMINUM CHARGE (FIRST SET)

A variety of experiments were made on several molten metals with different levels of cleanliness, and the curves maintained from Prefil were more or less the same. A charge of pure aluminum was used and casting conditions kept at a constant level. For example, the molten metal temperature was between 720° C and 735° C. Figure 34 shows the Prefil curves produced before and after mechanical stirring.



**Figure 34.** Prefil curves compared with LiMCA II measurement in pure aluminum (first set)

#### 4.5.2 LiMCA II RESULTS WITH A PURE ALUMINUM CHARGE (FIRST SET)

A charge of pure aluminum was selected for similar Prefil tests. Because it was not possible to fill the Prefil spoon when the LiMCA II was measuring, the cleanliness levels measured by the Prefil were compared with the average of four LiMCA II measurements; two before and two after the Prefil sampling. The melt temperature was in the range of 720° C and 735° C. In both the cases of Prefil and LiMCA II, tests were conducted in a 70 – lb electric furnace. The LiMCA II measurements as a function of time are shown in Figure 35.

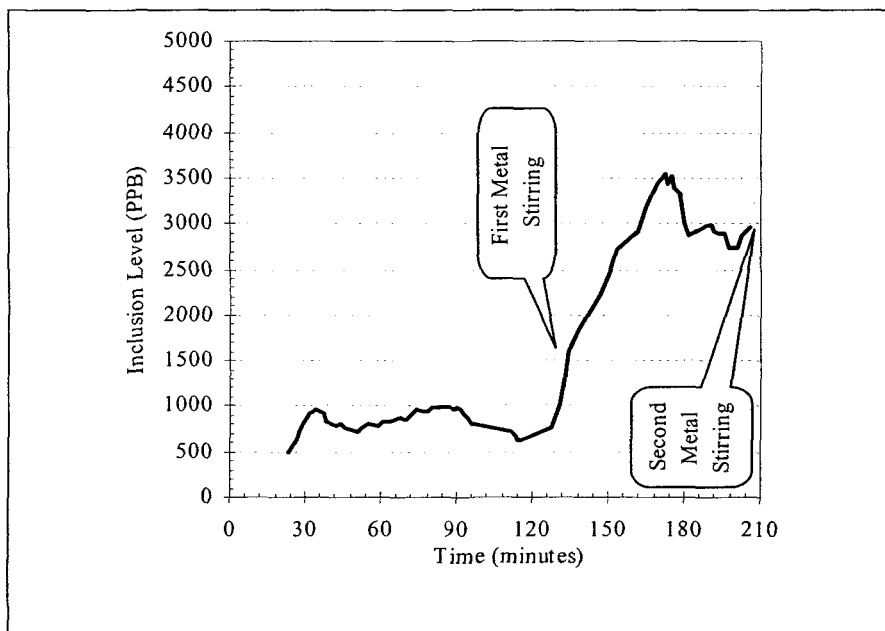


**Figure 35.** Inclusion level measured with the LiMCA II in pure aluminum (first set).

Stirring the metal causes an increase in the concentration of inclusions in molten metal. The effect of this parameter is clearly observed in the results obtained from Prefil

and LiMCA II techniques. As shown in Figure.34, after the first stirring the results of three Prefil tests (filtration rate) are definitely low. The second stirring caused the last Prefil curve to go even lower. Before the first stirring, the amount of inclusions measured by the LiMCA II was about 700 PPB and increased after stirring to 3800 PPB.

**4.5.3 PREFIL RESULTS WITH A PURE ALUMINUM CHARGE (SECOND SET)**

In the same furnace (70 lb electrical) and for the same charge (pure aluminum) the tests were carried out. In this case, the molten metal was allowed to settle after stirring. Figure 36 shows the corresponding results.

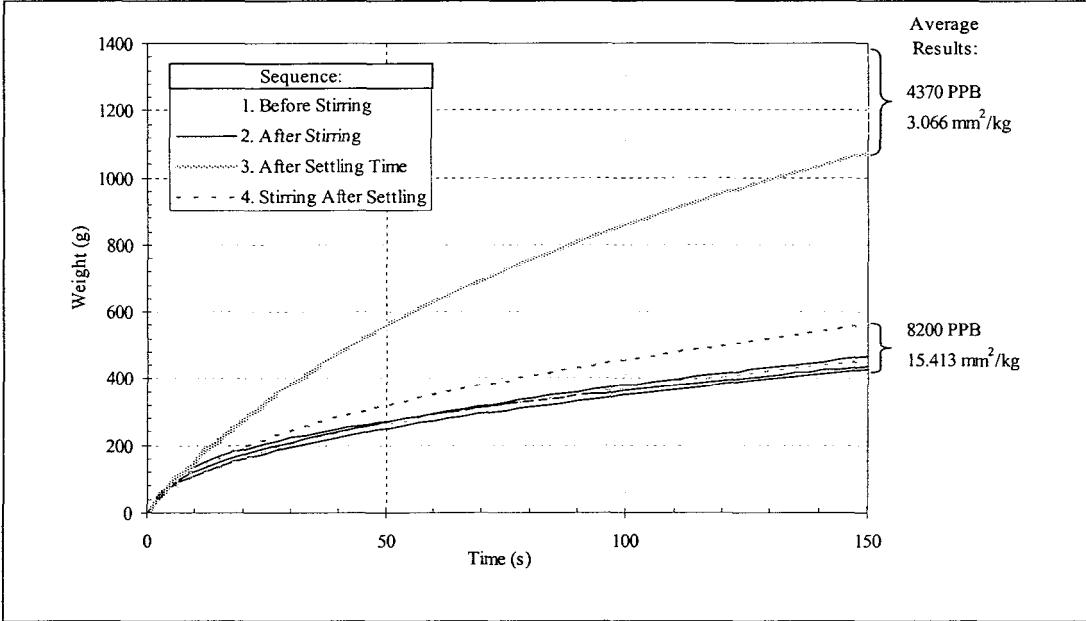


**Figure 36.** Prefil curves compared with LiMCA II instruments and metallographic analysis in pure aluminum (second set).

Metallographic analysis also showed a considerable increase in the total inclusion content after stirring, Figure 37.



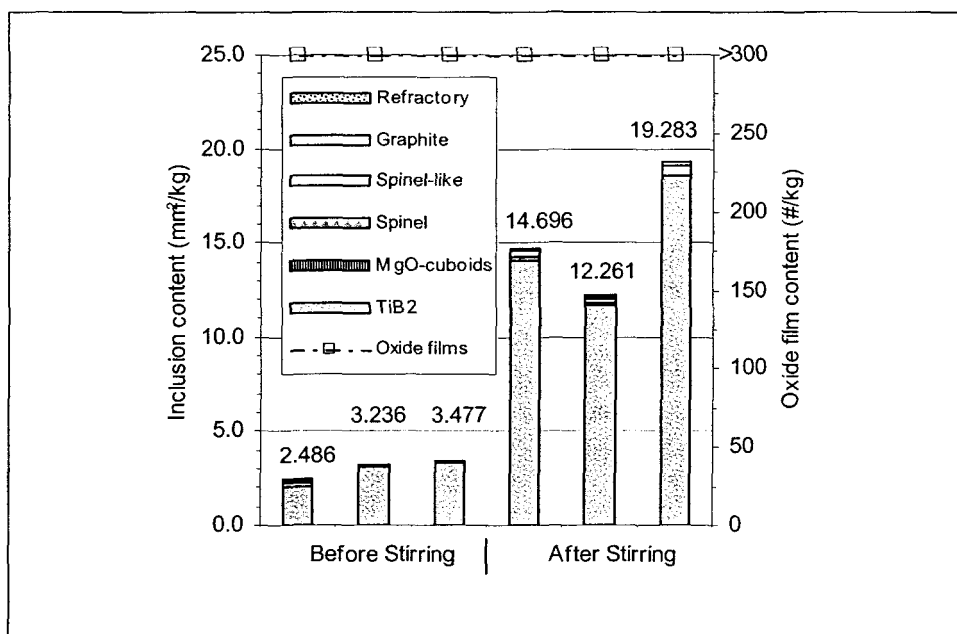


**Figure 37.** Metallographic analysis results from Prefil residues in pure aluminum (second set).

The curves were high before stirring and lowered after stirring. Overnight settling led to back up the level before the first stirring. However, after the second stirring, the curve dropped again.

#### **4.5.4 LiMCA II RESULTS WITH PURE ALUMINUM CHARGE (SECOND SET)**

In the case of LiMCA II, after overnight settling time the results were similar to those obtained before stirring (Figure.38).

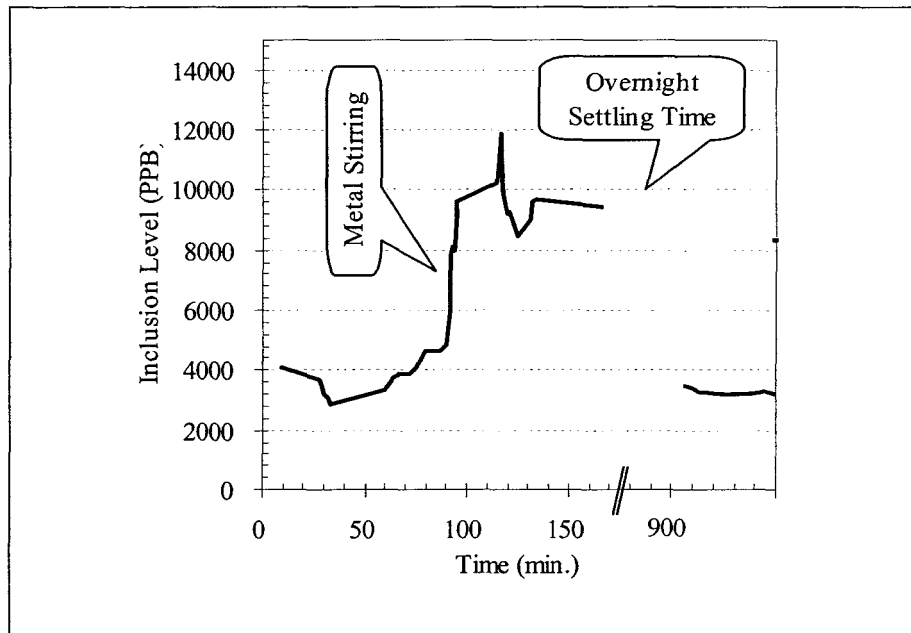


**Figure 38.** Inclusion level measured with the LiMCA II in pure aluminum (second set).

Titanium di-boride ( $TiB_2$ ) was the main inclusion that was found before and after stirring. All samples contained more than 300 aluminum oxide films.

#### ***4.5.5 THIRD SET AT A PRIMARY ALUMINUM PRODUCER PLANT***

This series of experiments were conducted in a primary aluminum production plant. Pure aluminum with a 99.7% grade in a launder with a 60 ton capacity and a T-bars of a period of one hour were selected.

#### 4.5.6 PREFIL RESULTS WITH A PURE ALUMINUM CHARGE (THIRD SET)

In each case, molten metal was degassed and samples were taken before and after degassing. For Prefil samples, metallographic analysis was done before and after degassing using the Alpur technique. The Prefil tests show that the metal has a higher concentration of inclusions before degassing than after degassing, as depicted in Figure 39.

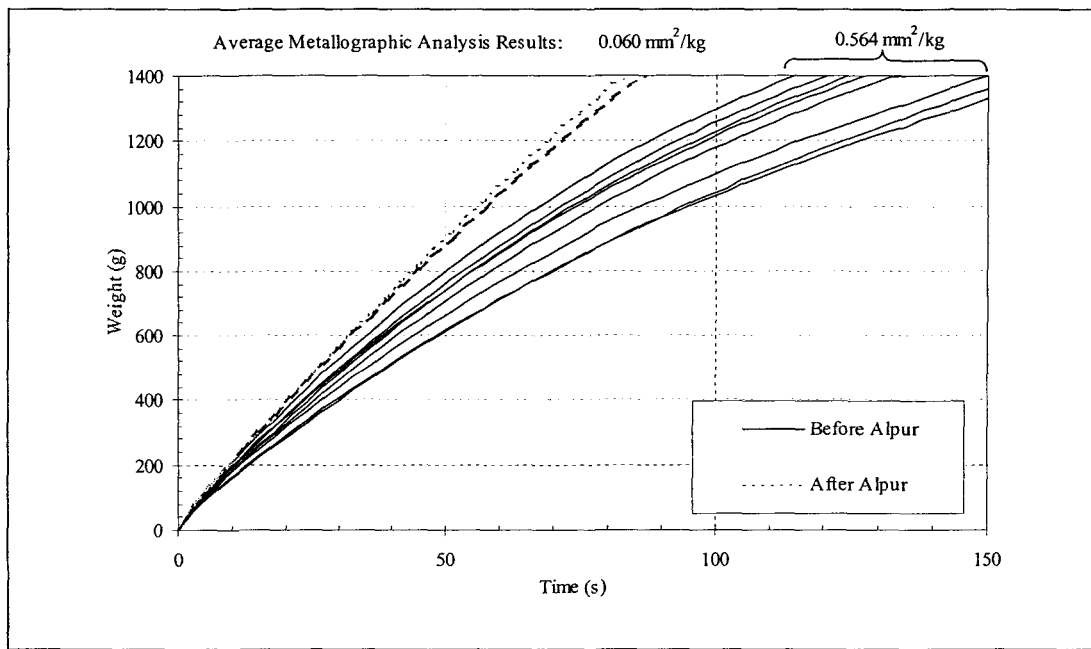


**Figure 39.** Prefil curves and metallographic analysis results in 99.7% pure aluminum (third set)

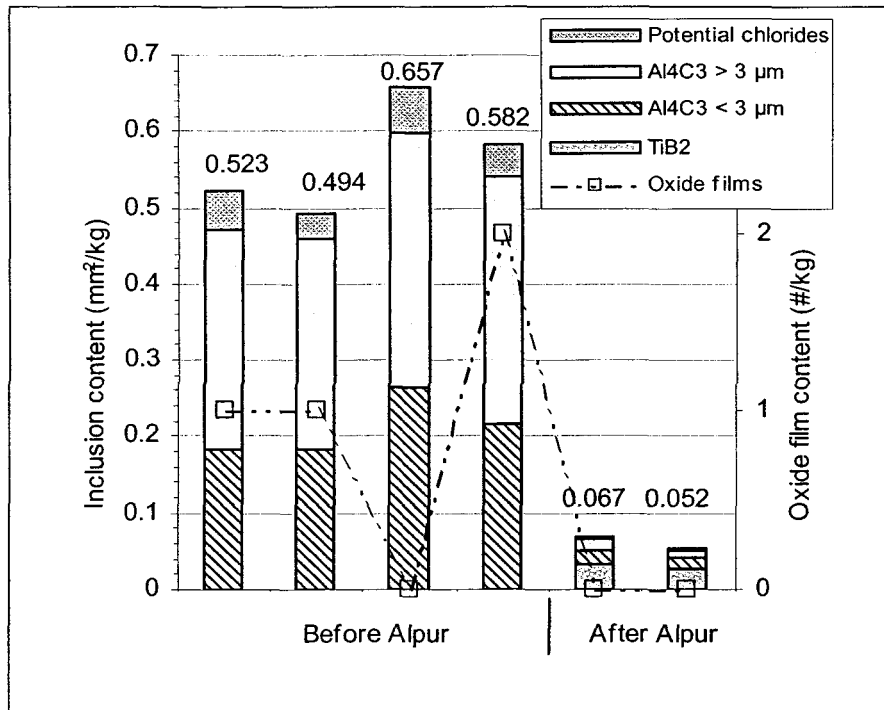


**Figure 40.** Metallographic analysis results from Prefil residues in 99.7% pure aluminum (third set).

Figure 40 illustrates that carbides of various size are present in the metal before and after degassing, whereas Figure 41 and Figure 42 are microstructures of two filter sections corresponding to before and after degassing.

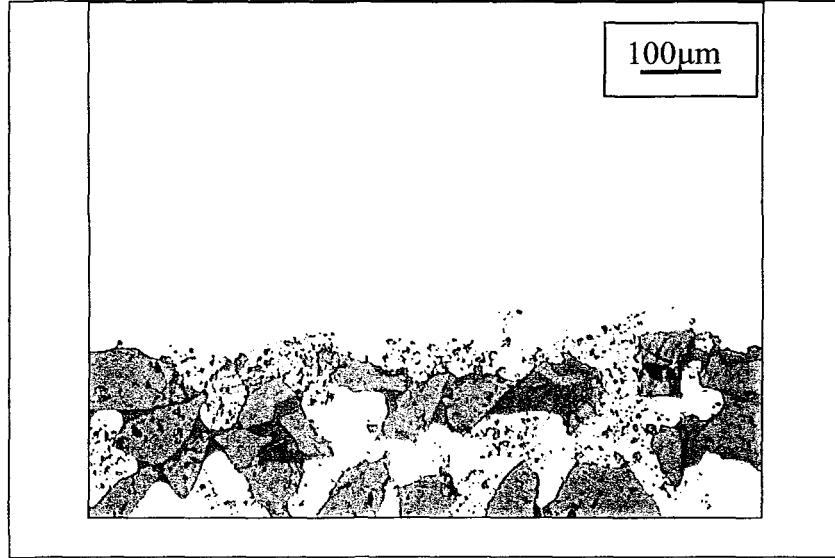


**Figure 41.** Microscopic aspect of the Prefil Filter before degassing (pure aluminum, third set).

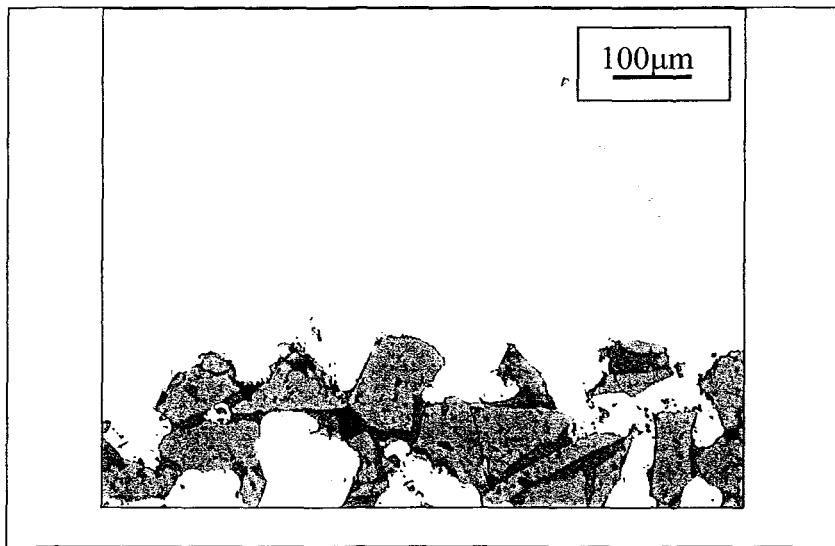


**Figure 42.**Microscopic aspect of the Prefil filter after degassing (pure aluminum, third set).

#### 4.5.7 LiMCA II RESULTS WITH PURE ALUMINUM CHARGE (THIRD SET)

Tests with LiMCA II were carried out before degassing. In the presence of argon bubbles in the liquid metal, LiMCA II apparatus was unable to start the test. Figure 43 shows the LiMCA II measurement as a function of time. LiMCA II has the capability of measuring inclusions from 20  $\mu\text{m}$  up to 300  $\mu\text{m}$ .

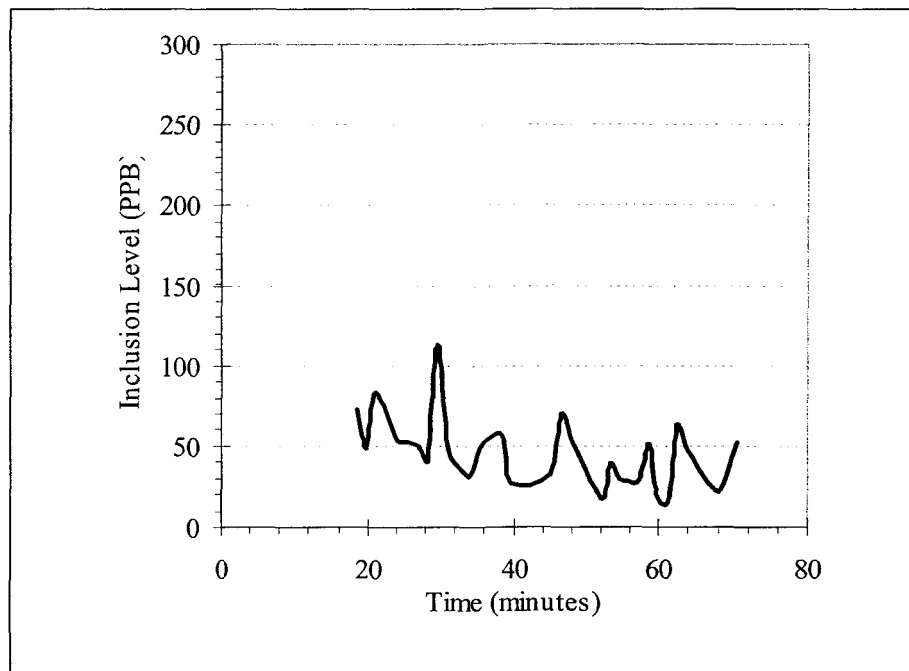


**Figure 43.** Inclusion level measured by LiMCA II before degassing in 99.7% pure aluminum (third set).

#### 4.5.8 TEST WITH AA4104 ALLOY

This alloy is normally used for car radiators. Tests were conducted at the same plant (as mentioned in section 4.5.5).

##### 4.5.8.1 Prefil Experiments

In these series of tests, metal treatment consisted of degassing and filtering using 30 ppi CFF filters. Samples were taken before and after metal treatment. Results obtained from these tests are shown in Figure 44.

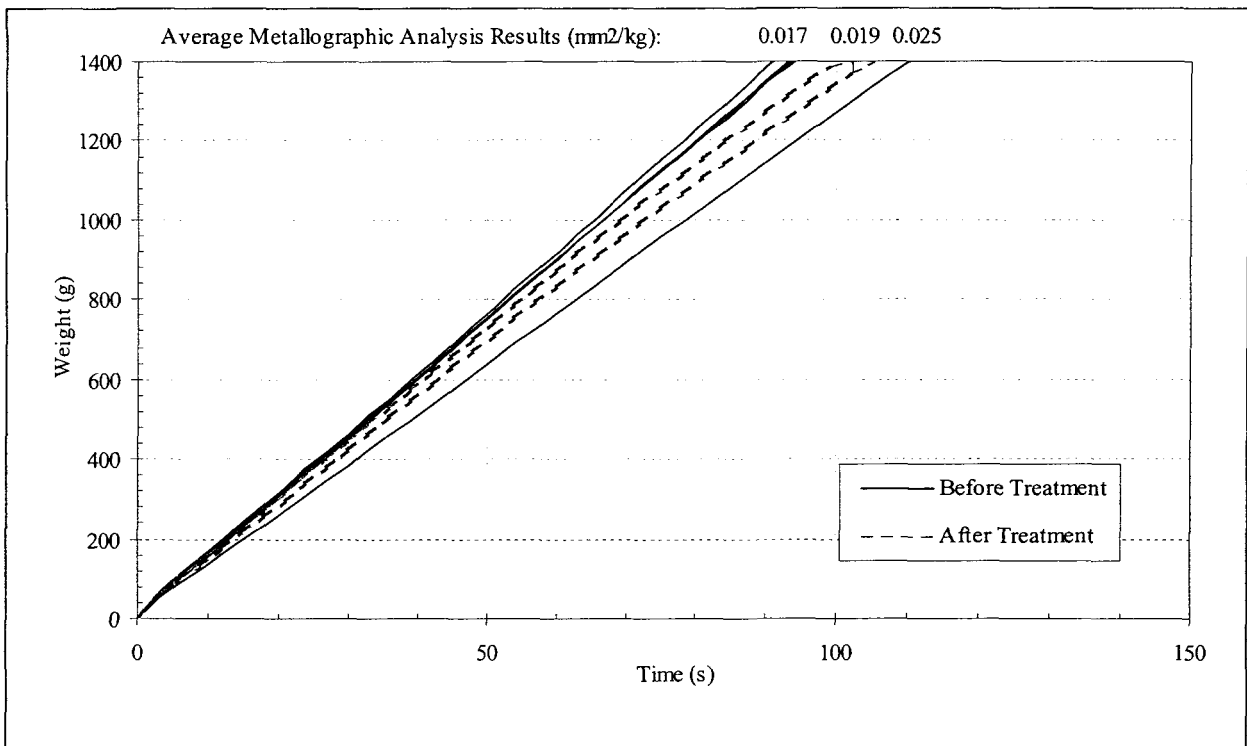


Figure 44. Prefil curves and metallographic analysis results in AA4104 alloy.

Metallographic analysis of the Prefil samples illustrated in Figure 45.

Figure 46 and Figure 47 are microstructures of filter sections before and after metal treatment.

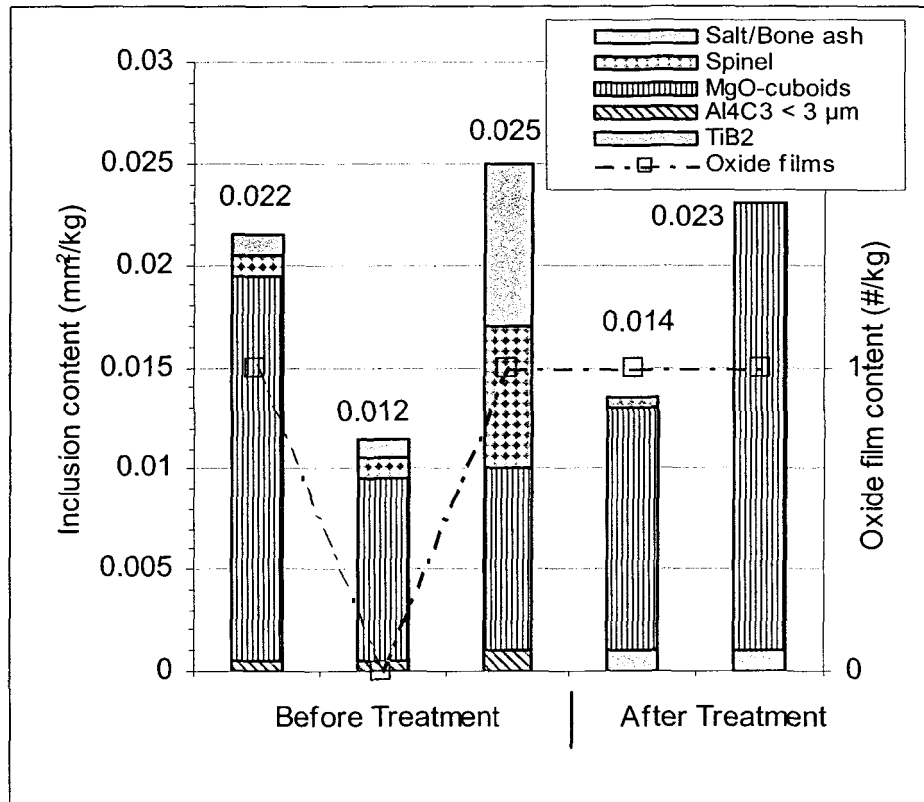
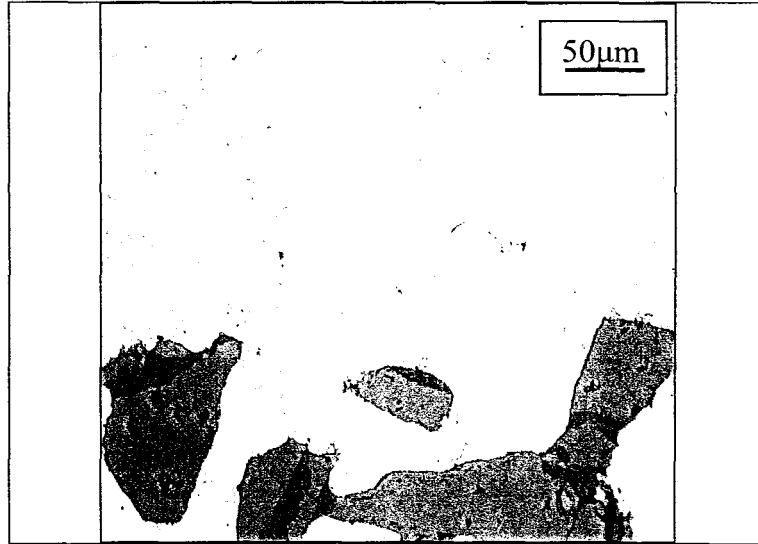
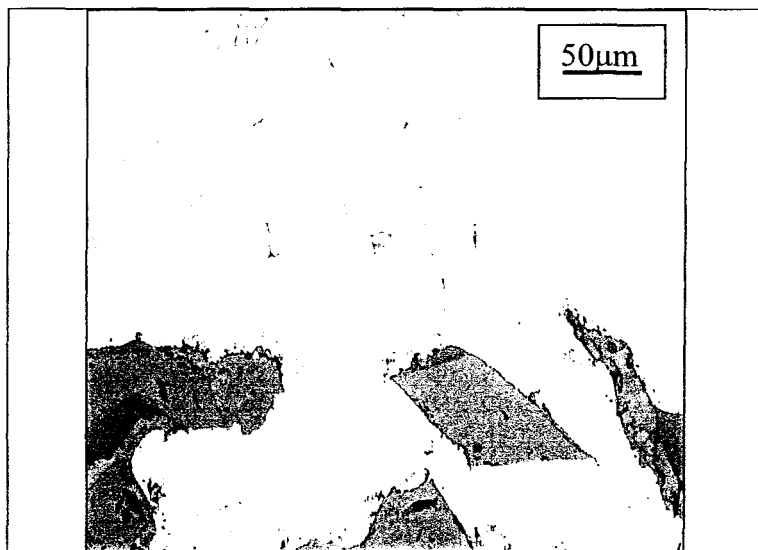


Figure 45. Metallographic analysis results from Prefil residues in AA4104 alloy.





**Figure 46.** Microscopic aspect of the Prefil filter before treatment in AA4104 alloy.



**Figure 47.** Microscopic aspect of the Prefil filter after treatment in AA4104 alloy.

It is clear that metal treatment has no significant role in the removal of inclusions. The grain refiner particles are seen in the metallographic results (Figure 45). The microscopic aspects of the Prefil filter are the same before and after treatment (Figure 46 and Figure 47).

#### 4.5.8.2 LiMCA II Experiments

For LiMCA II, tests were carried out before the metal treatment. The average of measured inclusions is about 50 PPB (2.5K/kg), as shown in Figure 48.

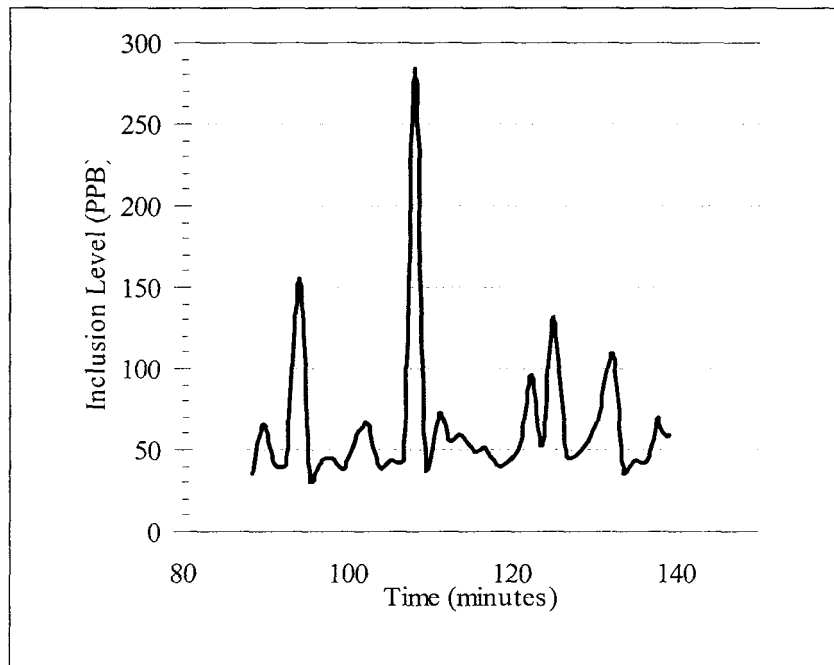


**Figure 48.** Inclusion level measured by the LiMCA II before metal treatment in AA4104 alloy.

#### 4.5.9 TEST WITH A356.2 ALLOY

##### *First Set at a Primary Aluminum Producer Plant*

The tests were conducted at the same primary aluminum plant with a launder where 70 tons of A356.2 alloy in T-Bars were cast in a one-hour period.

##### 4.5.9.1 Prefil Results

Samples were taken before and after degassing and filtration. The Prefil results are shown in Figure 49 and the metallographic analysis is illustrated in Figure 50.

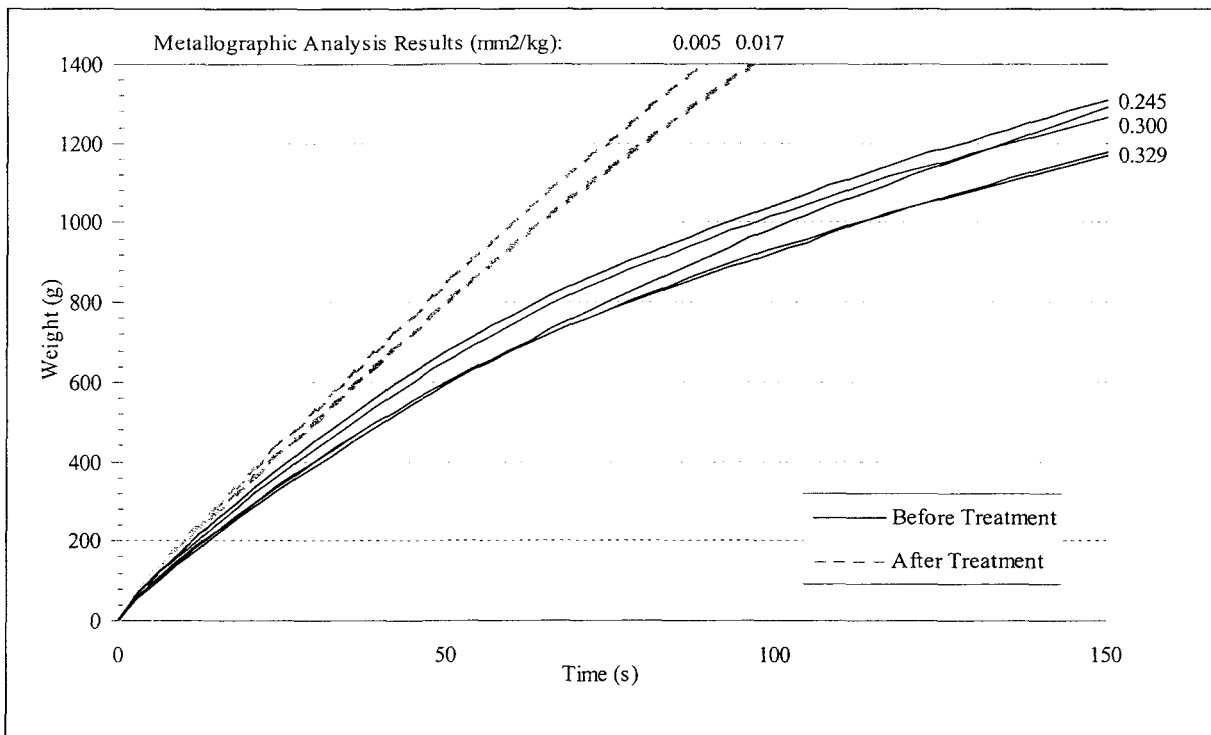


**Figure 49.** Prefil curve results with A356.2 alloy (first set).

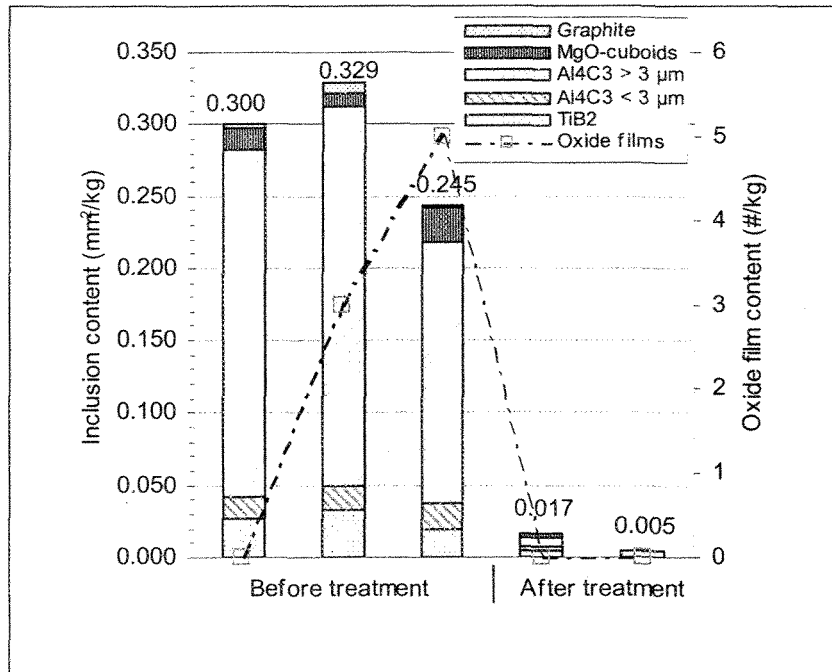


**Figure 50.** Metallographic analysis results from Prefil residues in A356.2 alloy (first set).

The small inclusions (carbides, MgO and TiB<sub>2</sub>) clearly affect the curvature of the Prefil curve. Also, these inclusions gradually clog the filter and reduce the filtration rate.

#### 4.5.9.2 LiMCA II Results

LiMCA II performed measurements before the melt treatment and the results are shown in Figure 51. Average inclusion concentration is about 75 PPB (3K/kg). The metallographic results for LiMCA II shows a good level of cleanliness with small carbides that are about 80 % of the total inclusions.

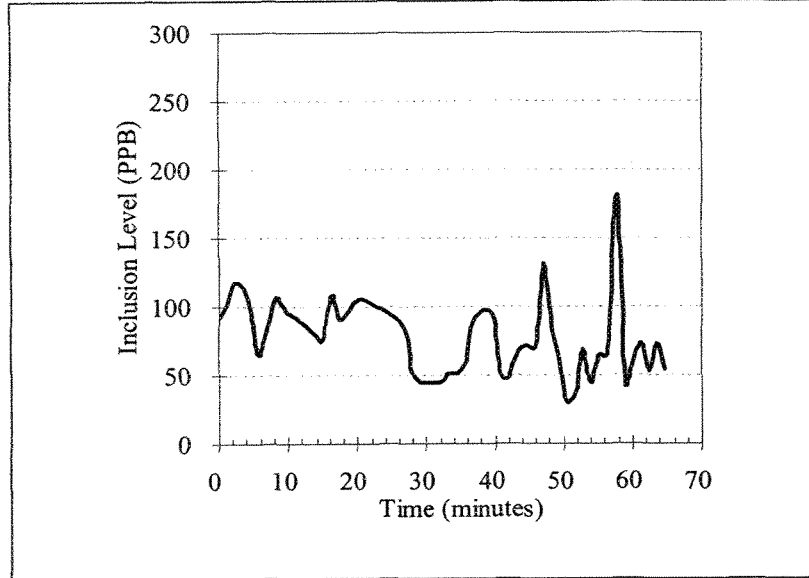


**Figure 51.** Inclusion level measured by LiMCA II before melt treatment in A356.2 alloy (first set).

Metallographic analysis results reveal the presence of large carbides, MgO and TiB<sub>2</sub> before melt treatment and small carbide particles after melt treatment. Figure 52 and Figure 53 show the corresponding microstructure aspects of carbide inclusions found in molten A356.2 alloys.

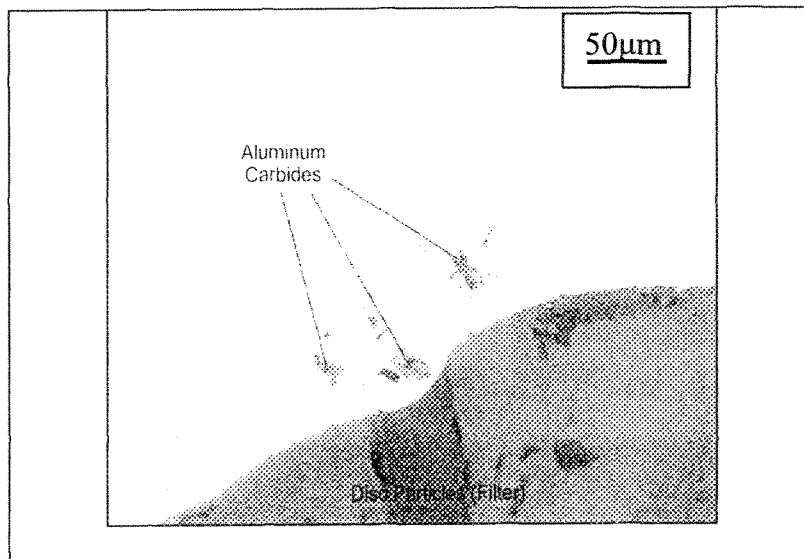


**Figure 52.** Microscopic aspects of carbides greater than 3 µm in A356.2 alloy (first set).

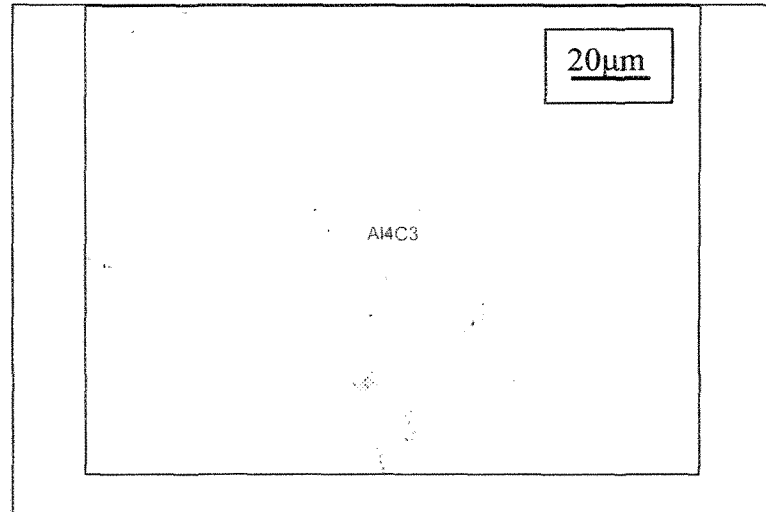


**Figure 53.** Microscopic aspect of carbide in A356.2 alloy (first set).

#### ***4.5.10 SECOND SET AT A PRIMARY ALUMINUM PLANT***

##### **4.5.10.1 Prefil Results**

All working conditions were similar to those used previously (i.e., A356.2 alloy, degassing and filtration using CFF). Samples for Prefil trials were taken before and after melt treatment. The results obtained from the first Prefil tests are shown in Figure 49 and those obtained from the second set are illustrated in Figure 54. The level of metal cleanliness before melt treatment seems to be relatively better in the second set.

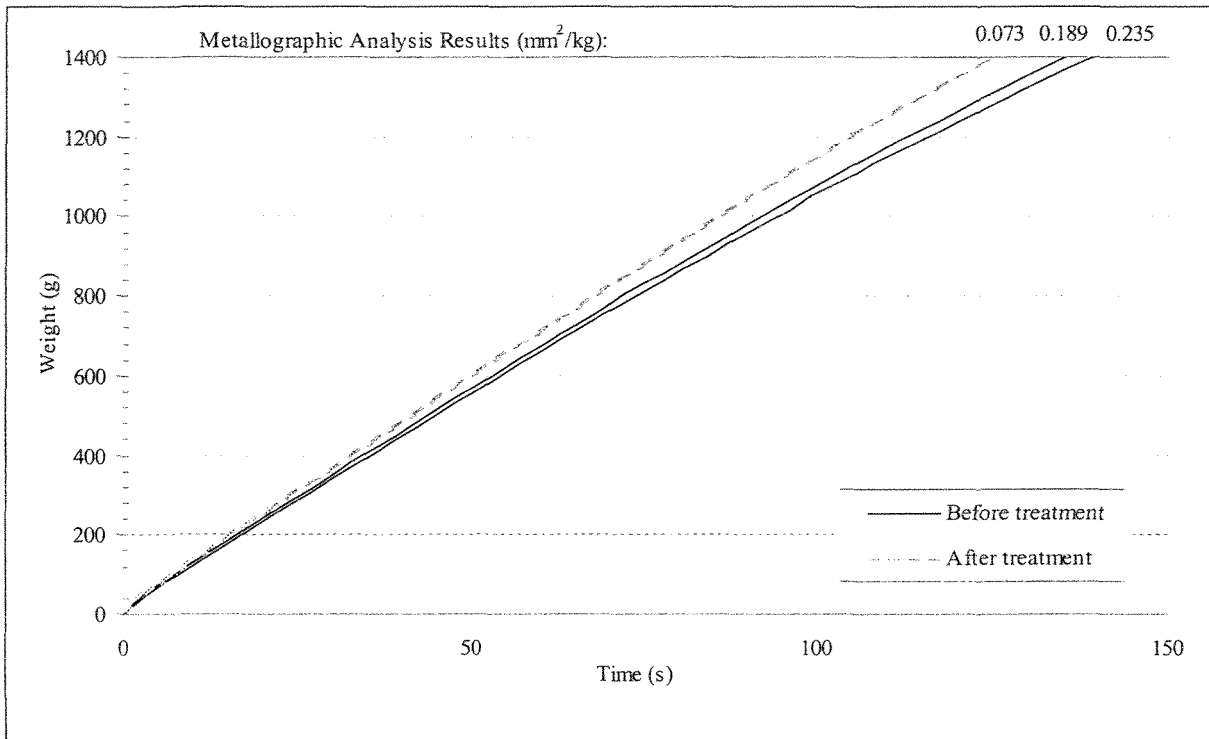


**Figure 54.** Prefil curves and metallographic analysis results in A356.2 alloy (second set).

#### 4.5.10.2 LiMCA II Results

For LiMCA II, measurements were taken before the melt treatment. The average of inclusion measurements in LiMCA II was about 300 PPB (10K/kg). In this case the results were opposite to the Prefil results (from 75 PPB in Figure 51 to 300 PPB in Figure 55) in the second set. Thus, the LiMCA II instrument is less affected by carbide but more affected

by  $TiB_2$  particles. These particles tend to agglomerate to create bigger clusters and, hence, are more easily detected by LiMCA II. Figure 55 illustrates the results of this test.

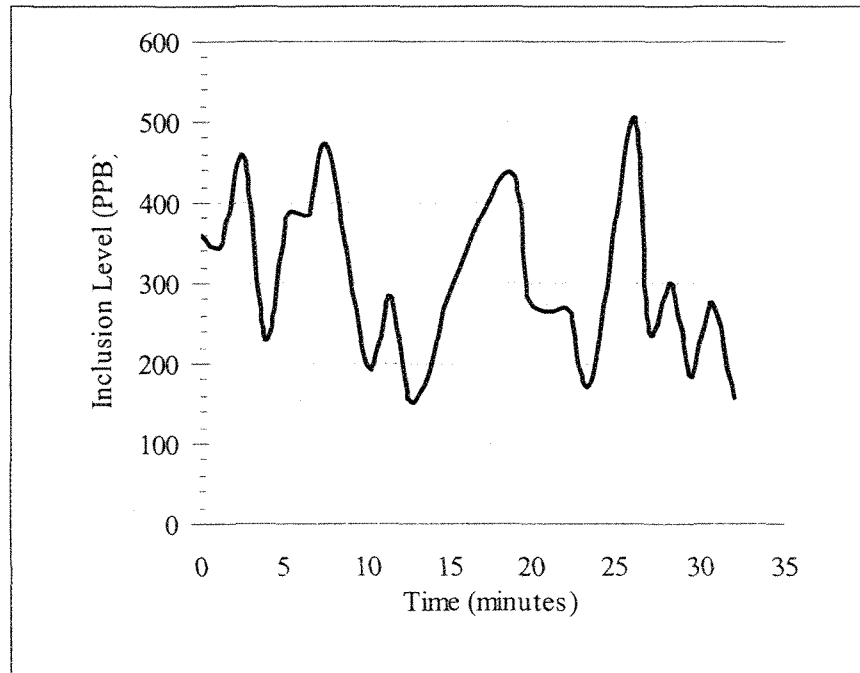


**Figure 55.** Inclusion level measured by the LiMCA II before melt treatment in A356.2 alloy (first set).

Metallographic analysis is shown in Figure 56, revealing in the first set more carbides and less grain refiner than in the second set (c.f. Figure 50 and Figure 56). The average inclusion content in the first set before melt treatment was  $0.3 \text{ mm}^2/\text{kg}$  and  $0.2 \text{ mm}^2/\text{kg}$  for the second set.



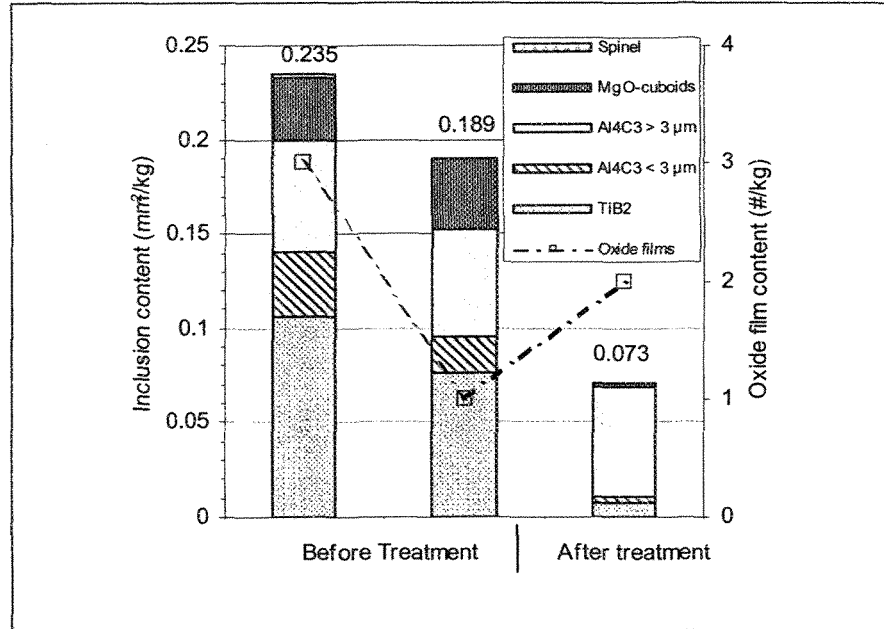


**Figure 56.** Results of metallographic analysis of Prefil residues in A356.2 alloy (second set).

Figure 57 and Figure 58 depict examples of the two different types of inclusions at high magnification.

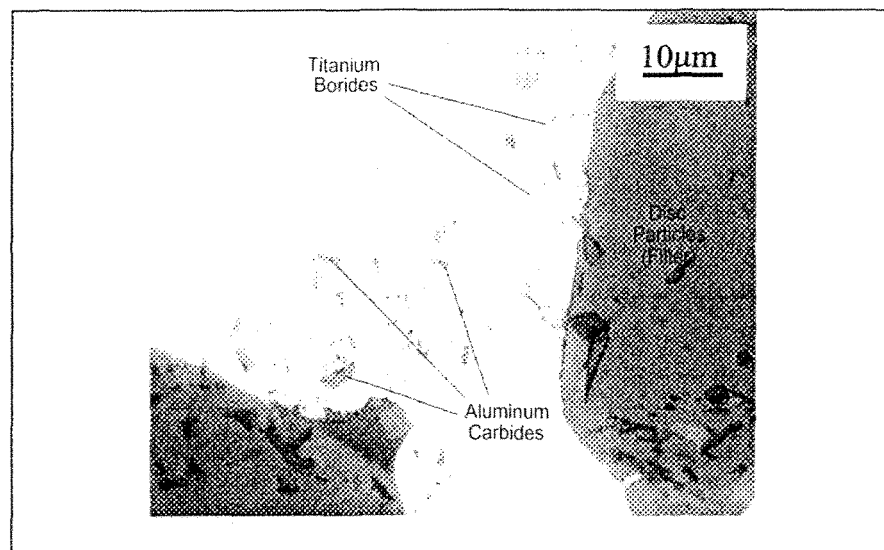


**Figure 57.** Microscopic aspect of titanium boride particles and aluminum carbides in A356.2 alloy (second set).

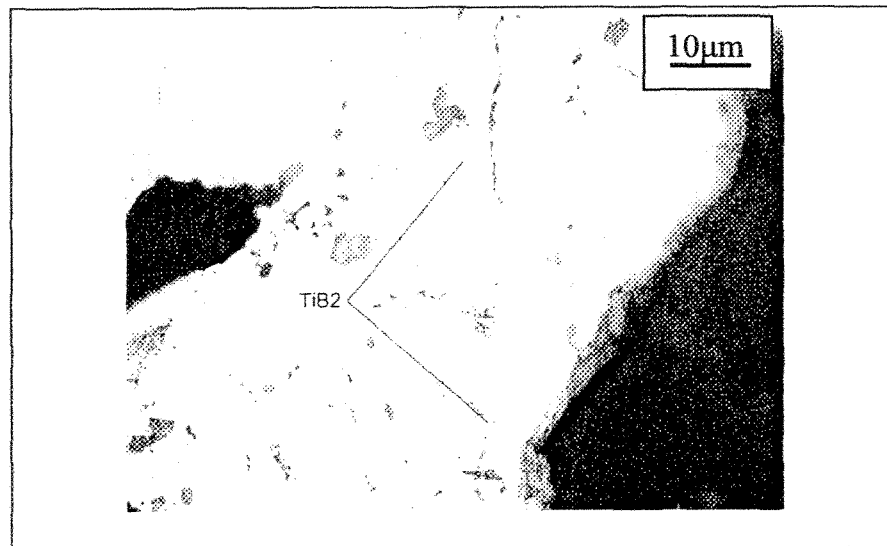


**Figure 58.** Microscopic aspect of TiB<sub>2</sub> particles in A356.2 alloy (second set).

#### 4.5.11 TEST WITH 319 ALLOY

These tests were carried out in a 35 kg capacity electrical resistance furnace. In this case, fresh ingot of 319 alloy was selected, and several tests were performed with the Prefil apparatus. Prefil curves and metallographic analysis results are shown in Figure 59 and Figure 60.

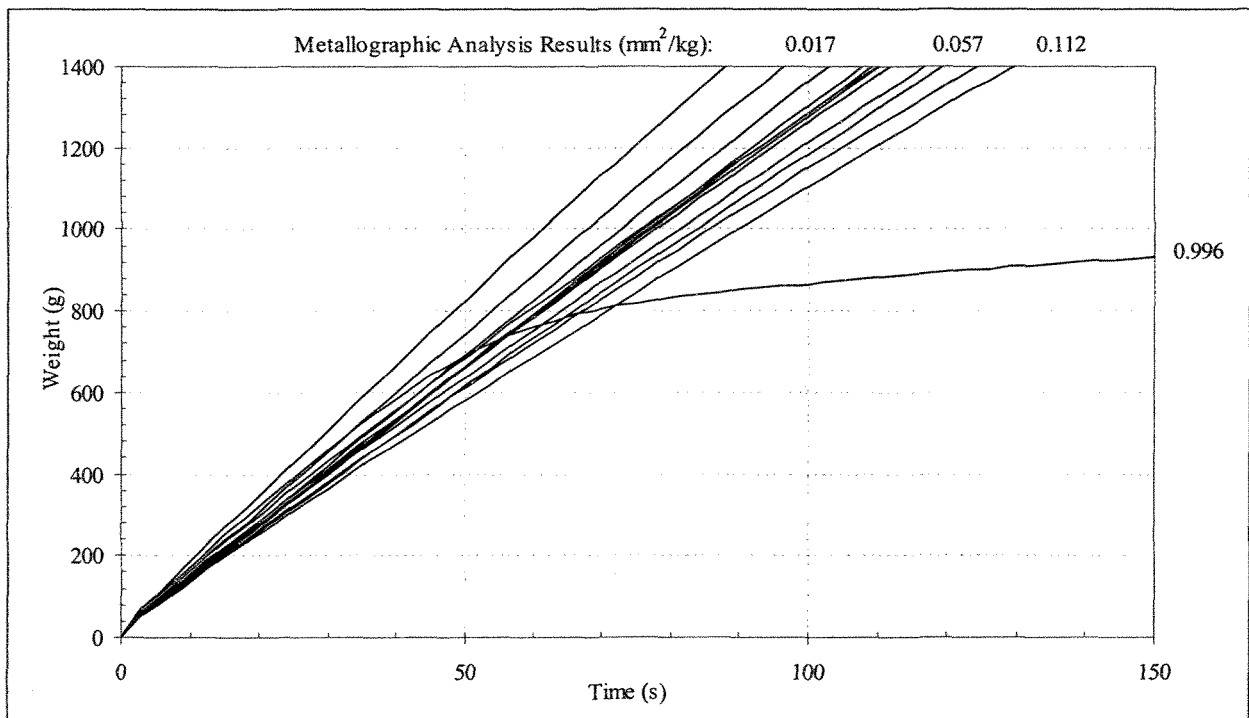


**Figure 59.** Prefil curves obtained with A319 alloy.

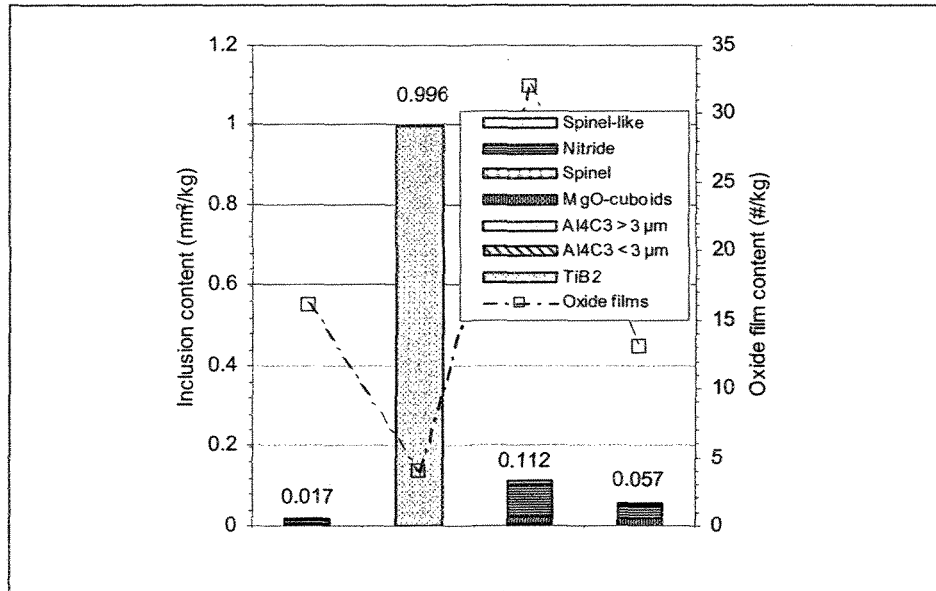


**Figure 60.** Metallographic analysis results from Prefil residues in A319 alloy.

Four metallographic analyses were performed to verify their correspondence with the Prefil curves. The lowest Prefil curve occurred due to the addition of grain refiner. Figure 61 illustrates the microscopic aspect of the Prefil filter section.

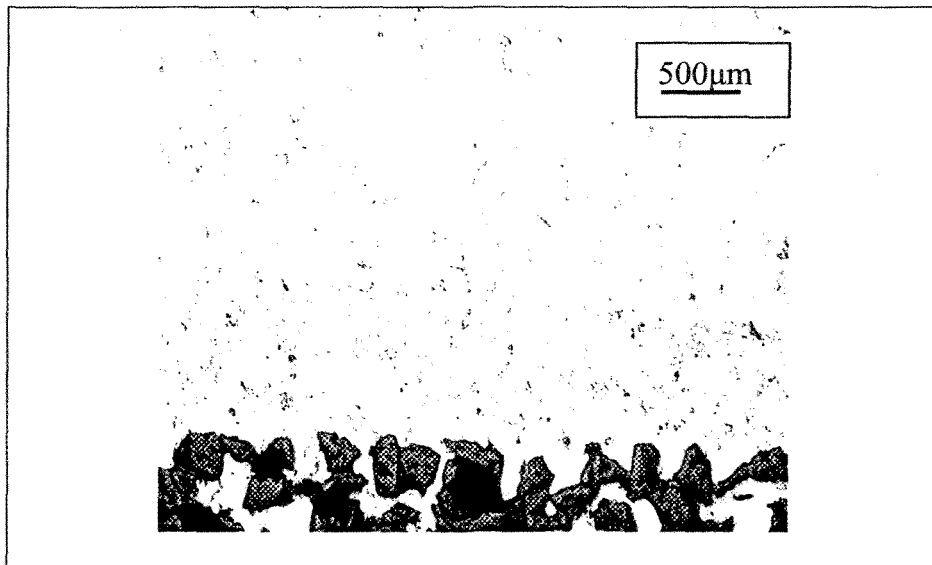


**Figure 61.** Microscopic aspect of Prefil filter in 319 alloys.

#### 4.5.12 EFFECT OF GRAIN REFINER

The tests were carried out under similar conditions described in the previous section. In this case A356.2 alloy was selected. For each test, the molten alloy was degassed for 15 minutes. Three samples were taken before the addition of a grain refiner. Six concentrations of grain refiner followed by 5 minutes degassing (after each addition) were employed. Two or three Prefil samples were taken after each addition. Figures 62 (a) and (b) shows the curves obtained from Prefil and the amount of inclusions generated from each grain refiner addition.

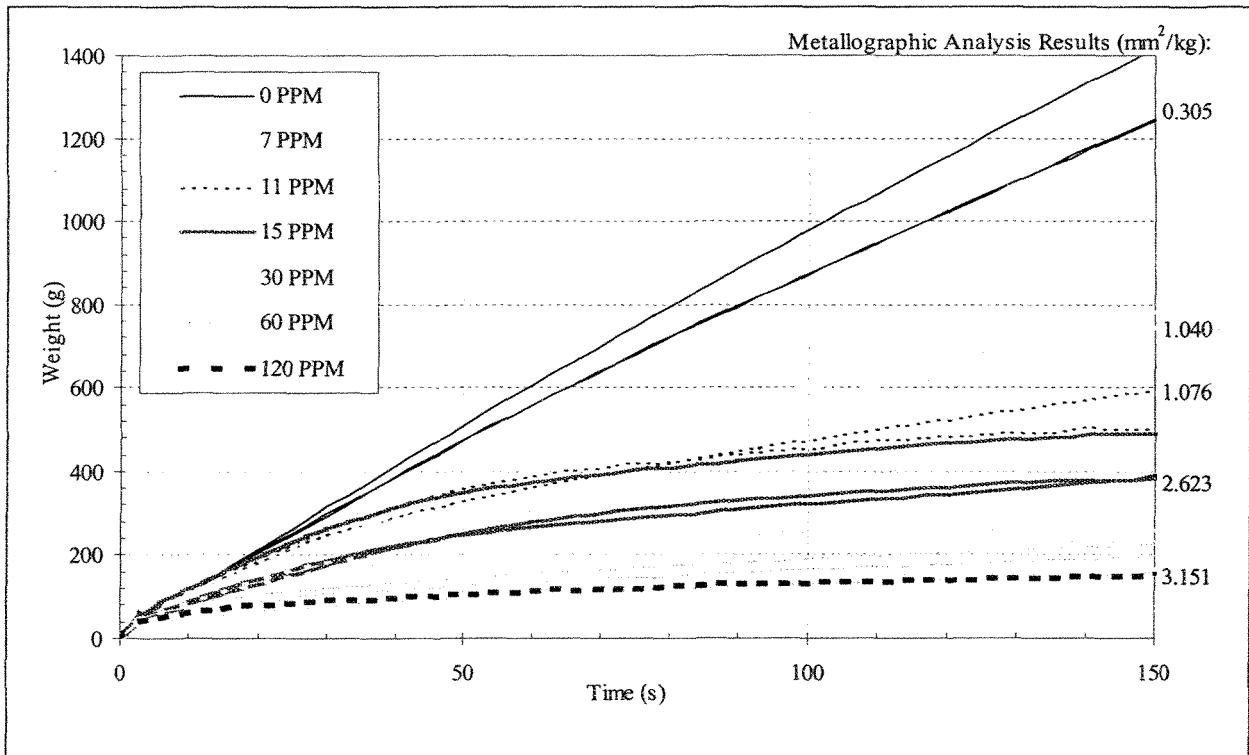
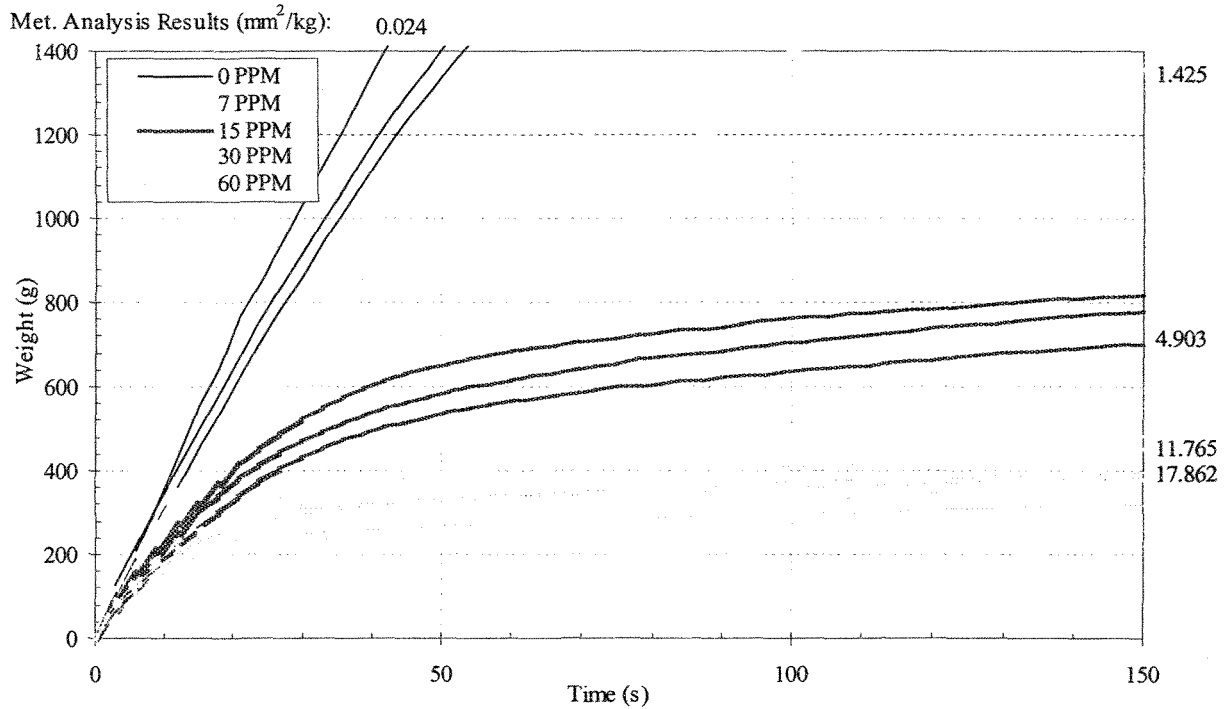


Figure 62 (a). Prefil curves and metallographic analysis results showing the effect of grain refiner on the filtration rate (fresh A356.2 alloy).



**Figure 62 (b).** Prefil curves and metallographic analysis results showing the effect of grain refiner on the filtration rate (fresh A356.2 alloy).

As are clearly shown in Figures 62(a) and (b), the filtration rate is greatly affected by grain refiner. The highest curve is the alloy without a grain refiner addition. The filtration rate progressively decreases with the increasing amount of grain refiner. When the total amount of boron in the grain refiner added to the melt reaches 60 ppm, the filtration rate is approximately nil.

#### 4.5.13 EFFECT OF MODIFICATION

In aluminum master alloys containing 3 – 10 wt% strontium, most of the strontium is present as strontium aluminidies ( $\text{Al}_4\text{Sr}$ ) and  $\text{Al}_2\text{SrO}_3$ .<sup>58</sup> The influence of the size of these

particles, as well as the influence of phosphorus on the degree of modification in a representative Al-Si hypoeutectic alloy (A356), are investigated by use of a metallographic and thermal analysis technique.<sup>59</sup>

In the present work, 200 ppm, 400 ppm and 600-ppm strontium were added to molten metal to highlight the effect of the presence of this element on the behavior of the Prefil curves. Figures 63(a) and (b) shows the Prefil results obtained for A356.2 alloys under different working conditions. Table 10. shows the inclusions concentrations as a function of Sr content and filter permeability.

Table 10. Inclusion Concentrations as a Function of Sr Content and Filter Permeability

Figure #	Curve #	Amount of Sr (ppm)	Filter Type	Amount of Inclusions (mm <sup>2</sup> /kg)
64(a)	1	200	HP	1.111
	2	400	HP	0.51
	3	200	SP	N/A
	4	200	SP	0.4
	5	200	SP	0.495
64(b)	1	600	HP	0.117
	2	600	HP	1.536
	3	600	SP	0.471
	4	400	SP	0.930
	5	600	SP	1.106

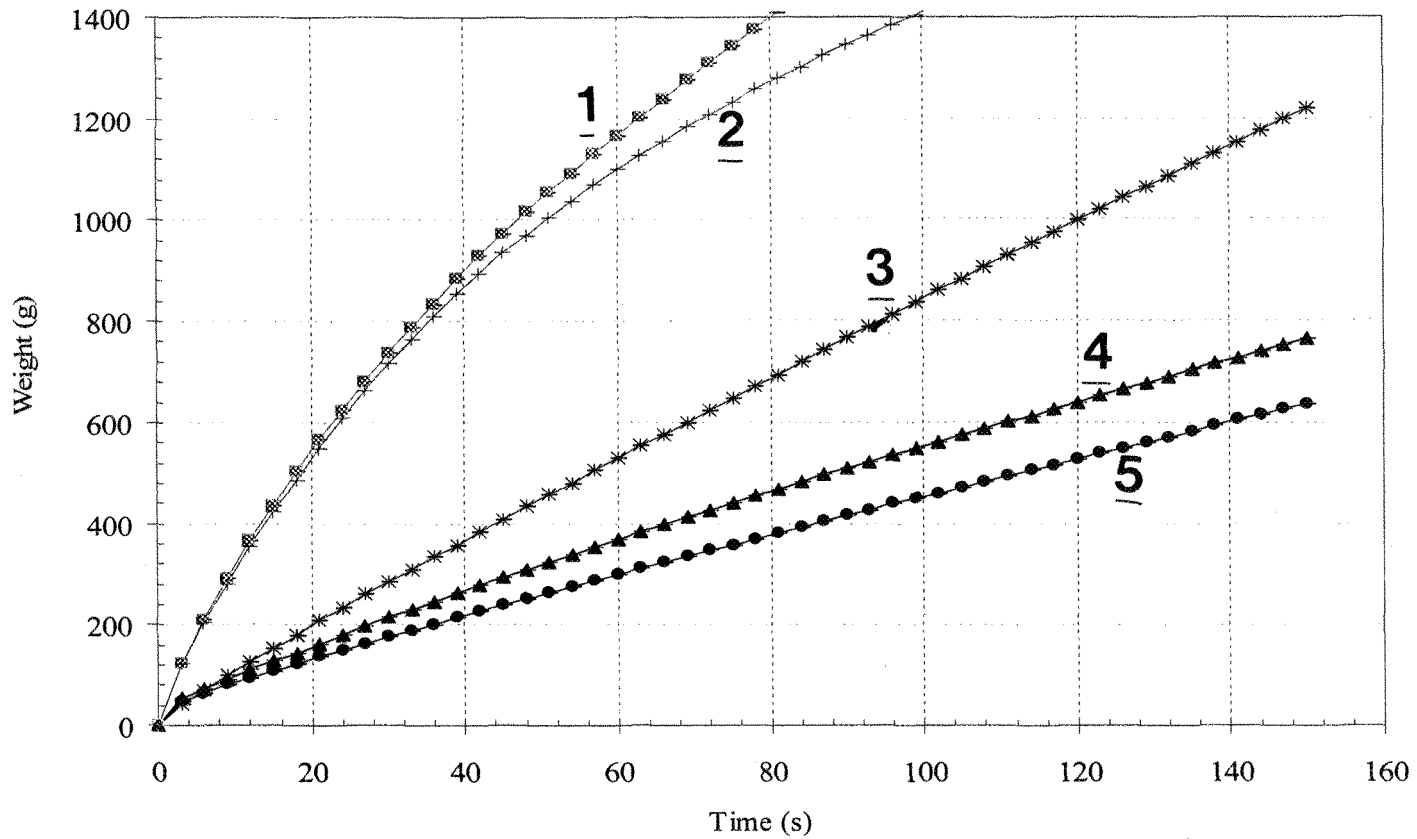
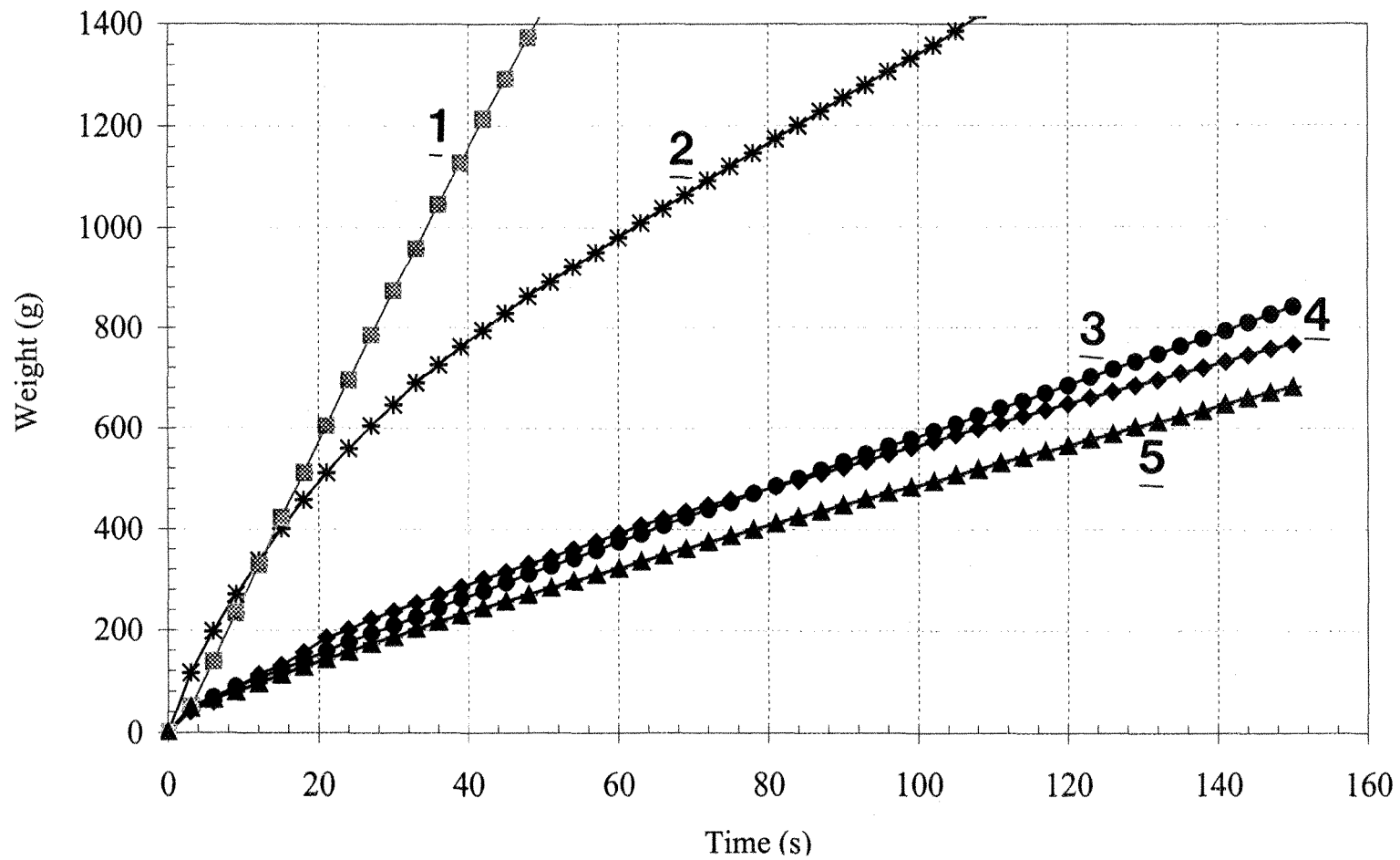


Figure 63(a). Effect of modification with 200-400 ppm strontium on Prefil curves using different filter permeability.





**Figure 63(b).** Effect of modification with 400-600 ppm strontium on Prefil curves using different filter permeability.

Figure 64 illustrates the microstructure of strontium oxide inclusion ( $\text{Al}_2\text{SrO}_3$ ). Whereas in Figure 65, the corresponding EDX analysis shows aluminum, strontium, and oxygen reflections.

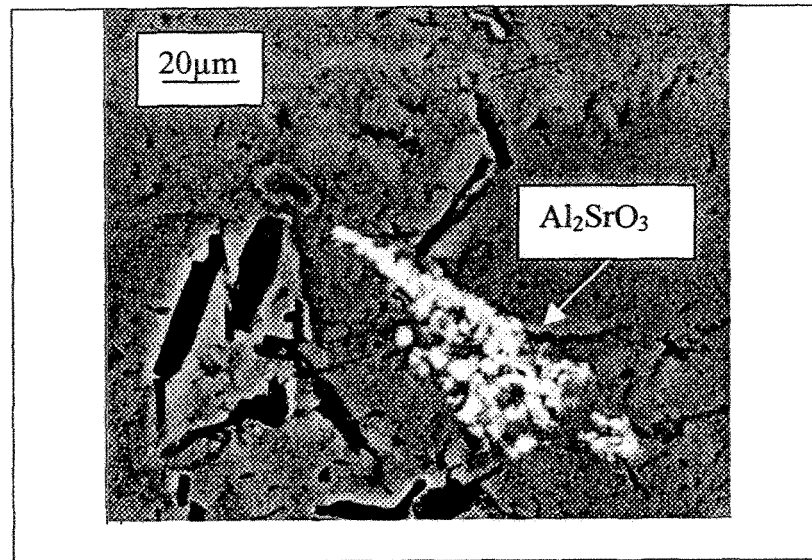


**Figure 64.**  $\text{Al}_2\text{SrO}_3$  inclusion particles in a 356.2 alloy.

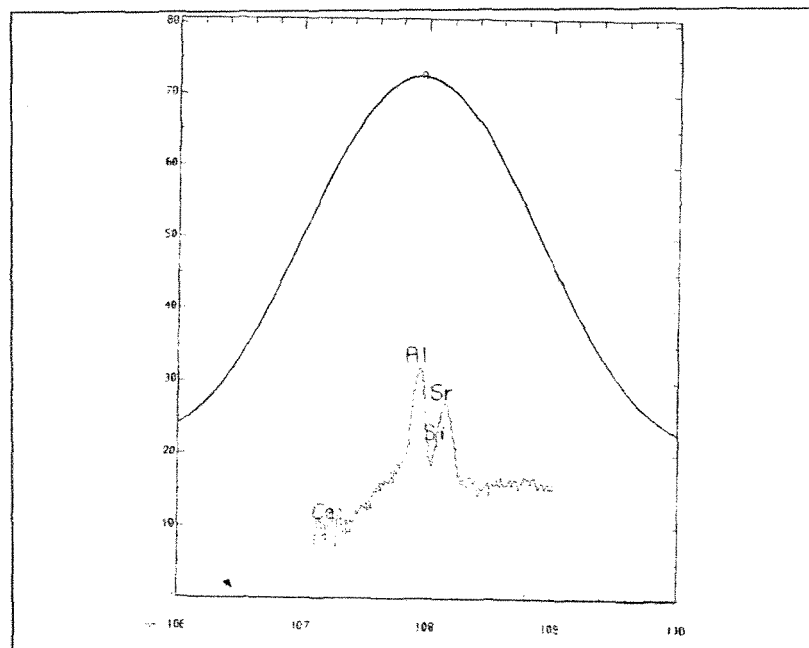


**Figure 65.** EDX analysis of O, Sr and Al observed in the white particles shown in Figure 65.

#### 4.6 PREFIL – FOOTPRINTER CURVES SENSITIVITY

Prefil sensitivity can be evaluated by comparing the variation in Prefil cleanliness curves. In the case of metallographic analysis the inclusion concentration is expressed in  $\text{mm}^2/\text{kg}$ , whereas for LiMCA II it is expressed in PPB. In order to establish correlation graphs and the expression of Prefil curves, it was necessary to find a numerical correlation. A very simple method was used to express a Prefil curve numerically – the filter metal weight was taken at 120 seconds. The best results from the Prefil test were obtained at 1400 grams of filtered metal with a maximum filtration time of 120 seconds. Under these conditions a linear extrapolation was made to obtain a value at 120 seconds. For pure aluminum tests, a correlation graph was made for the weight of filtered metal at 120 seconds as shown in Figures 66 and 67.

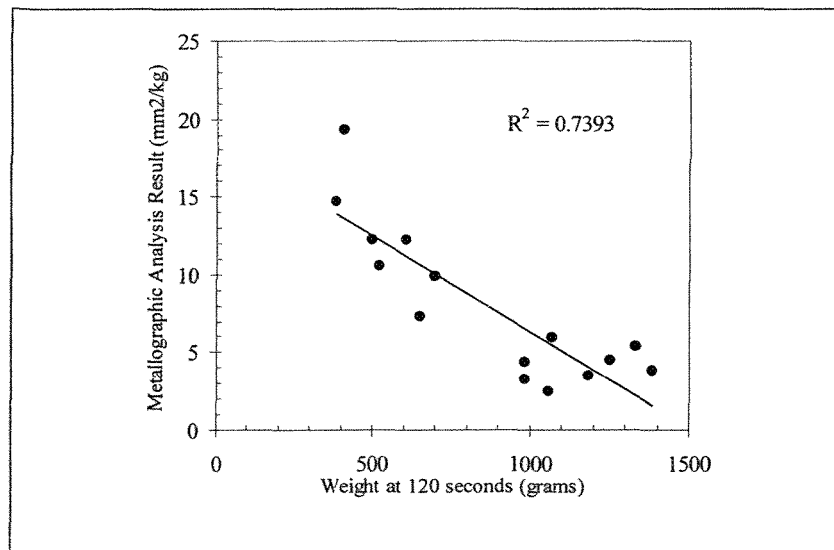


**Figure 66.** Correlation between Prefil curves and metallographic analysis results for pure aluminum.

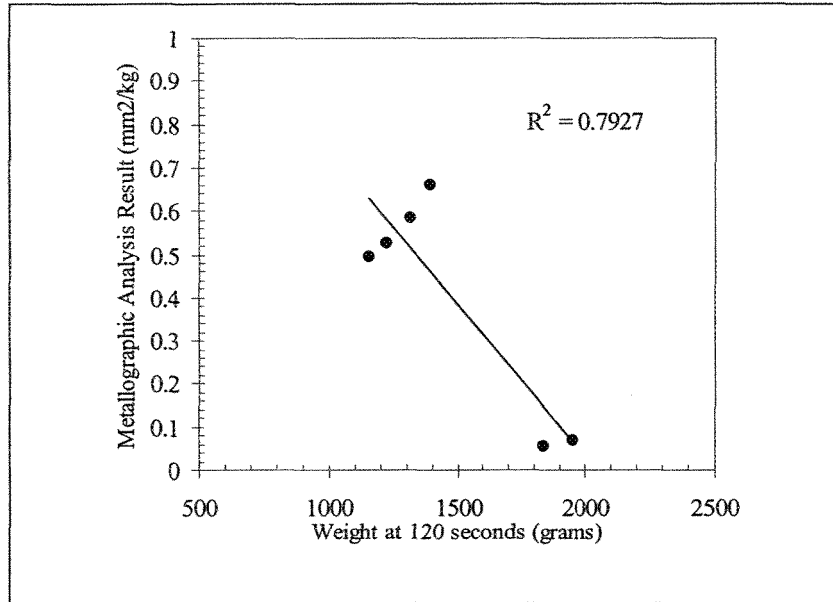


**Figure 67.** Correlation between Prefil curves and metallographic analysis results in pure aluminum for clean metal.

In addition, the correlation graph between the Prefil results and LiMCA II values was plotted in Figure 68.

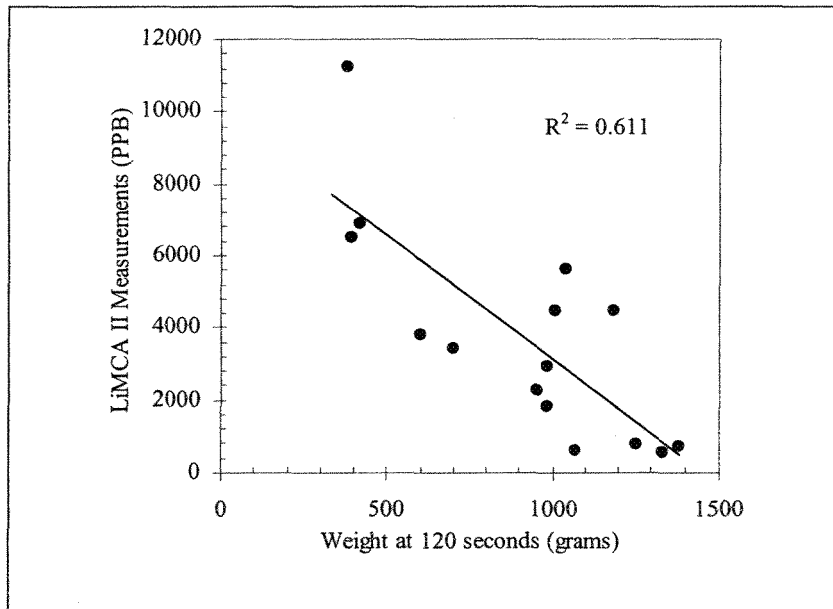


**Figure 68.** Correlation between Prefil curves and LiMCA II measurements for pure aluminum.

The same results were observed for tests performed on A356.2 alloy (Figure 69). A clear linear relationship between the Prefil tests and the metallographic analysis was obtained as demonstrated in Figure 69.

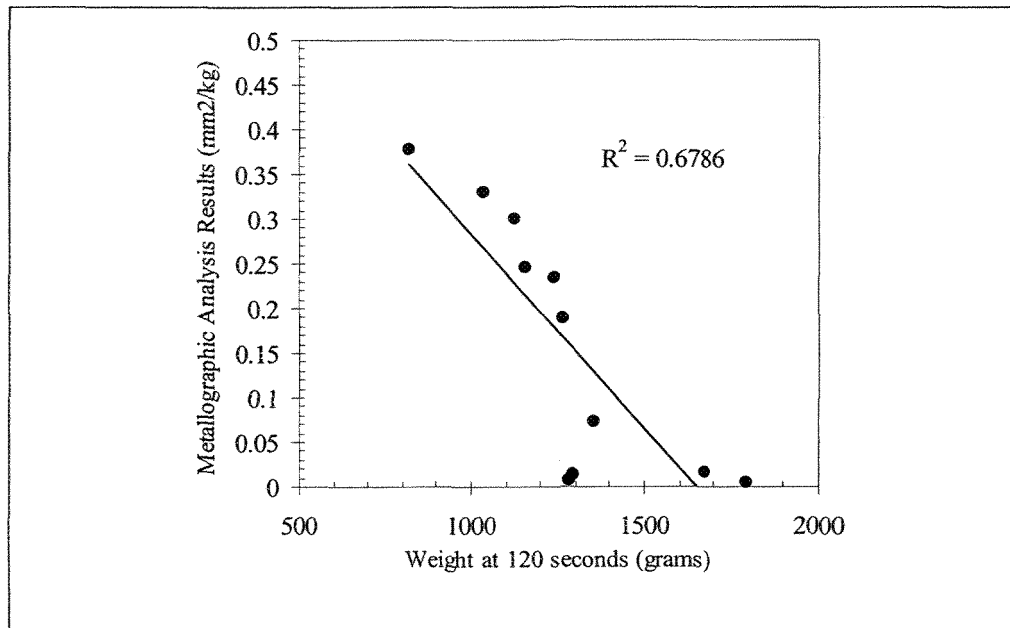


**Figure 69.** Correlation between Prefil curves and metallographic analysis results with A356.2 alloy.

Figures 66, 67 and 69 show a correlation between the Prefill tests and the metallographic analysis. When the metal is "dirty", the filtration rate is low, because inclusions captured at the surface of the Prefil filter clog the filtration process. For dirty metal, the filtered material at 120 seconds is low and metallographic results reveal a high concentration of inclusions (in mm<sup>2</sup>/kg). In contrast, when the metal is "clean", the filtered metal weight at 120 seconds is relatively high and the amount of inclusions in the metallographic analysis is low. There is also a good correlation between the Prefil curve and LiMCA II values.

Figure 68 shows that when the Prefil curve is low, the LiMCA II results are high. In this case, the metal is dirty (no degassing or filtration was applied). When the metal is clean, the Prefil curve is high and the LiMCA II results are low. When the metal is very clean, a maximum weight at 120 seconds is reached. This maximum depends on the fluidity characteristics of molten metal (mainly alloy, chemical composition, melt temperature).

In the present study, an exact correlation between LiMCA II measurements and Prefil measurements was not established. A transfer function for conversion of a Prefil curve into a LiMCA II value in PPB is not available. The first reason is that the metal sampled by both instruments is not the same. Metal cleanliness in a small furnace, such as the one used for these experiments, is not homogeneous. The second reason is that LiMCA II and Prefil are not affected in the same way by each type of inclusion. For example, Prefil is partly affected by small inclusions such as aluminum carbides, whereas the LiMCA II is insensitive to this type of inclusion. The third reason is that the principle of measurement of each technique is physically different. The Prefil produces filtration rate curves in g/s, whereas LiMCA II produces values in PPB (part per billion), or K/kg and metallographic analysis reports values in  $\text{mm}^2/\text{kg}$ . Metallographic analysis is a human evaluation of a surface covered by inclusions under the microscope. LiMCA II measures inclusions by electrical conductivity variations, while Prefil measures them by metal flow rate. Metallographic analysis is considered to be a semi-quantitative method because of the low precision of the area evaluation. Evaluation of the surface covered by inclusions under optical microscopy induces high uncertainty.<sup>61</sup>

#### 4.7 CURVES REPRODUCIBILITY

Reproducibility tests were performed under controlled environments in two research laboratories and a primary aluminum producer plant. The first laboratory had a 70-lb crucible filled with pure aluminum. A two days settling time with careful skimming of the surface was used to insure the stability of the metal cleanliness. Samples were taken consecutively to reduce metal disturbance to a minimum. There was no metal addition during the tests. The second laboratory had an 80-lb crucible containing A356 alloy. Settling time was more than two hours.

The other test conditions were the same as for the first laboratory. In the primary aluminum producer plant, a LiMCA II instrument measuring at all times during the testing ensured the stability of the aluminum cleanliness level. The reproducibility is determined empirically. The overall error induced by the Prefil instrument, the sampling itself and the possible variation in the metal cleanliness, are included. A total of 53 samples were taken. Standard deviation was calculated for all curves at 3-second intervals. Figure 70 shows an example of the average curve and standard deviation. The reproducibility calculated from the 53 tests is  $\pm 8\%$  at 95%. The calculation of the reproducibility gives approximately the same number at any time during the filtration. Considering that the standard deviation follows a chi-square distribution, a maximum standard deviation can be calculated using a level of confidence of 90%. Consequently, the reproducibility of the Prefil curve is increased to  $\pm 9\%$  at 95%.

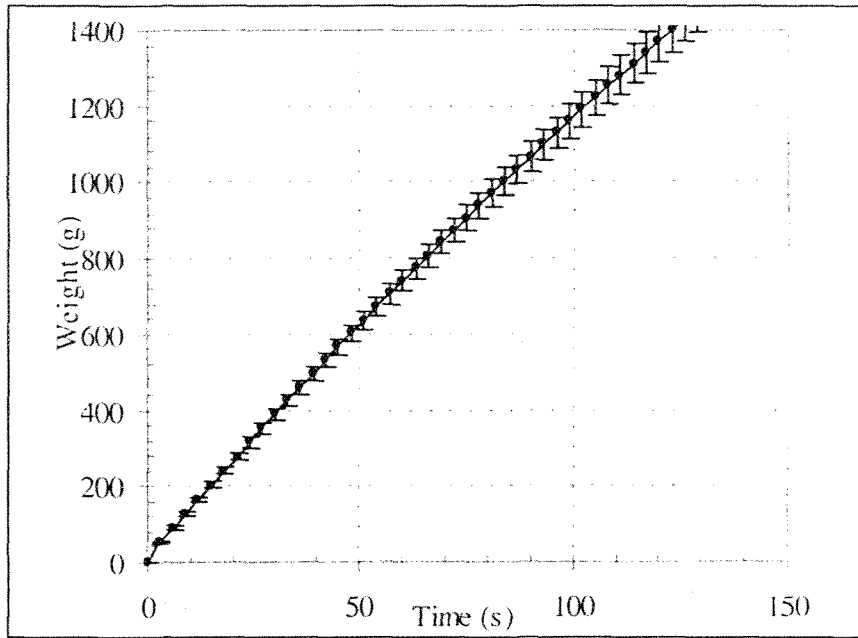


**Figure 70.** Average Prefil curves and standard deviation.



## 4.8 EXAMPLES OF INCLUSIONS

The main types of inclusions found in the alloy samples studied are borides ( $\text{TiB}_2$ ), aluminum carbides ( $\text{Al}_4\text{C}_3$ ) and magnesium oxides ( $\text{MgO}$  and  $\text{MgAl}_2\text{O}_4$ ).

### 4.8.1 BORIDES

The sample associated with a low curve is due to a high amount of inclusions (mostly  $\text{TiB}_2$ ) concentrated on the filter surface Figure 71. The inclusion was counted to be  $54.399 \text{ mm}^2/\text{kg}$  with three oxide films. The sample that revealed a higher Prefil curve showed an inclusion content of  $0.024 \text{ mm}^2/\text{kg}$  and five oxide films.

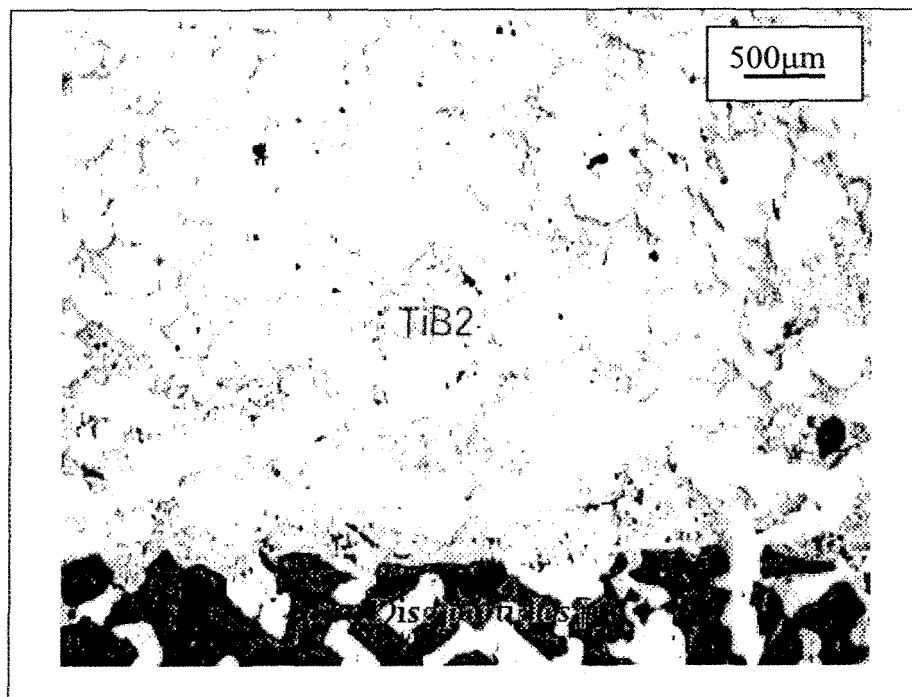


**Figure 71.** Microscopic aspect of the metal/filter interface.

With a high amount of grain refiner, it is noticed that a dense cake of  $TiB_2$  particles clogs the filter. Thus, it may be concluded that these particles affect the shape of the curves. Other types of inclusions consisting of boron are  $AlB_2$  and  $(Ti-V)B_2$ . Figure 72 and Figure 73 illustrate these inclusions.

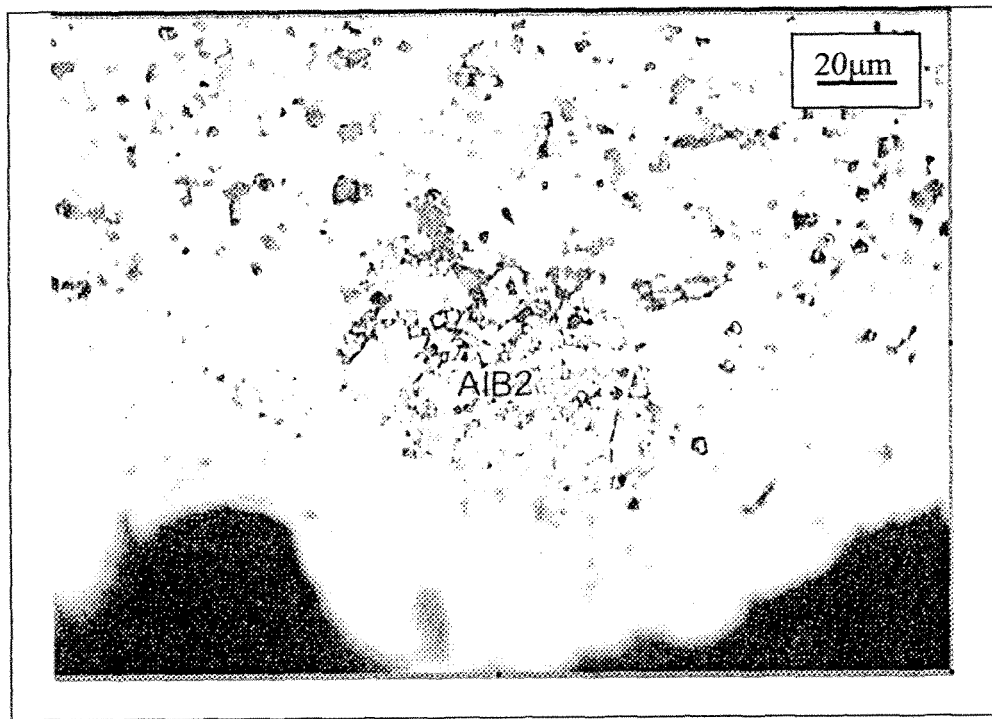


**Figure 72.**  $AlB_2$  as an inclusion in aluminum casting alloys.

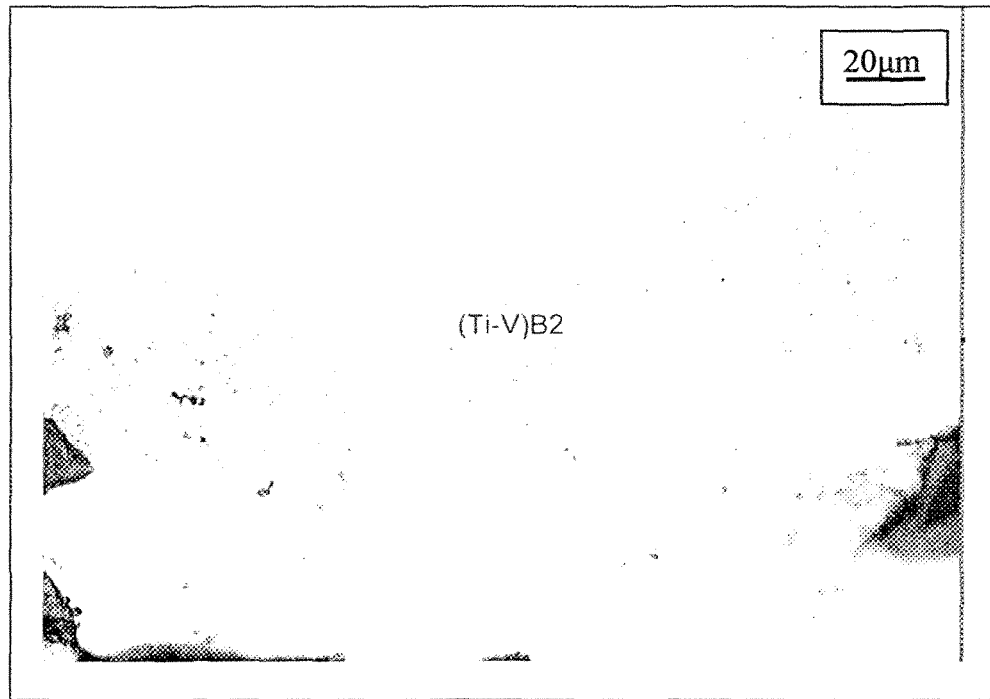
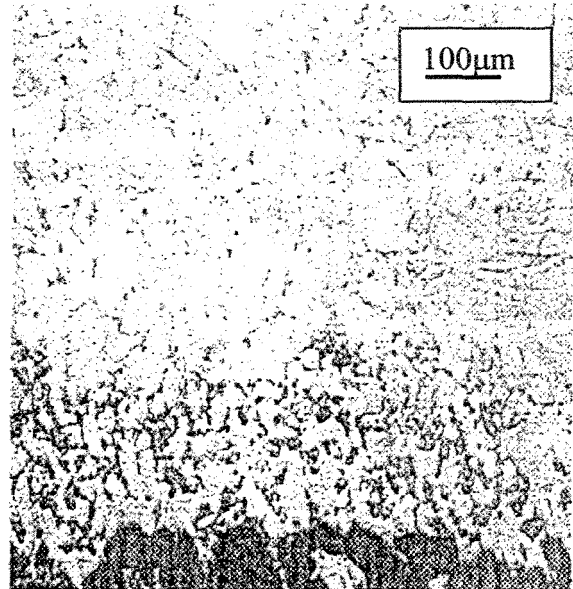


**Figure 73.** (Ti-V)B<sub>2</sub> as an inclusion in aluminum casting alloys.

The present crucibles (coded as C4) were found to be less affected than the other type of crucible by the small inclusions. The filter pore size for C4 is 130 µm compared to 90 µm for C5. Figure 74 illustrates the difference in the microstructure using the two types of filters i.e., C4 and C5.



C4 Filter



C5 Filter

**Figure 74.** Microstructure of Prefil-Test residues using C4 and C5 filters.

High permeability crucibles give higher curves than the standard one. However, with a high quantity of  $TiB_2$  particles, the filter clogs and the curves are low (more or less 0.5 kg).

Note that many samples have filtered weights of less than 0.5 kg. For accurate metallographic analysis, the amount of filtered metal should be more than 0.5 kg. Large amounts of small particles such as  $TiB_2$  or  $MgO$  could clog the filter. These samples should be rejected because of their low filtered weight. However, analyses were carried out to have an idea about the types of inclusions present in the batch.

The aluminum – titanium – boron master alloy is, in most cases, added to control grain refining in aluminum alloy, and forms titanium diboride inclusions ( $TiB_2$ ). Borides are small, hard inclusions but the clusters they form are considered to be “soft” inclusions and are sometimes discarded from the total Prefil or PoDFA counts. Sometimes these inclusions are tolerated at levels much higher than oxides.

#### **4.8.2 CARBIDES**

Aluminum carbides ( $Al_4C_3$ ) are essentially caused by carbon present in the melt from furnace coating, recycled metal, etc. Aluminum carbide agglomerates can cause degradation in the mechanical properties of the final product. In recycled metal, carbon may be introduced from plastics, wood, residual oil and various paints. In a casting furnace, carbon could originate from tooling or some linings. Small aluminum carbides ( $< 3 \mu m$ ) come from reduction cells. Large aluminum carbide inclusions ( $> 3 \mu m$ ) originate from graphite flakes or other large particles that degrade in contact with molten aluminum (Figure 75).

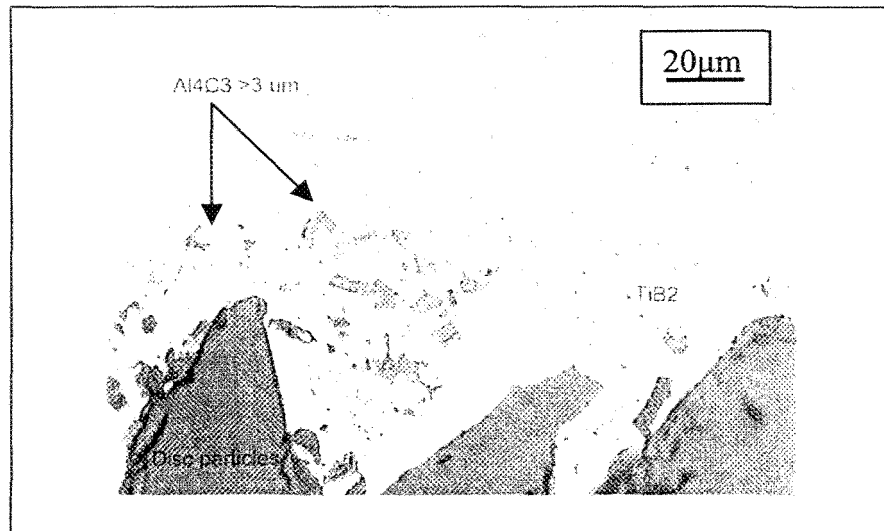


**Figure 75.** Large aluminum carbide inclusions.

Generally, the main source of carbides comes from the reaction between the melt, and the cathode and the anode in the reduction cells. Aluminum carbides larger than 3  $\mu\text{m}$  are counted in a separate category due to their detrimental effects on the alloy properties. Figure 76 shows an example of aluminum carbides.

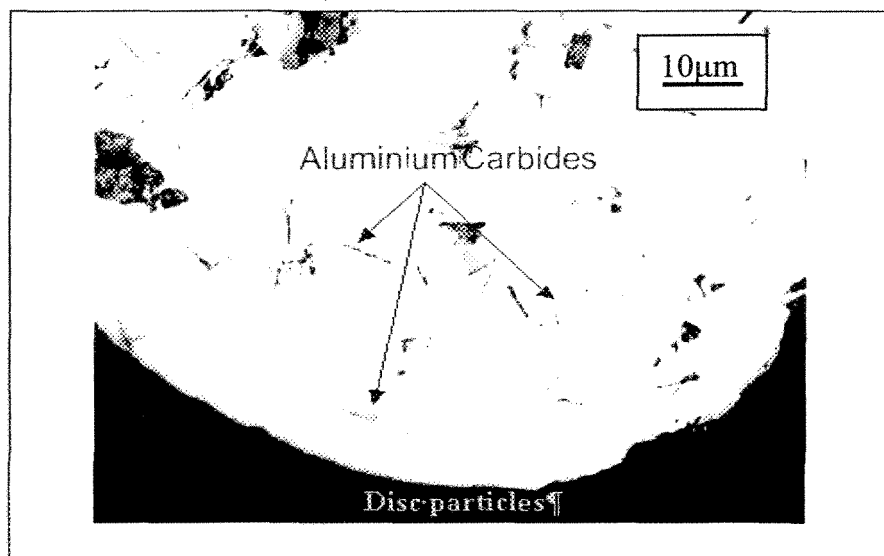


**Figure 76.** Microstructure aspect of aluminum carbides.

### 4.8.3 OXIDES

According to Lessiter and Rasmussen <sup>62</sup>, the most prevalent source of inclusions is through oxidation reactions with air. Molten aluminum reacts readily with oxygen in the air to form aluminum oxide ( $\text{Al}_2\text{O}_3$ ), which actually protects the melt from further oxidation. Disturbing the protective oxide skin, however, results in additional aluminum oxide formation when the skin breaks. These oxides are typically of skin-type morphology, although they may exist in small particles or in the form of flakes. In addition to  $\text{Al}_2\text{O}_3$ , magnesium oxide ( $\text{MgO}$ ) and magnesium aluminate spinel ( $\text{MgAl}_2\text{O}_4$ ) are the most prevalent oxides.

$\text{MgO}$  particles are created by contact of the molten metal with the atmosphere. Because of their small size, the magnesium oxide inclusions are detrimental to the filtration process only if they are present in large patches. Furthermore, they are always present with oxide films or with magnesium oxide spinel inclusions. Figure 77 and Figure 78 illustrate the two kinds of magnesium oxide inclusions.

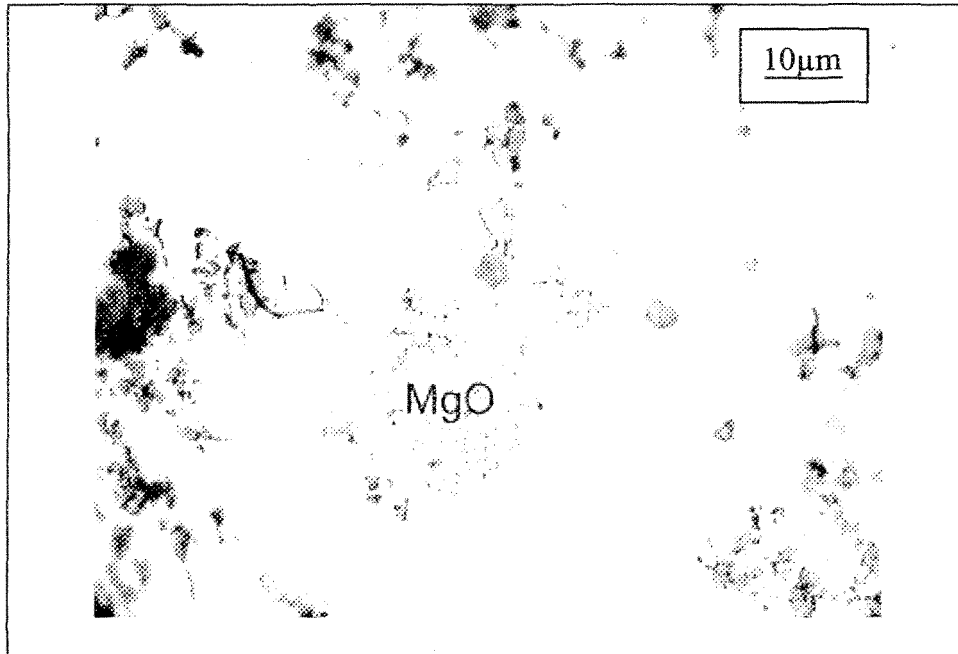


**Figure 77.** Presence of MgO at the metal/filter interface.

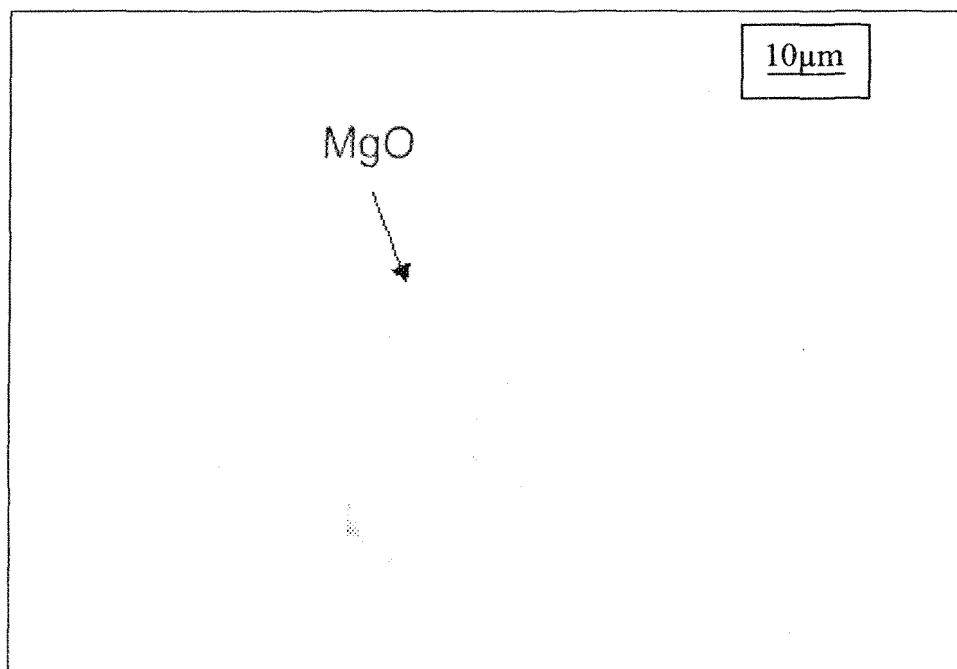


**Figure 78.** Presence of MgO in the matrix.



Figures 79 and 80 also illustrate other examples of magnesium oxide inclusions in aluminum casting alloys.



**Figure 79.** Magnesium oxides beside the filter section.

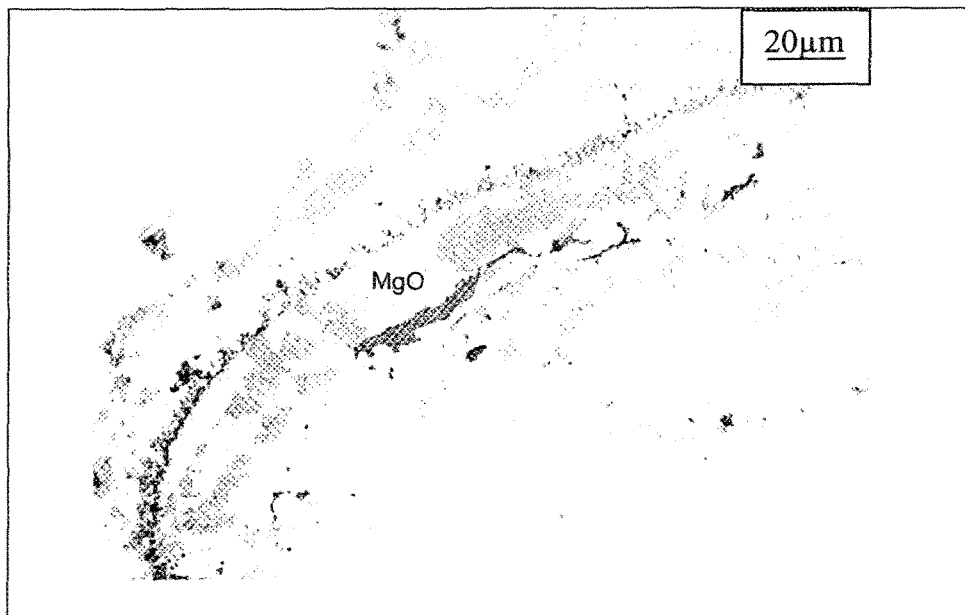


**Figure 80.** Magnesium oxide inclusion in the matrix.

Cuboid oxide inclusions are formed at high temperatures in remelting furnaces of magnesium containing alloys. Recycled metal is more susceptible to contain cuboid inclusions. Because cuboid inclusions are present along with spinel inclusions and oxide films, they are believed to be extremely detrimental to the filtration process. The cuboid inclusions are small, but always present together with large patches of magnesium oxide, spinel oxide and oxide films. They are very hard particles. Figures 81 and 82 show cuboids with oxide inclusions.

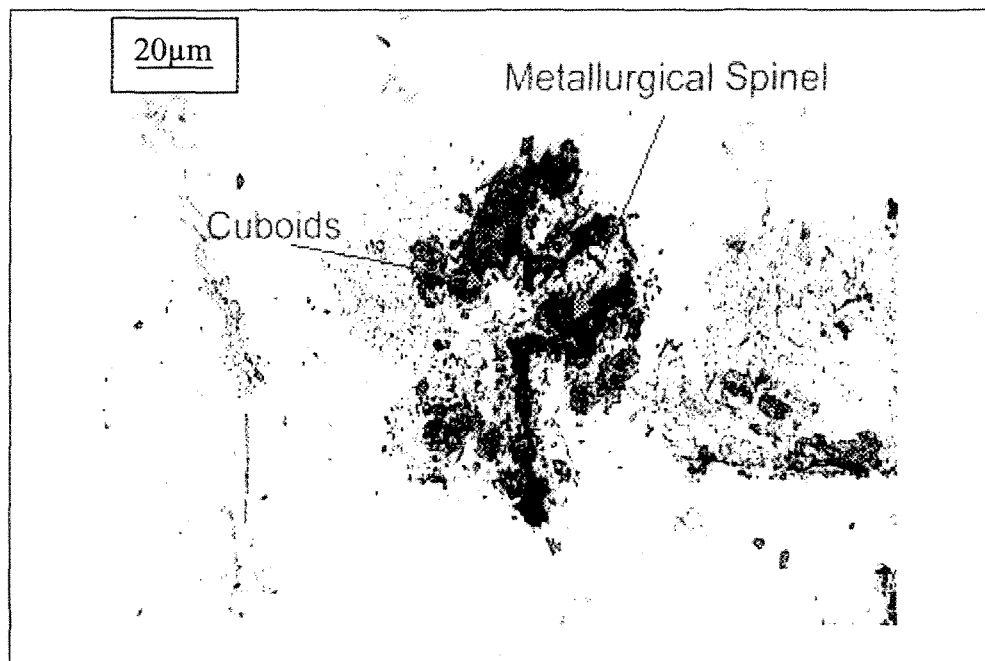
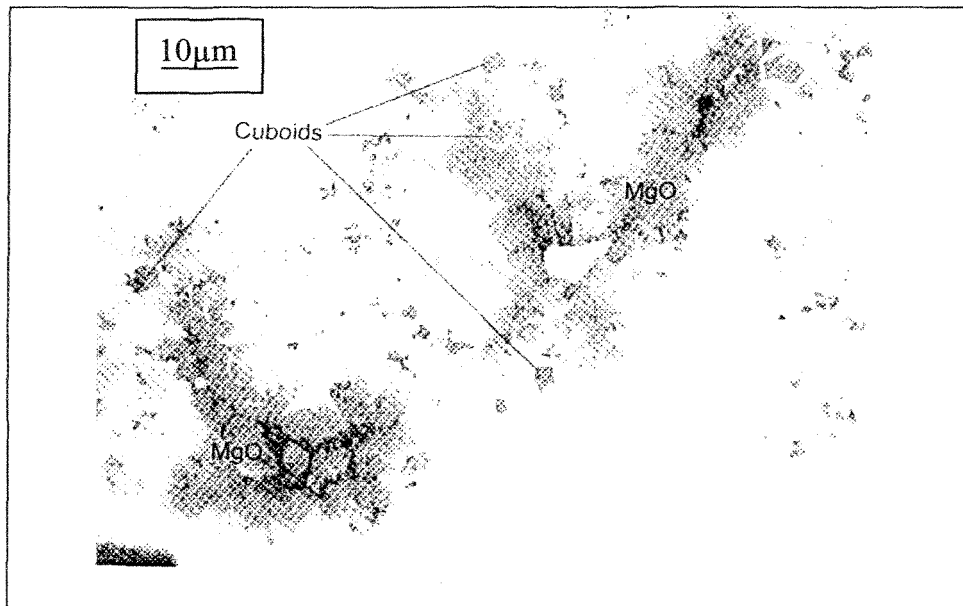


**Figure 81.** Presence of metallurgical spinel and cuboids at the interface.



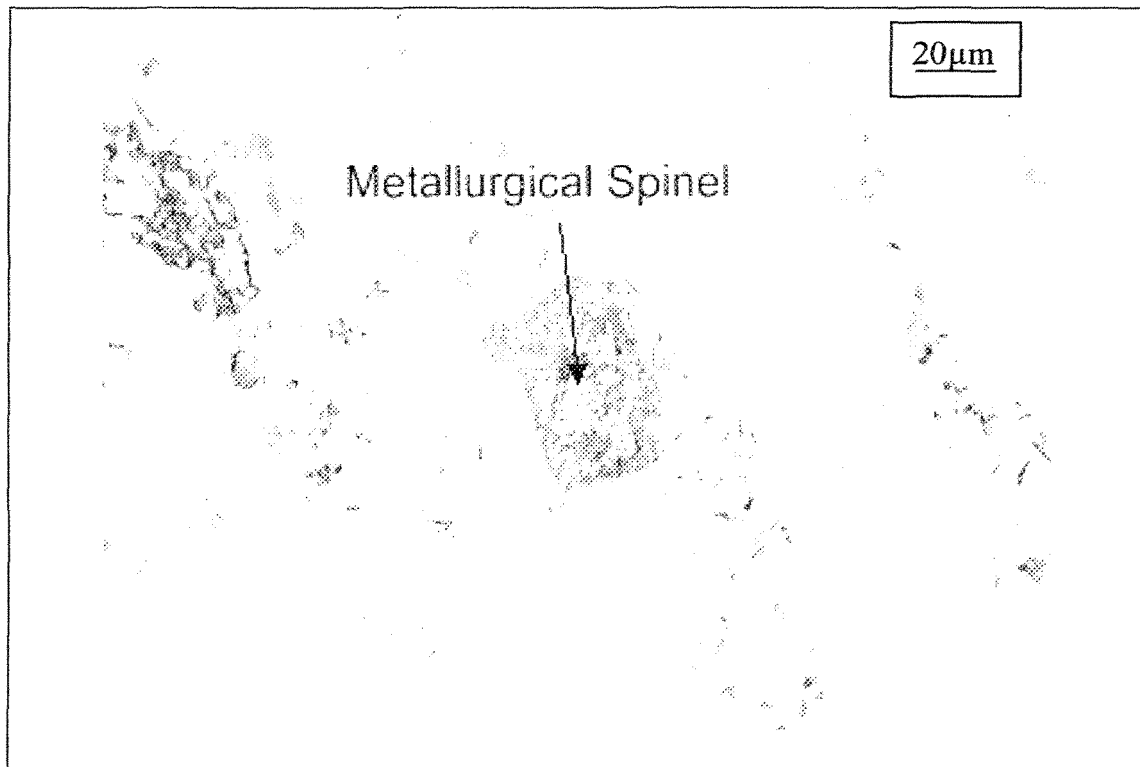
**Figure 82.** An example of cuboids with oxide inclusions.

Figure 83 shows an example of cuboid inclusions beside the magnesium oxides at the interface.



**Figure 83.** Cuboid inclusions with MgO at the interface.

The metallurgical spinels ( $\text{MgAl}_2\text{O}_4$ ) are the most detrimental inclusions found in aluminum because of their large size and hardness. An example of a metallurgical spinel is illustrated in Figure 84.



**Figure 84.** Presence of metallurgical spinel particles at the interface.

The rate of spinel formation increases with an increase in the melt temperature. Because of their large dimension, both spinel-like and metallurgical spinels can be easily

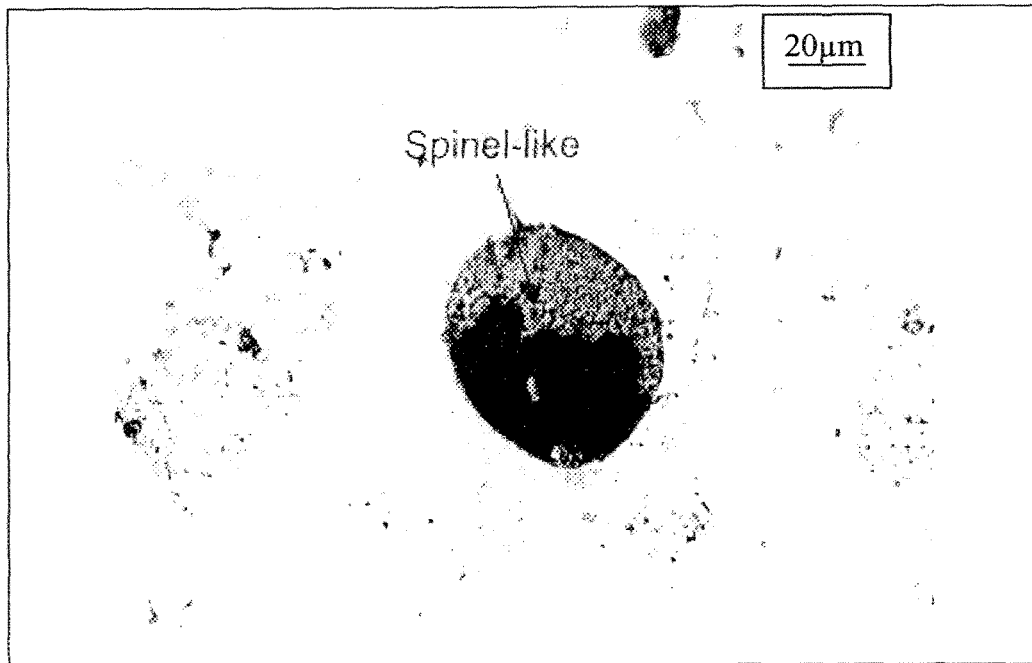


**Figure 86.** Presence of a spinel-like inclusion at the interface.

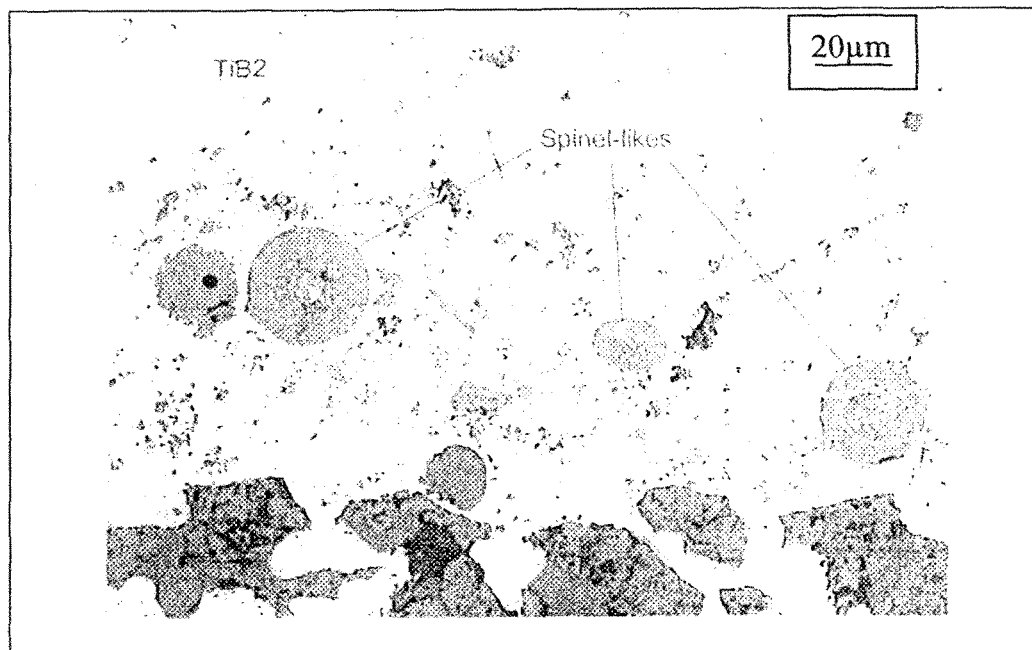


**Figure 87.** Spinel-like inclusion.

Oxide films are created in a short period of time when the molten metal is vigorously stirred (i.e., turbulence). Process handling (i.e. metal pouring or tool dipping) also creates turbulence.<sup>64,65</sup> The Prefil sampling can also cause turbulence and, thus, thin oxide films are formed in small quantities. Thin oxide films are defined as films with a thickness less than or equal to 1  $\mu\text{m}$ . Such oxide films can sometimes be removed by flotation due to fluxing action. Thus, the oxide films found in the Prefil of PoDFA samples may not necessarily be found in the ingot, as they are formed during the Prefil sampling operation. Two examples of different oxide films are shown in Figures 88 and 89.

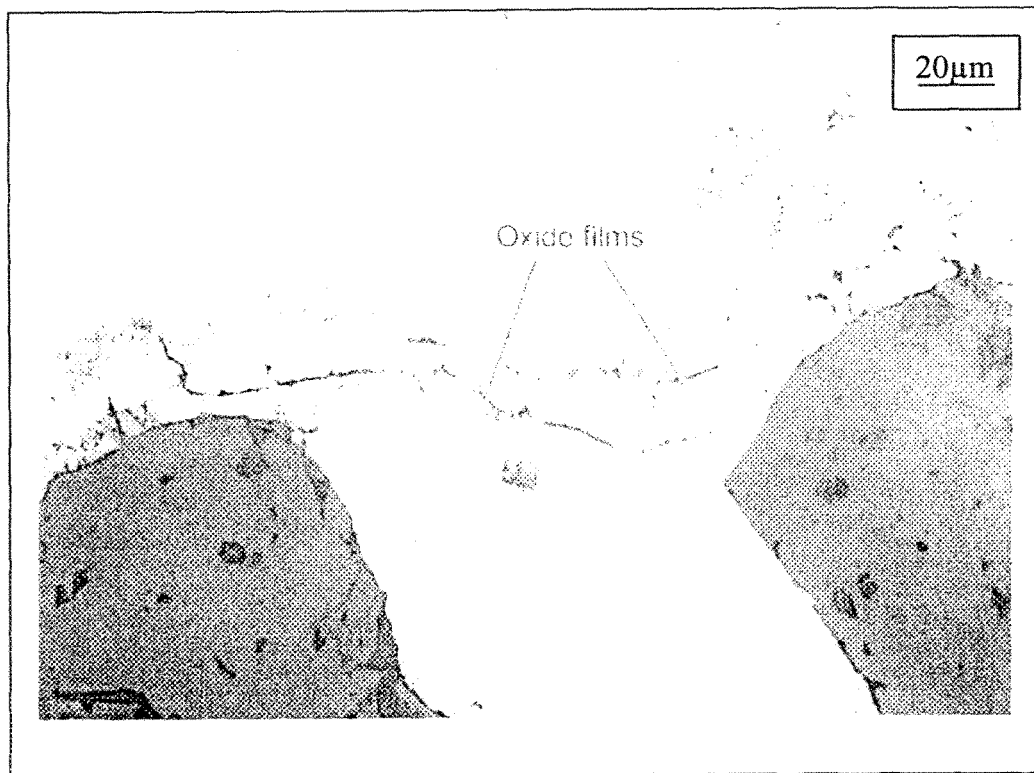


**Figure 88.** Example of a thick and long oxide film.

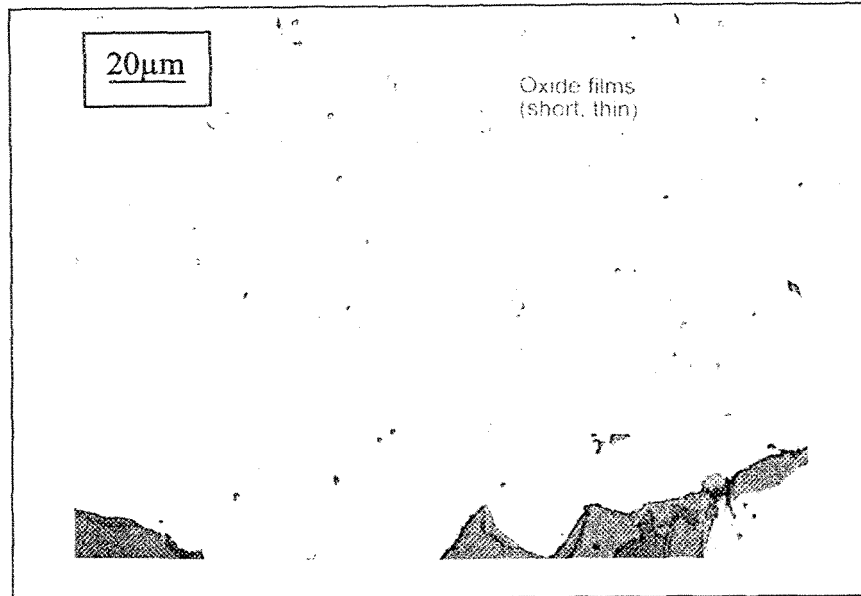


**Figure 89.** Example of a thin and short oxide film.

In some cases aluminum oxide inclusions appear as dispersed particles mixed with other types of inclusions such as  $TiB_2$ . Figure 90 illustrates this kind of inclusion.

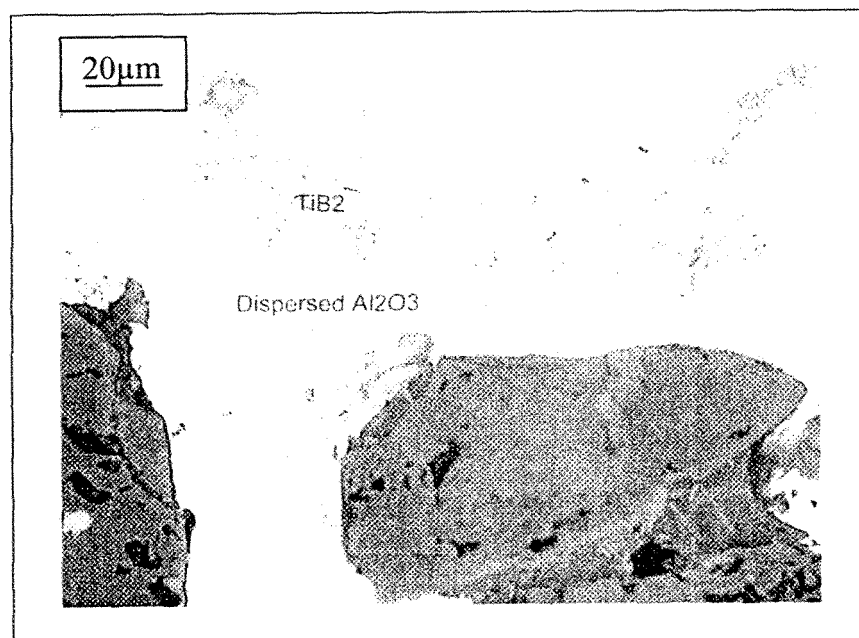


**Figure 90.** Dispersed  $Al_2O_3$  beside the filter section.

Other types of oxide inclusions that may be found in aluminum casting are bone ash and FeO/MnO. Figures 91 and 92 show these types of inclusions.

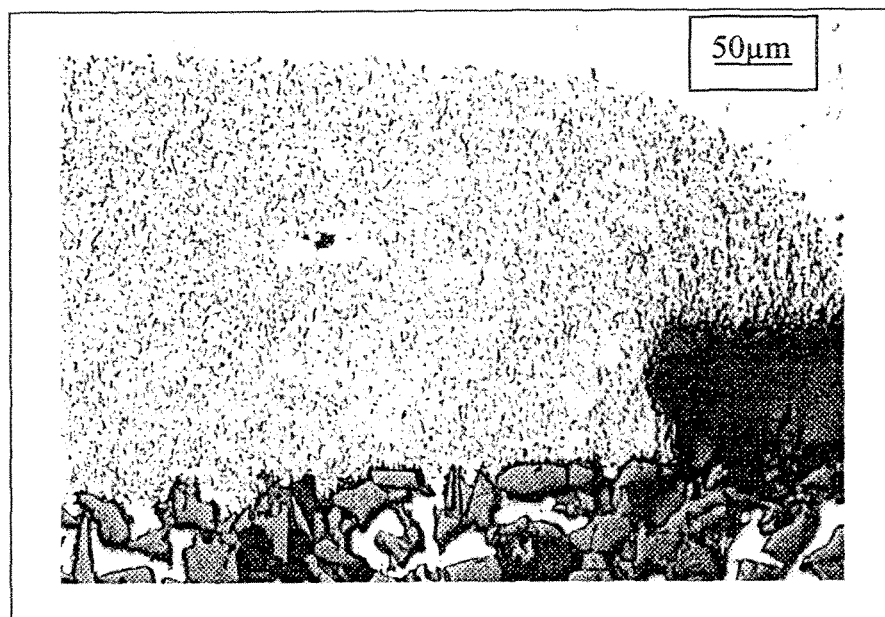


**Figure 91.** Example of Bone ash inclusions in aluminum casting.

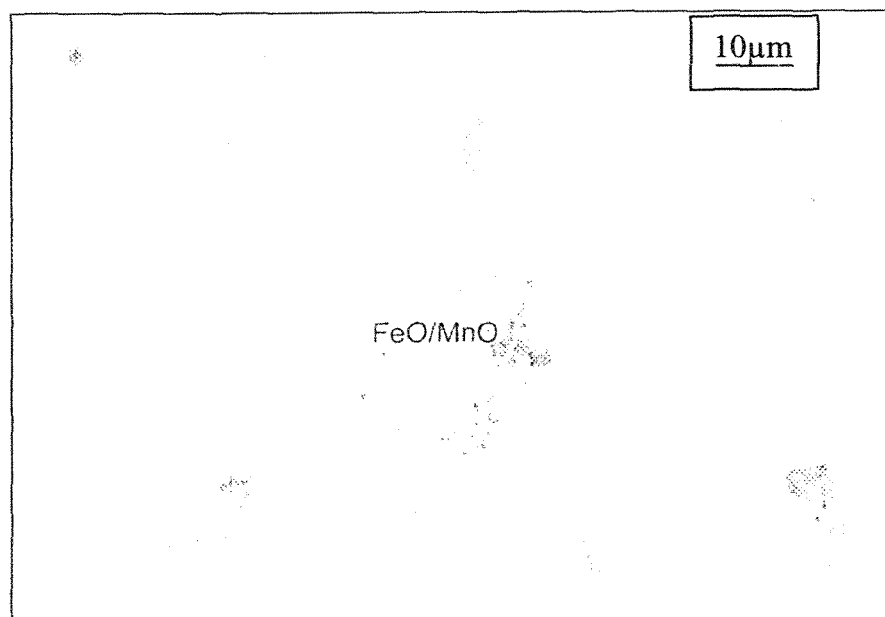


**Figure 92.** Example of FeO/MnO inclusions in aluminum casting.



Foreign material inclusions (also termed exogenous inclusions) are particles from outside the melt. Substances such as alumina, silica and silicon carbide, which arise from the wear and erosion of crucibles, refractories, sheaths and the like, are included in this group<sup>66</sup>. Also included in this group are particles of tool coating materials and inadequately dissolved alloying constituents. Foreign material inclusions invariably exist as discrete insoluble particles. They may vary in size from about 1  $\mu\text{m}$  to as much as 20 mm. Figure 93 shows an example of foreign inclusions (refractory particles).

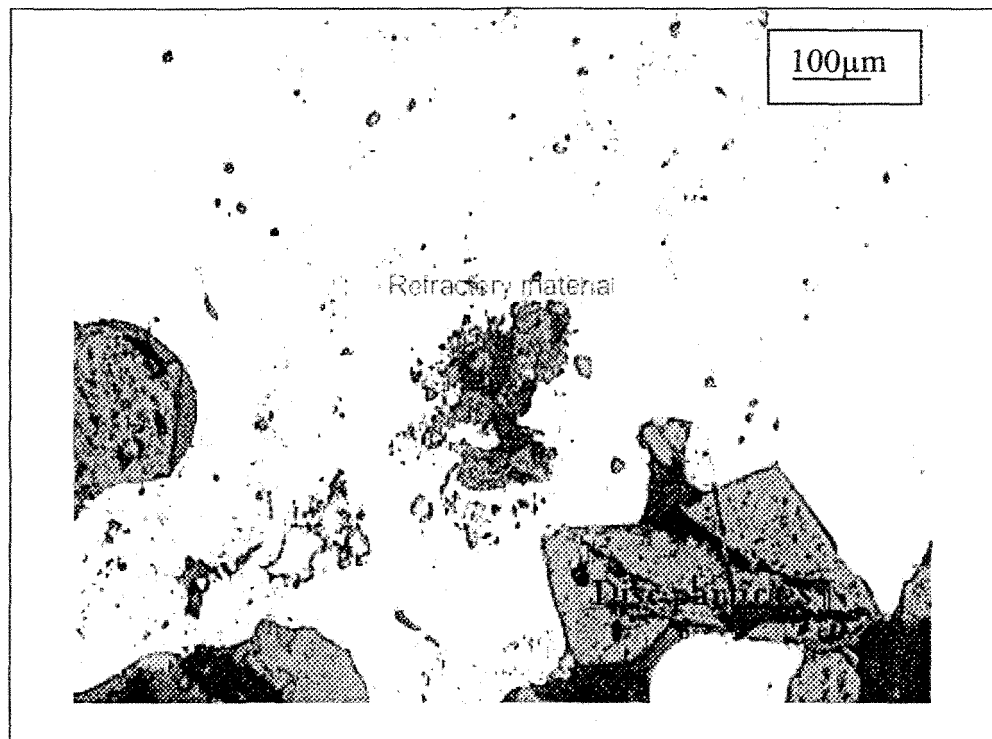


**Figure 93.** Presence of refractory material at the interface.

#### 4.8.4 GRAPHITES

Normally graphite inclusions were found in two popular forms in aluminum casting alloys:

- i) Nodular Graphite
- ii) Flake Graphite

Generally, the main source of graphite comes from the reaction between the melt and the components of the reduction cells. Other sources of these inclusions are the degassing unit.

Figures 94 and 95 display these two kinds of inclusions.

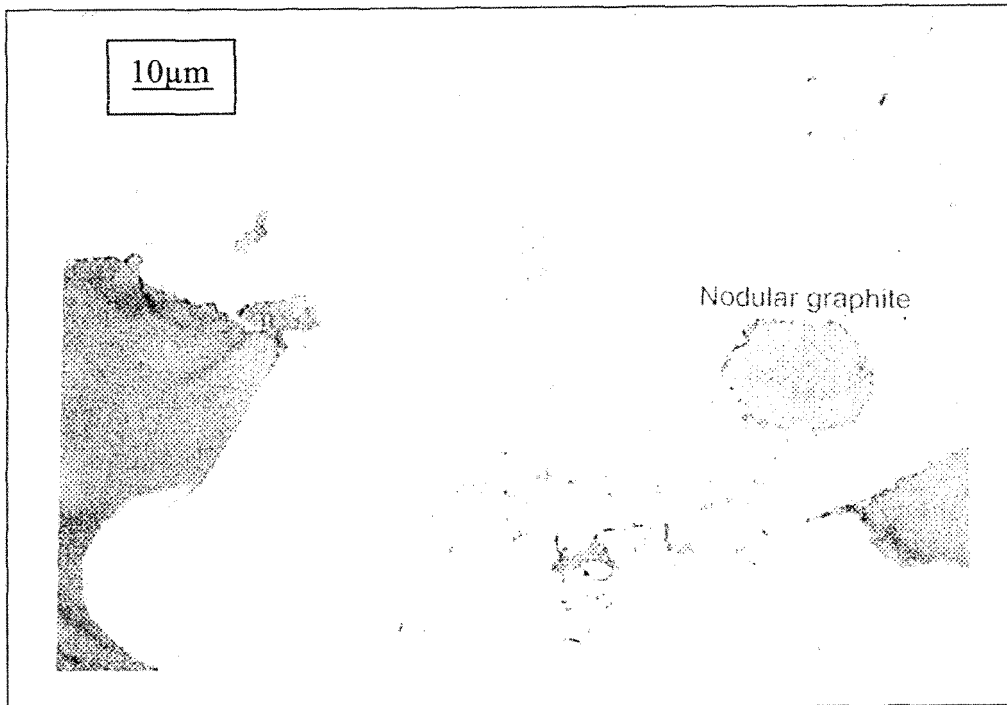


**Figure 94.** Nodular graphite inclusion in aluminum.

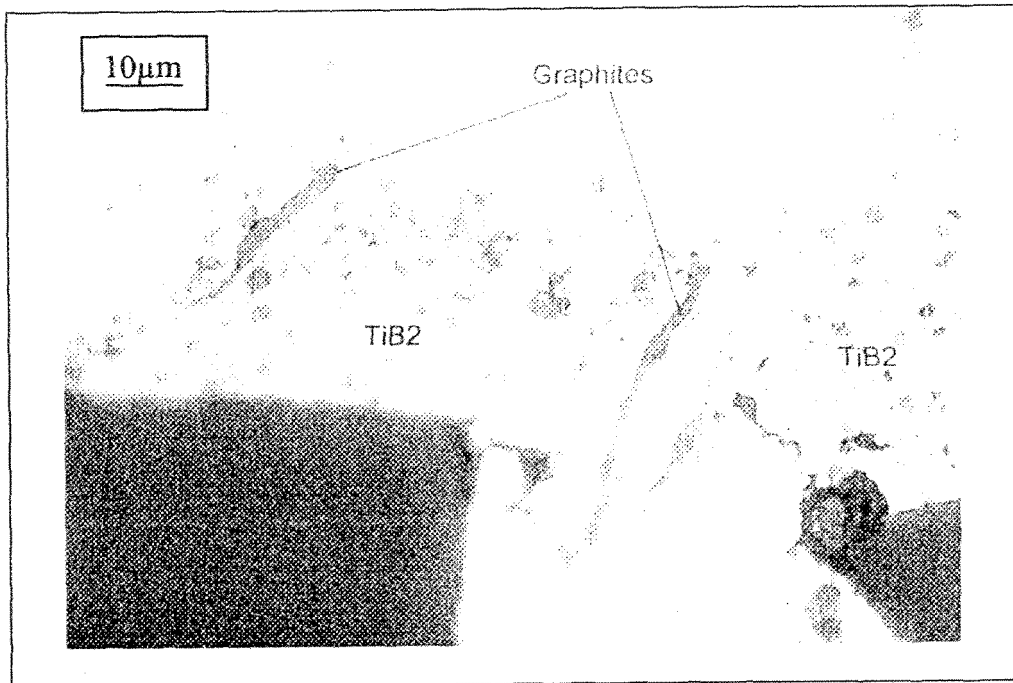


**Figure 95.** Flake graphite inclusion in aluminum.

**CHAPTER 5**  
**CONCLUSIONS**

## **CHAPTER 5**

### **CONCLUSIONS**

An intensive study was carried out for measuring and identifying inclusions in different aluminum casting alloys, under laboratory and industrial environments. Four automotive alloys were tested, viz., 356, 319, 4104 and pure aluminum. Eighty-nine Prefil samplings were taken under various conditions. The study addresses the concerns about the Prefil-Footer's capability to measure the cleanliness of liquid aluminum. More specifically, it demonstrates the sensitivity and reproducibility of the Prefil curve.

#### **Prefil and LiMCA II Results**

1. Prefil curves demonstrate very good sensitivities to the variations in the melt treatment conditions. There is a clear difference between the Prefil curves produced before and after metal treatment. Prefil curves are also greatly affected by settling time, metal stirring and grain refiner addition.
2. In the case of Sr modification, the correlation between the amount of strontium in the molten metal and the Prefil curve (Foot-Print) has yet to be correctly established. More experiments are needed to better understand this.
3. Reproducibility of the Prefil curves was empirically demonstrated using statistical methods.

3. Reproducibility of the Prefil curves was empirically demonstrated using statistical methods.
4. The filtration rate is greatly affected by grain refiner. The highest curve is the alloy without grain refiner addition. The filtration rate progressively decreases with increasing amount of grain refiner. When the total amount of boron in the grain refiner added to the melt reaches 60 ppm, the filtration rate is approximately nil.
5. The overall error on the Prefil curve is  $\pm 9\%$  at a level of confidence of 95% ( $2\sigma$ ) at any time during the filtration. This was determined in (a) laboratory environments where all parameters are controlled, and (b) a primary aluminum producer plant where a LiMCA II instrument ensured the stability of the melt cleanliness level. Due to the fact that it is impossible to perfectly control molten metal conditions and sampling variations, the real instrument error is probably lower. Thus, the Prefil-Footer is capable of measuring significant variations in the cleanliness of liquid aluminum alloys, including those used for automotive castings.
6. Good correlation was obtained between the results produced using the LiMCA II instrument and the metallographic analysis of the Prefil residues. Small differences in the inclusion concentrations measured by the LiMCA II and by metallographic analysis can be associated with the corresponding Prefil curves, indicating a good sensitivity of the Prefil technique.

### **Main Inclusions and Their Morphologies**

7. Oxides ( $\text{Al}_2\text{O}_3$ ,  $\text{MgO}$ ,  $\text{Al}_2\text{MgO}_4$ ) are found in the form of films (thin films  $<3\mu\text{m}$ , or thick films  $>3\mu\text{m}$ ), clusters, or oxide particles. They originate from the reaction between the molten metal and the surrounding atmosphere.
8. Carbides (mainly  $\text{Al}_4\text{C}_3$ ) exist in the form of clusters. These carbides are caused by the reaction between the molten aluminum and the components of the manufacturing cell (e.g. cathodes, anodes), lining of the melting furnace, charges and tools (e.g. graphite degassing impeller).
9. Borides ( $\text{TiB}_2$  and  $\text{VB}_2$ ) appear in the form of hexagonal or rectangular discs, and occur due to the addition of grain refiners such as Al-5% Ti-1% B.
10. Nitrides (mainly  $\text{AlN}$ ) are associated with other oxides, and originate from the reaction between the melt and surrounding atmosphere.
11. Graphite occurs in the form of nodules and flakes, resulting from broken pieces of the components of the reduction cells.
12. Bone ash and refractories appear in the form of particles, which arise from the wear and erosion of the furnace sheath.

## REFERENCES



## REFERENCES

1. ASM Specialty Handbook: "Aluminum and Aluminum Alloys", J.R. Davis, ASM International Materials Park, Ohio, (1993), pp. 3-4.
2. "Introduction to Physical Metallurgy", S.H. Avner (ed.), McGraw-Hill Book Company, New York, (1974), pp. 481-482.
3. S. Shivkumar, L. Wang and D. Apelian, "Molten Metal Processing of Advanced Cast Aluminum Alloys", JOM, January (1991), pp. 26-32.
4. H.E. Miller, "Relationship Between Inclusions Content of Casting and Final Product Quality", Aluminum Transactions, vol. 5 (1972), pp. 368-371.
5. "Aluminum viewed from within", A. Altenpohl (ed.), (1975).
6. Metals Handbook, (2<sup>nd</sup> Edition), vol. 1, Aluminum and Aluminum Alloys, American Society for Metals, Metals Park, Ohio (1998), pp. 417-420.
7. "The Treatment of Liquid Aluminum-Silicon Alloys", J.E. Gruzleski and B.M. Closset (eds.), American Foundrymen's Society, Inc., Des Plaines, Illinois, (1990), pp.186-189.
8. S. Shivkumar, D. Apelian and H. Brucher, "Melt Cleanliness in Die Cast Aluminum Alloys", Transactions of the 16<sup>th</sup> International Die Casting Congress and Expositions, Detroit, Michigan, USA. 30 September - 3 October (1991), pp. 143-152.
9. D. Doutre, B. Gariépy, J.P. Martin and G. Dubé, "Aluminum Cleanliness Monitoring: Methods and Applications in Process Development and Quality Control", Light Metals (1985), pp. 1179-1189.
10. ABB Bomem Inc., Metallographic Evaluation Reports for Prefil, January 2001.

11. P.S. Mohanty, F.H. Samuel and J.E. Gruzleski, "Studies on Addition of Inclusions to Molten Aluminum Using a Novel Technique", *Metallurgical and Materials Transactions B*, vol. 26 B (1995), pp. 103-109.
12. J. Langerweger, "Non-Metallic Inclusions as the cause of Structural Porosity, Heterogeneous Cell Structure and Surface Cracks in DC Cast Al Products", *Swiss Aluminum Ltd. J.* vol. 4 (1980), pp. 685-705.
13. J.E. Gruzleski and B. Closset, "Mechanical Properties of A356.0 Alloys Modified with Pure Strontium", *AFS Transactions*, vol. 99 (1982), pp. 453-464.
14. D.V. Neff and P.V. Cooper, "Clean Metal for Aluminum Foundries: New Technology Using a Rotor Degasser and Filter Pump", *AFS Transactions*, vol. 107 (1990), pp. 579-584.
15. S. King and J. Reynolds, "Flux Injection/Rotary Degassing Process Provides Cleaner Aluminum", *Modern Casting*, vol. 85 (1995), pp. 37-40.
16. T.A. Zeliak, "Effective Degassing of Aluminum Alloys For Foundry Applications", Internal Report.
17. D.P. Kanicki, and W.M. Rasmussen, "Cleaning Up Your Metal", *Modern Casting*, vol. 80 (1990), pp. 55-61.
18. H. Cong and X. Bian, "The Reduction of the Inclusions And Hydrogen in the Molten Aluminum Alloys", *Materials Sciences Forum*, vol. 33 (2000), pp. 325-330.
19. S. Shivkumar, L. Wang and R. Lavigne, "Quantitative Evaluation of Pore Characteristics in Cast Aluminum Alloys", *Light Metals* (1993), pp. 829-833.

20. J.F. Meredith, "Metal Treatment of Aluminum Alloys", *Metal Asia*, vol. 7 (1999), pp. 28-30.
21. D.W. Pattle, "Advances in degassing aluminum alloys" *American Foundrymen's Society, Inc., Des Plaines, Illinois*, (1998), pp. 232-235.
22. "Solidification Processing", M.C. Flemings (ed.), *McGraw-Hill Book Company*, New York, (1974), pp. 229-230.
23. B.L. Tuttle, "Molten Metal Processing Treatment for the Production of quality Die Casting", *SDCE 13<sup>th</sup> International Die Casting Congress and Expositions*, vol. 21 (1985), pp. 1-13.
24. D.E. Groteke, "The Reduction of Inclusions in Aluminum by Filtration", *Modern Casting*, vol. 73 (1983), pp. 25-30.
25. C.J. Simensen, "Sedimentation Analysis of Inclusions in Aluminum and Magnesium" *Metallurgical Transactions B*, vol. 12B (1981), pp. 733-737.
26. C.J. Simensen and U. Hartvedt, "Analysis of Oxides in Aluminum by Means of Melt Filtration", *Z. Metalkunde*, vol. 76 (1985), pp. 409-414.
27. L. Liu, "Evaluation de l-a propreté des alliages d'aluminium de Fonderie A356.2 et C357 à l'aide de la technique PoDFA", *M. Eng. Thétis, Université du Québec à Chicoutimi* (1997).
28. C.J. Simenson and G. Berg, "A Survey of Inclusions in Aluminum", *Aluminum Transactions*, vol. 56 (1980), pp. 335-340.
29. C.E. Eckert, "Inclusions in Aluminum Foundry Alloys", *Modern Casting*, vol. 81 (1991), pp. 28-30.

30. W. Simmons, "The Filtering of Molten Metal to Improve Productivity, Yield, Quality and Properties", *Indian Foundry J.*, (1988), pp. 21-28.
31. D. Apelian and S. Shivkumar, "Molten Metal Filtration – Past, Present and Future Trends", *Proc. 2<sup>nd</sup> International Conference on Molten Aluminum Processing*, Orlando, Florida, November 6-7, (1989), AFS, Des Plaines, IL, pp. 1-36.
32. M.J. Lessiter, "Understanding Inclusions in Aluminum Casting", *Modern Casting*, vol. 83 (1993), pp. 29-31.
33. D. Neff, "Effective Molten Filtration in Production Highest Quality Die Casting", *SDCE Conference, 14<sup>th</sup> International*, vol. 34 (1987), pp. 1-6.
34. E. Kato, Y. Ueda and T. Kabayashi, "The Influence of Inclusions on the Fracture Toughness of the High-Strength Aluminum", *J. of Japan. Institue. of Light Metals*, vol. 35 (1985), pp. 282-288.
35. J.R. Schmahl and N.J. Davidson, "Ceramic Foam Filter Technology for Aluminum Foundries", *Modern Casting Journal*, vol. 83 (July 1993), pp. 31-33.
36. W. Simmons and A.J. Broome, "Influence of Metal Filtration on the Production of High Integrity Cast Products", *SEAISI Conference*, Thailand, May 18-20, (1987), pp. 47-53.
37. H. Devaux, D. Hiebel, S. Jacob and M. Richard, "Filtration Techniques for Aluminum Castings", *Fonderie SEVRES J.* vol. 15 (1989), pp. 1-21.
38. "Applied Science in the Casting of Metals", K. Strauss (ed.), Pergamon Press, Oxford, U.K., (1970), pp. 241-293.

39. M.A. Easton and D.H. StJohn, "The Effect of Grain Refinement on the Formation of Casting Defects in Alloy 356 Casting", *Int. J. Cast Metals Res.*, vol. 12 (2000), pp. 393-408.
40. K. Dennis, R.A.L. Drew and J.E. Gruzleski, "Effect of Strontium on the Oxidation Behavior for an A356 Alloys", *Aluminum Transactions*, vol. 3 (2000), pp. 31-39.
41. P. Sandford, "Getting the Junk out of the Molten Aluminum", *AFS Transactions*, vol. 105 (1995), pp. 95-153.
42. M. Maniruzzaman and M. Makhlof, "The Removal of Solid Inclusions From Aluminum Alloys Melts by Flotation", 5<sup>th</sup> International AFS Conference on Molten Aluminum Processing, November 8-10, Orlando, (1998), pp. 61-67.
43. D.J. Lloyd, S.K. Das, C.P. Ballard and F. Marikar", *High Performance Composites for the 1990's*", TMS, (1991), pp. 33-45.
44. R. Taylor, "Melt treatments of aluminum alloys with particular reference to aluminum-silicon systems", *FWP J.*, January (1992), pp. 11-16.
45. J.R. Schmahl, N.J. Davidson, (eds.), "Ceramic Foam Filter Technology for Aluminum Foundries", *Modern Casting*, July (1993), pp. 31-33.
46. "Nondestructive Testing Handbook", 1<sup>st</sup> Edition, vol. 1, R.C. McMaster (ed.), The Reynolds Company, USA, New York, (1950), pp. 15-16.
47. F. Samuel, P. Ouellet, and A. Simard, "Assessment of Melt Cleanliness and Analysis of Inclusions in Aluminum – Silicon Alloys Using the Prefil Pressure Filtration Technique", *Int. J. Cast Metals Res.*, vol. 12 (1999), pp. 17-33.

48. "Liquid Aluminum Cleanliness Control Apparatus" Bomem Inc., Qualiflash User Manual, Revision 1.1.
49. C. Evans and W. Willmert, "Qualiflash as it Relates to Filtration and Degassing for Foundry and Extrusion Alloys", 5<sup>th</sup> International AFS Conference on Molten Metal Processing, Orlando, Florida, (1997), November 8-10, pp. 349-364.
50. F.H. Samuel, P. Ouellet, and A. Simard, "Measurement of Oxide Films in Aluminum (6-17) wt% Si Foundry Alloys Using the Qualiflash Filtration Technique", Int. J. Cast Metals Res., vol. 12 (1999), pp. 49-55.
51. C. Tian, F. Dallaire, R.I.L. Guthrie and L. Strom, "Inclusions Removal From Aluminum Melts Through Filtration", Recent Developments in Light Metals, Proc. Int. Symposium, M. Gilbert, P. Tremblay, and E. Ozberk (eds.), The Metallurgical Society of CIM, Montreal, Canada, (1995), pp. 153-161.
52. J.P. Martin and F. Painchaud, "On-Line Metal Cleanliness Determination in Molten Aluminum Alloys Using the LiMCA II Analyser", Light Metals, (1994), pp. 915-920.
53. P.G. Enright and I.R. Hughes, "A Shop Floor Technique for Quantitative Measurement of Molten Metal Cleanliness of Aluminum Alloys" Foundryman Magazine, IBF publication, November (1996), pp. 390-395.
54. A. Simard, F. Dallaire, J. Proulx and P. Rochette, "Cleanliness Measurement Benchmarks of Aluminum Alloys Obtained Directly At-Line Using the Prefil – Footprinter Instrument", Light Metals, (2000), pp. 379-385.

55. P.K. Singh and D.J. Mitchell, "Analysis of Metal Quality in a Low Pressure Permanent Mold Foundry", 105<sup>th</sup> AFS Casting Congress, Dallas Texas, April 28-May 1 (2001), pp. 88-102.
56. ABB Bomem Inc., Private Communication, April 2001.
57. X.G. Chen, R.I.L. Guthrie and J.E. Gruzleski, "Quantitative Measurement of Melt Cleanliness in Aluminum – Silicon Casting Alloys", 4<sup>th</sup> International AFS Conference on Molten Metal Processing, Orlando, Florida, (1996), pp. 15-28.
58. G. Chai and L. Bæckerud, "Some Factors Affecting the Modification of Aluminum Silicon Alloys by Addition of Strontium-Containing Master Alloys", AFS Transactions vol. 100 (1992), pp. 847-852.
59. ABB Bomem Inc., "Metallographic Evaluation Report for Prefil", January 2001.
60. ABB Bomem Inc., "Metallographic Evaluation Report for Prefil", June 2001.
61. S.T. McClain, A.S. McClain and J.T. Berry, "A Comparison of Image–Analysis and Pyknometry Results for the Percentage Porosity Evaluation of Two A356 Casting", 105<sup>th</sup> AFS Casting Congress, Dallas, Texas, April 28-May 1 (2001), pp. 62-72.
62. M.J. Lessiter and W.M. Rasmussen, "To Pour or Not to Pour – The Dilemma of Assessing Your Aluminum Melt’s Cleanliness", Modern Casting, vol. 86 (1996), pp. 45-48.
63. ABB Bomem Inc., Prefil Engineering Bulletin No. 3, (2001).
64. C.E. Eckert, R. Mutharasan, D. Apelian and R.E. Miller, "An Experimental Technique for Determining Specific Cake Resistance Value in the Cake Filtration of Aluminum Alloys", Light Metals, (1985), pp. 1281-1304.

65. S.A. Levy, "Application of the Union Carbide Particulate Tester", *Light Metals*, (1981), pp. 723-733.
66. L. Liu and F.H. Samuel, "Assessment of Melt Cleanliness in A356.2 Aluminum Casting Alloys Using the Porous Disc Filtration Apparatus Technique", *J. Mater. Sci.*, vol. 32 (1997), pp. 5927-5944.
67. L.A. Godlewski and J.W. Zindel, "Capability Study of a Filtration Process to Predict Aluminum Melt Quality", 105<sup>th</sup> AFS Casting Congress, Dallas, Texas, April 28-May 1 (2001), pp. 314-326.